Formation of thiocyanate in bioleaching residues and its effect in PGM recovery

By
Kathija Shaik

Supervisor
Professor Jochen Petersen

Submitted in fulfilment of the requirements for the award of the degree of Master of Science in Chemical Engineering,

University of Cape Town

2016

Plagiarism declaration

1. I know that plagiarism is wrong. Plagiarism is to use another's work and pretend that it is one's own.
2. Each significant contribution to, and quotation in, this assignment from the work(s) of the people has been attributed, and has been cited and referenced.
3. This assignment is my own work.
4. I have not allowed, and will not allow anyone to copy my work with the intention of passing it off as his or her own work.

Signature: Signed by candidate ***Date: 15 February 2016***

Acknowledgements

All praise belongs to the Almighty, the Lord of the worlds. The Most gracious, The Most Merciful.

I would like to express my sincere gratitude to Professor Jochen Petersen for giving me the opportunity to work on this project and introducing me to the world of hydrometallurgy, which I thoroughly enjoyed. Thank you for your encouragement, technical guidance and giving me intellectual freedom to work on this project in my own right.

I would also like to acknowledge Outotec in association with the South African Institute of Mining and Metallurgy for the Scholarship in Sustainable Mining, as well as the South African National Research Foundation for their financial support.

A heartfelt thank you to James Mwase, without whom this project would not have been possible. Thank you for your research which laid the foundation for my project. I speak on behalf of the Hydromet team, when I say thank you for making our lab a safe, organised space to conduct our research. The new lab manager has high standards to live up to.

To Rahul Ram, thank you for your invaluable input, editing and assistance towards my thesis. I genuinely appreciated your guidance and advice throughout the write-up of my thesis.

A huge thank you to Cody Burcher-Jones and Shalisa Lodewyk for their assistance on the thiocyanate kinetics study.

Many thanks to the CeBER staff, Emmanuel Ngoma and Tich Samganke for your commitment and technical support in the lab. To the UCT Analytical team, Russell Geland, Jessica Heyns, Zulfa le Rich, Stephanie La Grange and Riana Rossouw from Stellenbosch University, thank you for the endless hours spent analysing all my samples.

To my tea time buddies, Alexey, Buhle and Thandazile, thank you for all the interesting conversations. There was never a dull moment with the 3 of you around.

Last but not least, to my family, my parents Mohammed and Kathoon Shaik, my elder brother Hussain, my sisters Ayesha and Firdous and my brother-in-law Ismael, thank you for your continued support and encouragement. I am forever grateful to have you all in my life.

Abstract

A recent study investigated the feasibility of a sequential heap leach in low grade Platreef ore in order to recover PGMs (Platinum Group Metals), by a pure hydrometallurgical route. This method comprised of two stages, an initial thermophile bioleach stage to extract base metals followed by a cyanide leach to recover precious metals, PGMs. The study conducted assessed the possibility of excluding costly stages such as concentration by flotation, smelting and pressure leaching by directly leaching low grade Platreef ore. The findings showed successful base metal recoveries; however, the production of thiocyanate during the cyanide leach raised concerns in terms of significant cyanide loss but also whether thiocyanate contributed positively to PGM recovery.

Cyanide present in processing liquors is known to react with various sulphur species, depending on the mineralogy of the ore and the chemical constituents within the system. These interactions between cyanide and reduced sulphur species, generated through incomplete oxidation of sulphidic ores, are primarily responsible for thiocyanate formation. In addition, thiocyanate generated during these processes has been identified to mobilise both base metals and precious metals, forming highly stable and soluble complexes with precious metals. Recent work in the field has shown pronounced recoveries during thiocyanate leaching of PGMs from virgin catalytic converters. However, a significant portion of previous research work has focused on metallic gold, with a lack of knowledge regarding thiocyanate leaching of PGMs associated with sulphidic minerals.

This study investigates the chemical kinetics of thiocyanate formation in a thiosulphate, sulphite and polysulphide system in the presence of cyanide. The initial rate kinetics of thiocyanate formation, explored in homogenous systems, displayed fairly rapid reaction kinetics in the cyanide-polysulphide system relative to the thiosulphate-cyanide system. Additionally, sulphite exhibited a minor affinity for cyanide as no measurable concentration of thiocyanate was observed. This serves to verify that polysulphides generated during incomplete oxidation of sulphidic minerals are most likely responsible for SCN^- formation and not the direct interactions between sulphidic minerals and cyanide.

Further, this research is an initial attempt to investigate the effectiveness of thiocyanate leaching in Pt and Pd containing minerals under varied conditions. In the process, it seeks to establish whether thiocyanate and cyanide act synergistically to promote the dissolution of Pt and Pd. Preliminary test work carried out on Platreef concentrate demonstrated that the presence of base metals significantly limited the concentration of free thiocyanate available for leaching. From the results observed, Fe (under acidic conditions) and Ni displayed a strong affinity for thiocyanate, attributed to the formation of highly stable complexes. However, Cu demonstrated a negligible effect on thiocyanate consumption, forming an insoluble salt complex, CuSCN(s).

Confirmatory test work was conducted on highly pure minerals (cooperite, sperrylite and Pt sponge) in batch stirred tank reactors under varied conditions. The results indicated that rate of Pt extraction varied substantially among the minerals. Cooperite exhibited the fastest Pt dissolution kinetics for an acid SCN^-/Fe^{3+}, acid SCN^- and an alkaline mixed (SCN^-, CN^- & $[Fe(CN)_6]^{3-}$) system generating initial rates of $7.29x10^{-10}$, $6.66x10^{-10}$ and $532.97x10^{-10}$ $mol.L^{-1}.s^{-1}$, respectively. However, sperrylite dominated in cyanide systems yielding initial rates of $1.55x10^{-10}$ and $9.60x10^{-10}$ $mol.L^{-1}.s^{-1}$ for the alkaline CN^- and the alkaline $CN^-/[Fe(CN)_6]^{3-}$ system, respectively. Thiocyanate specifically promoted the leaching of Pt in cooperite while cyanide contributed to the leaching of Pt in sperrylite; this technique can be exploited to selectively dissolve Pt in both cooperite and sperrylite.

Final test work on Merensky concentrate in columns reactors, utilising various mixed systems showed reasonable Pt and Pd recoveries. It was established that a 3 component system comprising of SCN^-, CN^- and $[Fe(CN)_6]^{3-}$ displayed enhanced extraction in relation to a 2 component consisting of either CN^-/SCN^- or $CN^-/[Fe(CN)_6]^{3-}$; achieving 47.19% Pt extraction over a 55 day period and 100% Pd extraction over 30 days. It was concluded that ferricyanide acted as an oxidant promoting the dissolution of Pt and Pd, whereas the formation of heterogeneous (mixed) ligand complexes containing both thiocyanate and cyanide ligands, primarily ensured enhanced stability of the Pt and Pd in the leach solution.

Nomenclature

Abbreviations

AAS	Atomic absorption spectroscopy
BMs	Base metals
ICP-AES	Inductive coupled atomic plasma emission spectrometry
ICP-MS	Inductive coupled plasma mass spectrometry
MLA	Mineral liberation analysis
ORP	Oxidation reduction potential
PGMs	Platinum group metals
PLS	Pregnant leach solution
ppb	Parts per billion
ppm	Parts per million
UG 2	Upper Ground 2

Chemical Formula

Au	Gold
CN^-	Cyanide
CO_3^{2-}	Carbonate
Cu	Copper
$CuFeS_2$	Chalcopyrite
Fe^{2+}	Ferrous ion
Fe^{3+}	Ferric ion
FeS_2	Pyrite
$Fe_{(1-x)}S$	Pyrrhotite
$HCl + HNO_3$	Aqua regia
Ni	Nickel
O_2	Oxygen
OH^-	Hydroxide
Pd	Palladium
Pt	Platinum
$PtAs_2$	Sperrylite (Platinum arsenide)
PtS_2	Cooperite (Platinum sulphide)
Rh	Rhodium
S	Elemental sulphur
S^{2-}	Sulphide
$S_2O_3^{2-}$	Thiosulphate
SO_3^{2-}	Sulphite
$S_xO_6^{2-}$	Polythionate
S_xS^{2-}	Polysulphide
SCN^-	Thiocyanate
$(SCN)_2$	Thiocyanogen
$(SCN)_3^-$	Trithiocyanate

Symbols

A	Pre-exponential factor
E_a	Activation energy (kJ.mol^{-1})
i	Reaction order
k	Specific rate constant (min^{-1})
k_{app}	Apparent rate constant
R	Universal gas constant (8.314 J.mol^{-1}.K^{-1})
r_x	Initial rate (mol.L^{-1}.s^{-1})
t	Time (s)
T	Temperature (^{o}C or K)

Table of Contents

Plagiarism declaration i
Acknowledgements ii
Abstract iii
Nomenclature v
Table of Contents vii
List of Figures x
List of Tables xiii
1. Introduction 1
1.1 Background to study 1
1.2 Problem statement 2
1.3 Objectives 2
2. Literature review 4
2.1 Introduction to PGMs 4
2.2 Conventional matte-melting process 7
2.2.1 Refining of Platinum Group Metals 8
2.2.2 Limitations of the conventional smelt-refine route 10
2.3 Sequential heap leach process 11
2.3.1 Bioleach 11
2.3.2 Cyanide leach 14
2.3.3 Findings 16
2.3.4 Thiocyanate conversion 17
2.4 Thiocyanate formation 19
2.4.1 Chemistry of cyanide and sulphur species in pure minerals 19
2.4.2 Reaction kinetics of thiocyanate formation 22
2.5 Thiocyanate hydrometallurgy 24
2.5.1 Chemical properties of thiocyanate 24
2.5.2 Thermodynamics of thiocyanate leach systems 24
2.5.3 Au-SCN complexes 25
2.5.4 Fe-SCN complexes 26
2.5.5 Cu-SCN complexes 27
2.5.6 Stability of thiocyanate 28
2.5.7 Thiocyanate complexation to Pt and Pd 31
2.6 Leaching of precious metals in thiocyanate solutions - Dissolution rates 32

2.6.1 Effect of thiocyanate concentration on rate dissolution 32
2.6.2 Effect of oxidant concentration 34
2.6.3 Effect of temperature 35
2.6.4 Effect of pH 36
2.7 Research approach 38
3. Experimental materials and methods 40
3.1 Materials 40
3.1.1 Platreef and Merensky concentrate 40
3.1.2 Pure minerals 41
3.1.3 Reagents 42
3.2 Equipment 42
3.2.1 Column reactors 42
3.2.2 Batch stirred tanks reactors 44
3.3 Methods 45
3.3.1 Phase 1: Chemical reaction kinetics of thiocyanate formation 45
3.3.2 Phase 2: Preliminary test work on Platreef concentrate 47
3.3.3 Phase 3: Confirmatory test work 48
3.3.4 Phase 4: Final test work on Merensky concentrate 49
3.4 Analysis techniques 50
3.4.1 pH and redox analysis 50
3.4.2 Elemental analysis of solids 50
3.4.3 Elemental analysis of solutions 50
3.4.4 Thiocyanate analysis 50
4. Results and discussion 51
4.1 Chemical kinetics of thiocyanate formation 51
4.2 Preliminary test work: Platreef concentrate 58
4.2.1 Ammonia leaching 58
4.2.2 Thiocyanate leaching 58
4.2.3 Influence of base metal on thiocyanate consumption 60
4.3 Pure Mineral leach 63
4.3.1 Cooperite (platinum sulphide) 63
4.3.2 Sperrylite (platinum arsenide) 64
4.3.3 Platinum sponge 65
4.3.4 ORP and pH 66

4.3.5 Reaction rates 68
4.4 Final test work on Merensky concentrate: dual lixiviant system 75
4.4.1 Bioleach 75
4.4.2 SCN-CN leach 77
5. Conclusions and recommendations 80
6. References 82
7. Appendices 87

List of Figures

Figure 1: Schematic of the Bushveld complex showing the location and depth of the Merensky, UG 2 and Platreef ore (Cawthorn, 2010). 6
Figure 2: Conventional method of extracting PGMs (Mpinga et al., 2015) 8
Figure 3: Sequential heap leach, (Mwase et al., 2014) 11
Figure 4: (a) Thiosulphate pathway and (b) polysulphide pathway (Schippers & Sand 1999; Schippers et al. 1996). 13
Figure 5: Percentage conversion of NaCN to thiocyanate. Column 1: -25+1mm, Column 2: -6+1mm: both columns leached at 5 L/m^2 with 5 g/L NaCN solution; aeration rate: 130 mL/min (Mwase et al., 2014). 16
Figure 6: Thiocyanate in cyanide effluent solution. Column 1: -25+1mm, Column 2: -6+1mm: both columns leached at 5 L/m^2 with 5 g/L NaCN solution; aeration rate: 130 mL/min (Mwase et al., 2014). 17
Figure 7: Concentration profiles for the reaction of cyanide with a 10:1 excess of Frasch sulphur: ΔΔ CN^-_{WAD}, ○○ CN^-_{WAD} reacted, □□ SCN^- produced. Conditions for the experiment were: 0.0401g of Frasch sulphur in 0.50L of 0.25mM CN^- at 25^{o}C (Wilmot, 1997). 19
Figure 8: Concentration profiles for the reaction of cyanide with a 10:1 excess of pyrite: ΔΔ CN^-_{WAD}, ○○ CN^-_{WAD} reacted, □□ SCN^- produced. Conditions for the experiment were: 0.0750g of pyrite in 0.50L of 0.25mM CN^- at 25^{o}C (Wilmot, 1997). 20
Figure 9: Concentration profiles for the reaction of cyanide with a 10:1 excess of pyrrhotite: ΔΔ CN^-_{WAD}, ○○ CN^-_{WAD} reacted, □□ SCN^- produced. Conditions for the experiment were: 0.1040g of pyrrhotite in 0.50L of 0.25mM CN^- at 25^{o}C (Wilmot ,1997). 21
Figure 10: Concentration profiles for the reaction of cyanide with a 10:1 excess of chalcopyrite: ΔΔ CN^-_{WAD}, ○○ CN^-_{WAD} reacted, □□ SCN^- produced. Conditions for the experiment were: 0.1147g of chalcopyrite in 0.50L of 0.25mM CN^- at 25^{o}C (Wilmot, 1997) 21
Figure 11: Comparison of production rates for formation of thiocyanate from reaction of equimolar concentrations of cyanide and polysulfide, and cyanide and thiosulfate (Luthy & Bruce, 1979). 22
Figure 12: Possible reactions of cyanide with reduced sulfur species in aqueous solution to yield thiocyanate (Luthy & Bruce, 1979) 23
Figure 13: Resonance structures of thiocyanate (Li et al. 2012a) 24
Figure 14: E_h-pH diagrams for the Au-SCN-H_2O system at SCN concentrations of 0.005, 0.1 and 0.5M, and Au concentration of 2mg/L at 25^{o}C. Dashed lines indicate water stability (Li et al., 2012a) 25
Figure 15: E_h–pH diagram for the Fe–SCN–H_2O system at Fe concentration of 0.1 M, SCN concentration of 0.1M at 25^{o}C. Dashed lines indicate water stability limits (Li et al. 2012a). 26
Figure 16: E_h–pH diagrams for the Cu–SCN–H2O system at Cu concentration of 0.2 g/L and SCN concentrations of 0.1M at 25 °C. Dashed lines show water stability limits (Li et al. 2012a). 27
Figure 17: E_h–pH diagrams for the SCN–H2O system at SCN concentrations of 0.5 and 0.005 M at 25 °C. Concentration of all other dissolved species 0.1 M. Short dashed lines show water stability limits (Li et al., 2012a). 28
Figure 18: LFER for the formation constants of Pt(II) and Pt(IV) complexes against those for Pd(II) complexes. Tu = thiourea, Su = selenourea, py =pyridine.(Hancock et al. 1977) 30
Figure 19: Reaction mechanisms for Pt and Pd complexes in thiocyanate solution 31

Figure 20: Dependence of leaching rate of gold from chemical product by KSCN solutions on pH value solution KSCN =0.4 M (Kholmogorov et al., 2002) 37
Figure 21: (a) Dickie and Stockler (Pty), (b) 10kg rotary splitter and (c) 1kg rotary splitter, Rotary micro riffler 40
Figure 22: Schematic of column and experimental setup 42
Figure 23: (a) Slurry coated onto support rock and (b) column packed with coated support rock. 43
Figure 24: Experimental set-up of batch stirred tank reactors. 44
Figure 25: SCN concentration profile for the reaction of cyanide with ■ 5:1 ratio, ▲ 3:1 ratio, ◆ 1:1 excess thiosulphate at 60°C 52
Figure 26: SCN concentration profile for the reaction of cyanide with ■ 5:1 ratio and◆ 1:1 ratio excess sulphite at 45° 53
Figure 27: SCN concentration profile for the reaction of cyanide with polysulphide: ■ 1.12:1 ratio, ▲0.56:1 ratio, ◆ 0.28:1 ratio at 25°C 53
Figure 28: SCN concentration profile for the reaction of cyanide and thiosulphate with 1:1 M ratio at ■ 75°C, ▲ 60°C and ◆ 45°C. 54
Figure 29: SCN concentration profile for the reaction of cyanide and polysulphide with 0.56:1 mol ratio at ■ 45°C, ▲ 35°C and ◆ 25°C. 54
Figure 30: Initial rate kinetic data for the ■ thiosulphate-cyanide and ● polysulphide-cyanide reaction. 55
Figure 31: Linear plot of rates against the inverse of absolute temperature for ■ thiosulphate-cyanide and ● polysulphide-cyanide reaction. 55
Figure 32: (a) Cu and (b) Ni extractions at 4M NH_4OH, 1M $(NH_4)_2CO_3$, 40°C, pH. 9.5-10.5 and aeration rate of 80mL/min. 58
Figure 33: Pt extractions at (a) 0.2M and (b) 0.3M SCN^- concentration, 50°C, 500rpm, gentle air flow and pH. 1.5 – 2 using pre-treated concentrate: ▲ Sample A [6M NH_3] ● Sample B [6M NH_3 + 1M H_2SO_4 (1hr)] and ■ Sample C [1M H_2SO_4 (24 hrs)] 59
Figure 34: Pd extractions at (a) 0.2M and (b) 0.3M SCN- concentration, 50°C, 500rpm, gentle air flow and pH. 1.5 – 2 using pre-treated concentrate: ▲ Sample A [6M NH_3] ● Sample B [6M NH_3 + 1M H_2SO_4 (1hr)] and ■ Sample C [1M H_2SO_4 (24 hrs)]. 59
Figure 35: Stacked diagram showing the total base metal recoveries achieved during pre-treatment and thiocyanate leaching for (a) Fe (b) Ni and (c) Cu. 61
Figure 36: Pt extractions achieved for synthetic cooperite under varied conditions at 50°C and 500rpm 63
Figure 37: Pt extractions achieved for natural sperrylite under varied conditions at 50°C and 500rpm. 64
Figure 38: Pt extractions achieved for Pt sponge under varied conditions at 50°C and 500rpm. 65
Figure 39: pH profile for cooperite, sperrylite and Pt sponge in ◆ acid SCN^-/Fe^{3+} and ▲ acid SCN^- systems. 66
Figure 40: pH profile for cooperite, sperrylite and Pt sponge in ■ alkaline SCN^-, ● alkaline mixed, ✖alkaline CN^- and ✱alkaline $CN^-/[Fe(CN)_6]^{3-}$. 66
Figure 41: ORP profile for cooperite, sperrylite and Pt sponge in ◆ acid SCN^-/Fe^{3+}, ▲ acid SCN^-, ■ alkaline SCN^-, ● alkaline mixed, ✖alkaline CN^- and ✱alkaline $CN^-/[Fe(CN)_6$. 67
Figure 42: ◆ k_{app} using the SCM1 for cooperite 70

Figure 43: ◆ k_{app} using the SCM1 for sperrylite 71
Figure 44: Platinum extractions achieved for (a) cooperite and (b) sperrylite under varied conditions at 500rpm 73
Figure 45: Linear plot of initial rates against the inverse of absolute temperature for (a) cooperite and (b) sperrylite at ◆0.5g/L (SCN^-,CN^-) and ■2g/L (SCN^-,CN^-) concentration..... 73
Figure 46: (a) Cu, (b) Fe and (c) Ni extractions achieved during bioleach process at 10g/L H_2SO_4, 0.2g/L Fe^{2+}, 65°C and aeration rate of 130mL/min. 75
Figure 47: (a) pH and (b) ORP achieved during bioleach process at 10g/L H_2SO_4, 0.2g/L Fe^{2+}, 65°C and aeration rate of 130mL/min 76
Figure 48: (a) Pt and (b) Pd extractions achieved for mixed systems at 50°C and aeration rate of 130mL/min. 77
Figure 49: Ferric nitrate standard curve 87

List of Tables

Table 1: A summary of the bulk minerology of Merensky reef, UG2 reef and Platreef that occur in the Bushveld igneous complex (Shamaila & Connor, 2008). 5
Table 2: Methods of extraction used in PGMs refinery (Crundwell et al., 2011) 9
Table 3: Overall stability constants of selected metal-cyano complexes 14
Table 4: PGM complexes formed during cyanidation process (Chen and Huang, 2006). 14
Table 5: Concentration of Pt in solution (Mwase et al., 2014) 16
Table 6: Thiocyanate formation reactions (Luthy & Bruce, 1979; Wilmot, 1997) 23
Table 7: Stability constants for selected thiocyanate complexes 29
Table 8: Stability constants for selected Pt and Pd complexes at 25^{o}C (Mountain & Wood, 1988; le Roux et al., 2014) 30
Table 9: Effect of thiocyanate concentration on the initial rate of gold dissolution (Barbosa-Filho & Monhemius, 1994) 32
Table 10: Effect of thiocyanate concentration on the initial rate of gold dissolution (Li et al., 2012b) 33
Table 11: Summary showing the effect of thiocyanate concentration on gold and PGM recovery 33
Table 12: Effect of Fe (III) concentration on the initial rate of gold dissolution (Barbosa-Filho & Monhemius, 1994) 34
Table 13: Effect of Fe (III) concentration on the initial rate of gold dissolution (Li et al., 2012b). 35
Table 14: Summary showing the effect of Fe(III) concentration on gold and PGM recovery 35
Table 15: Effect of temperaure on the rate of gold dissolution at 0.10 M SCN, 0.055M Fe(III), and at pH. 1.5 (Barbosa-Filho & Monhemius, 1994) 36
Table 16: Apparent activation energies for gold dissolution at 0.055M Fe (III), pH. 1.5(Barbosa-Filho & Monhemius, 1994) 36
Table 17: Total BM and PGM analysis of Platreef concentrate 41
Table 18: Total BM and PGM analysis of Merensky concentrate 41
Table 19: Size distribution analysis 41
Table 20: Experimental plan used in determining the reaction order and activation energy in thiosulphate and cyanide reaction 45
Table 21: Experimental plan used in determining the reaction order and activation energy in polysulphide and cyanide reaction 46
Table 22: General outline of preliminary test work on Platreef concentrate 47
Table 23: Experimental design used during the leaching of pure minerals 48
Table 24: Cyanide-thiocyanate leach for Merensky ore 49
Table 25: Reaction rate equation for thiosulphate and polysulphide in cyanide systems 55
Table 26: Activation energy equation for thiosulphate and polysulphide in cyanide systems 56
Table 27: Kinetic coefficients for thiosulphate-cyanide and polysulphide-cyanide systems 56
Table 28: Oxidation states of elements in thiocyanate related compounds 57
Table 29: Initial rate of Pt leaching in thiocyanate and cyanide solutions for cooperite, sperrylite and Pt sponge under different conditions 68
Table 30: Initial rates and k_{app} for cooperite 70
Table 31: Chemical reactions involving cooperite in acid systems 71
Table 32: Initial rates and k_{app} for sperrylite 71

Table 33: Chemical reactions involving sperrylite in alkaline cyanide systems 72
Table 34: Pt dissolution rates and apparent activation energies observed at varied temperature and SCN^-, CN^- concentrations 74
Table 35: Chemical reactions involving cooperite and sperrylite in alkaline mixed system (SCN^- /CN^-/$[Fe(CN)_6]^{3-}$) 74
Table 36: Initial rates and k_{app} for the bioleach process 76
Table 37: Initial rates and k_{app} for Pt in mixed systems 77
Table 38: Initial rates and k_{app} for Pd in mixed systems 77
Table 39: Homogenous and heterogeneous, Pt and Pd complexes, adapted from Kabesova & Gazo (1980) 78
Table 40: Thiosulphate raw data at varied concentration 87
Table 41: Thiosulphate raw data at varied temperatures 87
Table 42: Polysulphide raw data at varied concentration 87
Table 43: Polysulphide raw data at varied temperatures 88

1. Introduction

1.1 Background to study

More than 75% of the world's platinum and 35% of palladium are produced in South Africa, originating from the Bushveld Igneous Complex. The primary platinum ores mined include the Merensky reef, UG2 reef and Platreef (Mpinga et al., 2014). Presently PGMs (Platinum Group Metals) are recognised for being a high value precious metal as well as having major industrial uses (Rao & Reddi, 2000).

The traditional route utilised for the recovery of PGMs in South Africa encompasses the concentration of ore by flotation, followed by smelting to produce a PGM rich matte, which is then digested hydrometallurgically to solubilise base metals and PGMs. PGM dissolution is usually by aggressive aqua regia or chlorine/HCl systems; this is generally an aggressive process associated with high maintenance costs as well as environmental concerns (Mpinga et al., 2014). Furthermore, the lengthy concentration and smelting process are energy and capital intensive, adding substantially to the production cost of PGMs. This has led to a need to derive new methods of creating economical processes that extract metal. Many studies recently have focused on the extraction of PGMs from low-grade ore/concentrate by adopting purely hydrometallurgical routes.

A study conducted by Mwase et al. (2014) investigated the use of a low-cost hydrometallurgical method, which comprised of a thermophilic heap leach to extract base metals, followed by a cyanidation heap leach to extract PGMs in low grade ore. During the cyanidation process, cyanide reacts with several other scavenging constituents in the ore, namely sulfur species which progresses to thiocyanate. According to Mwase et al. (2014) 39% of the cyanide was consumed for a non-leaching purpose, as analysis of the cyanide leachate revealed high levels of thiocyanate. To date there has been a number of studies that explores the formation of thiocyanate with particular focus on the reaction between reduced sulphur species with cyanide (Luthy & Bruce, 1979) as well as the reactions between cyanide and pure sulphidic minerals (Wilmot, 1997) in support of the observations made by Mwase et al. (2014).

Another key observation made was the corresponding trends between high levels of thiocyanate formation and elevated levels of platinum extraction within the first 4 days (Mwase et al., 2014). Evidently this implied that the thiocyanate ligand could intervene with the leaching process, functioning as a lixiviant which may have contributed positively to PGM extraction. Recent work has shown pronounced recoveries during thiocyanate leaching of PGMs from virgin catalytic converters (Kriek, 2008), ranging from 80-90% Pt, 90-100% Pd and 29-32% Rh, respectively. However, further experimental work needs to be conducted on pure minerals to validate whether thiocyanate is responsible for increased extractions. Extensive research has been carried out on thiocyanate dissolution of gold and will thus serve as a reference, as the chemistry of PGMs closely mirrors that of gold. Previous researchers (Broadhurst, 1987; Kholmogorov et al., 2000; Li et al., 2012b) have

investigated the speciation and kinetics of gold leaching in thiocyanate solutions. A study by Li et al. (2012a) assesses the chemistry and thermodynamics involved in metal-thiocyanate systems, with particular focus on the E_h/pH diagrams for the SCN–H_2O, Au–SCN–H_2O, Cu–SCN–H_2O, and Fe–SCN–H_2O systems. However, the majority of work done was on metallic gold with inadequate focus on PGMs associated with sulphidic minerals.

The increased inertness of PGMs dictates the conditions required for ligand substitution, which include high concentration reagents, high temperature and prolonged reaction times. This study looks at alternatives to aggressive chloride-based lixiviants; it focusses on acidic and alkaline thiocyanate systems, in the presence and absence of cyanide for Pt and Pd recovery from sulphide-bearing minerals. The overall objective of this thesis is to explore an alternate lixiviant to treat PGM bearing ores and concentrates directly to simplify the overall process, with the purpose of providing a route that is economical and environmentally friendly.

1.2 Problem statement

Reduced sulphur species, thiosulphate and polysulphide, are generated during bioleaching of sulphidic minerals. The degradation of acid insoluble metal sulphides, especially pyrite, gives rise to the formation of thiosulphate, while polysulphides are created through the degradation of acid soluble metal sulphides, specifically chalcopyrite and pyrrhotite. Therefore, the synthesis of thiocyanate is inevitable in a subsequent cyanidation process owing to the strong reactivities of cyanide with reduced sulphur species as well as direct interaction between minerals such as chalcopyrite, pyrrhotite and pyrite, commonly associated with precious metal ores (Mpinga et al., 2014).

The corresponding trends between high levels of thiocyanate formation and elevated levels of platinum extraction observed in the secondary cyanide leach following the bioleach of PGM materials (Mwase et al., 2014) generated an interest, as to whether thiocyanate may have possibly promoted PGM recovery. Moreover, thiocyanate readily forms complexes with Pt and Pd. This affinity is demonstrated by the increased stability relative to conventional chloride based reagents (Mountain & Wood, 1988). It is postulated that apart from cyanide acting as a lixiviant, the presence of thiocyanate improves the recovery of PGMs.

1.3 Objectives

Therefore the investigation herein intends to develop an improved understanding by addressing the following objectives:

- Investigate the kinetics of thiocyanate formation in a thiosulphate, sulphite and polysulphide system.
- Evaluate the effectiveness of thiocyanate leaching of Pt and Pd under varied conditions.

- Determine the degree of base metal influence on thiocyanate consumption and hence propose a suitable pre-treatment method.
- Establish whether thiocyanate and cyanide act synergistically to promote the dissolution of Pt and Pd.

The experimental procedure undertaken to fulfil the study's objectives included a chemical kinetic study on thiocyanate formation explored in homogenous systems, thiosulphate, sulphite and polysulphides in the presence of cyanide. In addition, thiocyanate leach studies were conducted on pure minerals, in batch stirred tank reactors and in low grade concentrate, in column reactors do develop an improved understanding of the leaching behaviour.

2. Literature review

The purpose of this chapter is to lay the foundation for the research work in this thesis, with particular focus on the significance of this study in an industrial context, as well as to identify gaps in literature where a contribution can be made. This chapter presents a review on the current smelt-refine route used for PGM recovery and the limitations associated with it. It discusses a low-cost hydrometallurgical process proposed for treating low-grade concentrate and highlights the key findings. Lastly, it presents an in-depth discussion on the use of thiocyanate as an alternate lixiviant in PGM extraction with respect to the chemistry involved during formation, complexation and leaching.

2.1 Introduction to PGMs

The Platinum Group Metals (PGMs) consist of platinum (Pt), palladium (Pd), rhodium (Rh), ruthenium (Ru), iridium (Ir), and osmium (Os). The above mentioned metals have similar geochemical characteristics and are often concentrated together geologically (Jones, 2005). PGMs are categorised as noble metals owing to them being chemically inert to various substances as well as their high resistance to oxidation and corrosion.

Platinum and palladium are widely used commercially, and rhodium to a lesser extent. However, ruthenium, iridium and osmium are used in limited speciality applications. PGMs are valuable commodities that have important applications such as industrial catalysts and autocatalytic converters. The aesthetic quality of platinum makes it ideal for the production of jewellery and further serves as an investment (Rao & Reddi, 2000).

Approximately 75% of the world's platinum production and 35% of the world's palladium production originates from the Bushveld Igneous Complex in South Africa. The leading PGM reefs mined include the Merensky, Upper Group Two (UG2) and Platreef (Mpinga et al., 2014). These three layers are differentiated by their distinct mineralogical characteristics. The Merensky reef has PGMs associated with base metal sulphides whereas Platreef has an increased base metal sulphides and palladium quantity. In addition, the UG2 chromitite layer possesses a rich chromite layer in conjunction with low quantities of base metal sulphides (Jones, 1999). The three layers are discussed in detail below.

Merensky

The Merensky reef is usually considered as a uniform reef type despite the fact that there are substantial variations that occur within the reef (Schouwstra & Kinloch, 2000). The Merensky zone is also referred to as the pegmatoid zone, which contains base metal sulphide grains and associated platinum group metals. It is located for 300 km surrounding the outcrop of the eastern and western limbs of the Bushveld complex, at depths of up to 5km (Schouwstra & Kinloch, 2000).

Ore obtained from the Merensky reef incorporates up to 3% base metal sulphides which further comprises of 40% pyrrhotite, 30% pentlandite, 15% chalcopyrite and 2-4% pyrite and trace amounts of troilite, millerite and cubanite. PGMs occur in the form of minerals

such as cooperite, braggite, laurite and ferroplatinum as well as in conjunction with base-metal sulphides. Merensky Reef consists primarily of orthopyroxene (≈60%), plagioclase feldspar (≈20%), pyroxene (≈15%) and phlogopite (≈5%) (Schouwstra & Kinloch, 2000).

UG2

The UG-2 Reef is a chromitite layer which is generally located 20 to 400m below the Merensky reef, depending on the location within the complex. The chromitite layer can vary between 0.4 to up to 2.5m but is normally 1m thick. The UG2 body is made of 60-90% chromite (by volume) with lesser silicate minerals, approximately 5-30% pyroxene and 1-10% plagioclase. Additional minerals present in lower concentration include silicates (phlogopite and biotite), oxides (ilmenite, rutile and magnetite) as well as base metal sulphides (Schouwstra & Kinloch, 2000). The total PGM content is expected to be within the average range of 4 and 7 g/ton. The typical base metal content comprises of 200-300 ppm Ni as nickel sulphide and 200ppm Cu occurring as copper iron sulphide. The UG2 ore is usually categorised by the abundant occurrence of PGM sulphides, such as laurite, cooperite and braggite (Schouwstra & Kinloch, 2000).

Platreef

Platreef is a layer of ultramafic rock located along the Northern limb of the Bushveld complex. The Platreef zone consists of pyrroxenites, serpentinites and calc-silicates. The distribution as well as the content of base metals and PGMs is highly irregular in the Platreef zone. The base metals associated with the Platreef zone include pyrrhotite, pentlandite, chalcopyrite and pyrite. The predominant class of PGMs is in the form of Pt-Pd tellurides. Even though PGM minerals normally occur in or on grain boundaries of base metal sulphides a large amount of PGM minerals associated with silicate minerals is observed in this region. The Platreef grains are normally coarser than those that occur in the Merensky and UG2 ore. Additionally, minerals such as arsenide and tellurides are often encapsulated in the silicate gangue.

Table 1: A summary of the bulk minerology of Merensky reef, UG2 reef and Platreef that occur in the Bushveld igneous complex (Shamaila & Connor, 2008).

	Merensky	Platreef	UG2
Bulk minerology	Pyroxene Feldspar Plagioclase Base metal sulphides	Pyroxene Serpentine Calc silicates Plagioclase Base metal sulphides	Chromite Pyroxene Feldspar Plagioclase Base metal sulphides
PGM distribution	Tellurides ~ 30% Arsenides ~ 7% Alloys ~ 7% Sulphides ~ 36% Rest ~ 20%	Tellurides ~ 30% Arsenides ~ 21% Alloys ~ 26% Sulphides ~ 3% Rest ~ 20%	Tellurides < 5% Arsenides < 5% Alloys ~ 20% Sulphides ~ 70% Rest < 5%

The Merensky and UG2 reefs are thin natured (~ 1m) and for this reason require narrow mining techniques. Whereas, Platreef is substantially thicker (~ 4m) and mined by open pit methods a result of the shallow reef depth (Glaister & Mudd, 2010).

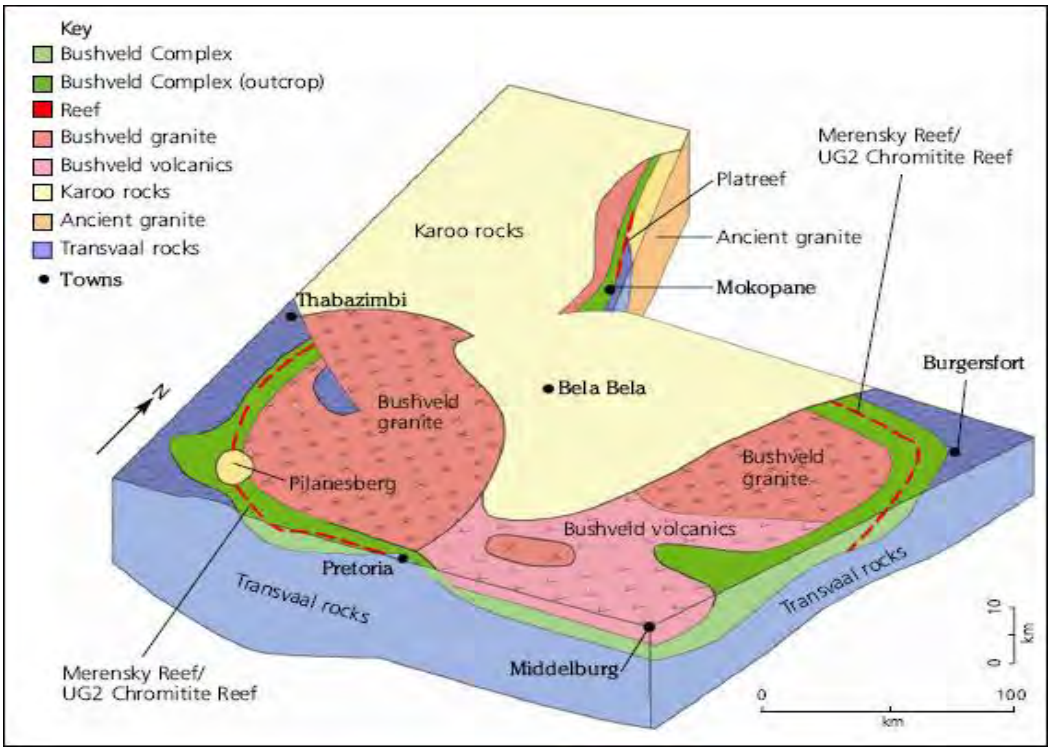

Figure 1: Schematic of the Bushveld complex showing the location and depth of the Merensky, UG 2 and Platreef ore (Cawthorn, 2010).

2.2 Conventional matte-melting process

The extractive metallurgy of platinum-group metals is a relatively complex process. With each processing stage designed to further increase the concentration of the precious metal within the ore. In the first stage the mined ore undergoes comminution, where the ore particle size is reduced through multistage crushing and ball milling (Mpinga et al., 2015). This is followed by the flotation stage, where sulphide ores associated with PGMs, are concentrated through a separation technique based on exploiting the difference in surface properties of the material to separate them. Flotation of chromite enriched ores is typically carried out in mill-float-mill-float (MF2) open circuit thus preventing the build-up of chromite fines produced during overgrinding in recirculating loads. Subsequently the flotation concentrates are subjected to smelting and converting, to create a PGM-containing nickel-copper matte.

The concentrate is smelted in electric furnaces at elevated temperatures necessary to melt chromite concentrate. Usually these furnaces operate at 1350^{o}C and approximately 1600^{o}C for UG2 ores. It is essential for the concentrate to be an appropriate composition for it to produce a fluid slag at the desired temperature. During smelting the concentrate is separated into two layers, a lighter silicate/oxide iron rich slag on the top and the iron sulphide-rich green matte at the bottom. The silicate/oxide iron is discarded, whereas the iron sulphide-rich green matte is transferred to the converter, where predominantly Fe is removed as oxide into the slag phase (Crundwell et al., 2011).

The converter matte is granulated or slow cooled and milled before further processing (Jones, 2005). During slow cooling, PGMs accumulate in the alloy phase which is then isolated from the BMs through magnetic separation. The non-magnetic fraction is transferred to the base-metal refinery to extract Cu, Ni and Co while the magnetic phase is transferred to the precious metals refinery to separate PGMs. This slow cooling process is specific to Anglo American while other refineries utilise the whole-matte leaching process. In the whole-matte leaching process, the converter matte is treated hydrometallurgically to isolate base metals, Cu, Ni, Fe and Co in order to produce a slime comprising 30-50% precious metals which is then transferred to the precious metals refinery (Crundwell et al., 2011).

The PGM refinery step comprises of three separation stages which include, the primary separation where PGMs are isolated from impurities followed by secondary purification to produce a metal salt and lastly reduction, resulting in a saleable metal. Different technologies are used to separate the saleable components. In modern refineries, PGMs are leached in hydrochloric acid using chlorine gas to generate a leach solution of precious metals, Pt, Pd, Rh and Au (Crundwell et al., 2011; Jones, 2005). During the refining stage (primary separation and purification stage), the differences in solubilities of PGM chloro complexes are exploited.

The concentration of PGMs recovered increases through each stage of processing. Initially, the starting ore comprises of 3-5g/t PGMs. This is upgraded to 150-250g/t during the concentration stage, and further increased to 1000-2000 g/t in the matte as a result of smelting. The refinery residue contains 50-70% precious metals giving an overall recovery from feed ore of approximately 80%.

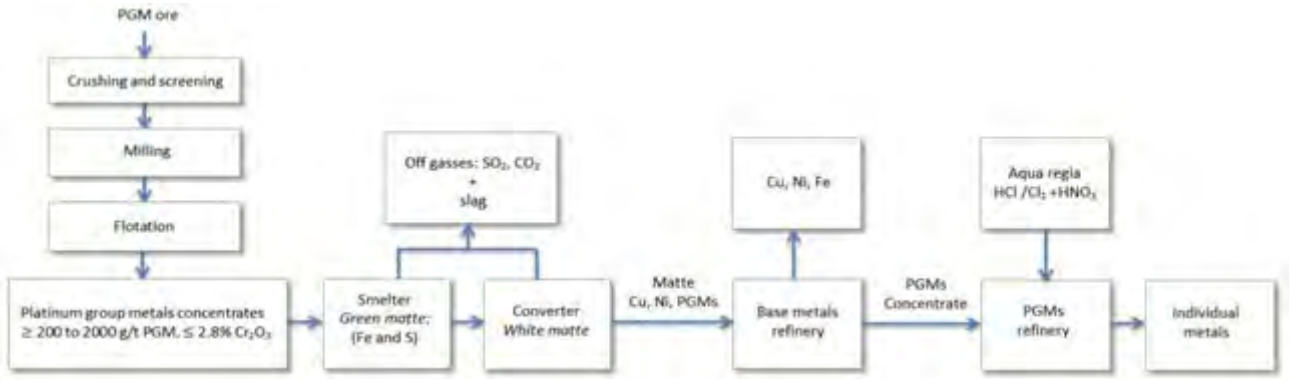

Figure 2: Conventional method of extracting PGMs (Mpinga et al., 2015)

2.2.1 Refining of Platinum Group Metals

The PGM refinery stage is a significantly important step in PGM processing, to obtain precious metals of high purity (>99.9% purity). The successful operation of the PGM refineries is crucially dependant on Pt and Pd separation. This can be achieved through different processing routes namely, dissolution, precipitation, hydrolysis, distillation, solvent extraction, ion exchange and metal reduction which are currently used in the mining sector. The precipitation process specifically used by Lonmin and the solvent extraction process used by Anglo American are described in this section.

Lonmin

Lonmin exploits the precipitation technique to refine PGMs. Feed containing 65-70% PGMs is dissolved in HCl (6M) at 65^{o}C for approximately 6 hours in the presence of chlorine gas. This is followed by Au precipitation by hydrazine (N_2H_4) reduction. The pH is then raised to 1 to precipitate the remaining base metals. Upon removal of precipitates the filtrate is transferred to a distillation step where ruthenium and osmium are oxidised with $NaClO_3$ to ruthenium tetroxide (RuO_4) and osmium tetroxide (OsO_4), respectively. These volatile compounds are then drawn through scrubbing columns where they are reduced by reaction with HCl. This is followed by the hydrolysis of rhodium and iridium, achieved by increasing the pH of the remaining solution to 5 which precipitate as $Rh(OH)_4$ and $Ir(OH)_4$ (Crundwell et al., 2011).

The solution is acidified with HCl and the redox potential altered to 900-1000mV with hydrogen peroxide. Platinum is then precipitated by the addition of ammonia chloride which gives rise to an ammonia hexachloroplatinate [$(NH_4)_2PtCl_6$] complex otherwise known as yellow salt. Ammonia acetate is added and the solution is boiled to increase the pH to 4.2. Upon cooling palladium precipitates as diamino-palladous dichloride, $(NH_3)_2PdCl_2$

which is filtered to obtain the precipitate. These primary separation steps described results in impure metals or metal salts which is subjected to further purification steps to obtain saleable products (Crundwell et al., 2011).

Anglo American

Alternately, Anglo American utilises solvent extraction to achieve PGM separation. Similarly, concentrate feed, containing between 50-60% PGMs is dissolved in HCl using chlorine gas at 120^{o}C and at 4bar pressure. In this high intensity dissolution step, both PGMs and BMs are dissolved while osmium is oxidised to OsO_4 and recovered as K_2OsO_4 using KOH. The next step involves gold removal, which is separated from the filtrate through solvent extraction using methyl isobutylketone (MIBK) under highly acidic conditions and reduced using oxalic acid. Palladium is then removed from the gold raffinate (aqueous solution from extraction stage) by solvent extraction with ketoxime and β-hydroxyoxime and then stripped from the loaded solvent with HCl (6M). This is followed by palladium precipitation from solution with ammonium hydroxide to form diamino-palladous dichloride, $(NH_3)_2PdCl_2$ (Crundwell et al., 2011).

Similarly, platinum is removed from palladium raffinate using secondary amines and is stripped with 11M HCl. Platinum is further precipitated with NH_4Cl to form hexachloroplatinate, $(NH_4)_2PtCl_6$. Both $(NH_3)_2PdCl_2$ and $(NH_4)_2PtCl_6$ complexes are reduced to metals using hydrazine. Subsequently ruthenium is oxidised to volatile RuO_4 using $NaClO_3$ and precipitated as $(NH_4)_2RuCl_6$ from solution using HCl. Iridium is then separated by solvent extraction using *n*-iso-tridecyltri-decanamide and stripped using HCl followed by precipitation with NH_4Cl to generate an $(NH_4)_2IrCl_6$ complex. Both $(NH_4)_2RuCl_6$ and $(NH_4)_2IrCl_6$ are further reduced to metal using cracked ammonia. Lastly rhodium is extracted from iridium raffinate using diethylene tri-ammine and precipitates to form $[RhCl(NH_3)_5]Cl_2$ which is reduced to rhodium sponge (Crundwell et al., 2011).

Table 2: Methods of extraction used in PGMs refinery (Crundwell et al., 2011)

Metal	Lonmin	Anglo American
Gold extraction	Au precipitation by hydrazine (N_2H_4) reduction	Solvent extraction with methyl isobutylketone (MIBK) followed by reduction with oxalic acid
Palladium extraction	Precipitation with ammonium acetate ($NH_4CO_3CO_2$)	Solvent extraction with β-hydroxyl oxime and then stripped ammonium hydroxide (NH_4OH)
Platinum extraction	Precipitation with ammonium chloride (NH_4Cl) to form ammonia hexachloroplatinate [$(NH_4)_2PtCl_6$]	Solvent extraction with tertiary amine, tri-*n*-octylamine stripped with HCl and precipitated with ammonium chloride (NH_4Cl)
Ruthenium extraction	Distillation with sodium chlorate ($NaClO_3$) and bromate ($NaBrO_3$)	Distillation with sodium chlorate ($NaClO_3$ and bromate ($NaBrO_3$)
Iridium extraction	Precipitation with ammonium chloride (NH_4Cl)	Solvent extraction with secondary ammine organic, *n*-iso-tridecyltri-decanamide
Rhodium extraction	Precipitation as $Rh(NH_3)_5Cl_3$ followed by purification with ammonium chloride (NH_4Cl)	Ion-exchange followed by precipitation with diethylene tri-ammine

2.2.2 Limitations of the conventional smelt-refine route

The traditional matte-smelting-refining technique is used to recover platinum groups from high-grade concentrate (150-250 g/t PGM containing 0.4–2.8% Cr_2O_3). However, high-grade precious metal reserves have been depleted and the remaining reserves comprise mainly of low-grade ores associated with either high chromite grades (in the case of UG2) or high pyrrhotite content (in the case of Platreef). These particular properties invariably lead to high smelting costs (low-grade) and smelter integrity risks (due to the chromite). Consequently, the increased mineralogical complexity of lower grade PGM ores, high capital investment and stringent environmental regulations has restrained the implementation of smelter based processes on low grade ore (Mpinga et al., 2015).

There are several limitations associated with the conventional smelt-refine route. This process route imposes harsh environmental conditions releasing approximately 162kg CO_2 equivalence and 0.47kg SO_2 as well as consuming 693m^3 of water per metric tonne of ore milled (Anglo American, 2014). In addition, the milling, grinding and smelting stage is severely energy intensive. Anglo American Platinum has reported that their energy consumption for 2014 amounted to R4688 million, approximately 86% of the utility cost, representing 11% of the operational cost (Anglo American, 2014). The electricity costs have increased by 26% in the mining sector, from 2007 to 2012 and are predicted to further increase by an additional 12% by 2018 (Nair et al., 2014). A further problem posed is the energy crisis that South Africa is currently experiencing with electricity supply interruptions and increased price leading to loss of production. While ESKOM needs to implement new strategies to avoid future supply interruptions, likewise mines need to minimise their energy usage through improved process design.

An ongoing environmental concern is the SO_2 gas emissions generated during the converting process. In order to satisfy the SO_2 dispersion criteria in certain parts of the world, the smelters are shut down during specific climatic phases (temperature fluctuations and low wind velocities). Inoperative converters results in a time and money loss. Additionally, during the processing of ores containing low sulphide contents, base metal concentrates are added to produce a matte to allow for collection of valuable metals which further adds to the cost (Ferron et al., 2006).

Since South Africa is home to the world's largest known deposits of platinum, it is in a unique position to benefit from the expansion of new mining projects and secondly, to lead initiatives in novel methods in extracting platinum. Hence, many studies recently have focused on the extraction of precious metals from low-grade ore/concentrates driven by the industrial need for these metals and their limited sources (Rao & Reddi, 2000). This has led Mwase et al. (2014) to develop and patent a novel integrated hydrometallurgical method, suitable to treat low-grade PGM sulphide concentrates known as the sequential leach.

This low-cost hydrometallurgical process has been proposed for treating low-grade Platreef concentrate (Mwase et al., 2012) and whole ore (Mwase et al., 2014). It comprised of a heap bioleach process to initially extract base metals, followed by caustic rinse of the residue material and lastly a heap cyanidation process to extract PGMs. The findings obtained from the sequential heap leach forms the basis of the present study, which are highlighted in the following section.

2.3 Sequential heap leach process

The sequential heap leach process developed by Mwase et al. (2014) intended to eliminate costs associated with flotation, smelting and the pressure leach stage, by directly leaching crushed whole ore. Two samples of drill core Platreef ore were studied comprising of different size distributions, -25 +1mm (column 1) and -6+1mm (column 2), respectively. The samples were subjected to an acidic bioleach at 65^{o}C followed by an alkaline cyanide leach at 50^{o}C in cylindrical columns to simulate heap leaching.

Figure 3: Sequential heap leach, (Mwase et al., 2014)

2.3.1 Bioleach

There are several hydrometallurgical methods utilised in base metal extraction, one of them being bioleaching. Bioleaching is a hydrometallurgical process whereby metals encapsulated in mineral sulphides are liberated through microbially mediated oxidation. This process mechanism involves the oxidation of reduced sulphur species to sulphate and ferrous to ferric by microorganisms. In bioleaching, mesophilic microorganisms such as *Acidithiobacillus ferrooxidans*, *Acidihiobacillus thiooxidans* and *Leptospirillum ferroxidans* are employed at 40-45^{o}C at pH 1.8. However, at increased temperatures thermophiles are used. This method has been established as an environmentally friendly alternative and proven to show favourable base metal recoveries (Ngoma, 2015).

Leaching mechanism

Earlier work (Archer, 1997) suggested that bioleaching of sulphide minerals were catalysed by microorganisms through a direct or indirect leaching mechanism, however this topic has been under much contention. More recent work by Tributsch (2001) has challenged the direct leaching mechanism with observations made by electron microscopy images, which show that bacteria does not directly attach to the surface of particles but instead interacts with a extracellular polymeric substances (EPS) layer to dissolve the particle.

In the indirect leaching mechanism, ferric ion functions as an oxidant during mineral sulphide oxidation. Ferrous sulphate is generated through mineral oxidation which advances to ferric sulphate by iron oxidising biocatalysts. Subsequently, the ferric iron oxidises the mineral sulphides to corresponding sulphides and elemental sulphur, in the process liberating the metal of interest (Ngoma, 2015).

The bacterial oxidation of metal sulphides proceed via two oxidation pathways, namely the thiosulphate or polysulphide mechanism. The particular mechanism followed is largely dependent on the mineralogy and acid solubility of metal sulphides and therefore influences the intermediate sulphur compounds formed during leaching. These pathways have been identified in mesophilic bacteria, *Acidithiobacillus ferrooxidans*, *AcidiThiobacillus thiooxidans*, and *Leptospirillum ferrooxidans* (Schippers & Sand, 1999; Schippers et al., 1996; Sand et al., 2001; Vera et al., 2013). It is assumed that similar pathways exist in thermophilic bacterial leaching of metal sulphides.

Pyrite (FeS_2) and other acid non soluble metal sulphides are associated with the thiosulphate pathway. The degradation of pyrite, FeS_2 involves an iron (III) ion-mediated leaching mechanism. The Fe-S_2 bond is cleaved after the S_2 group has been oxidised by iron (III) hexahydrate ions to thiosulphate, as shown in Figure 4a. Subsequently, thiosulphate is successively oxidised via tetrathionate, disulfane-monosulfonic acid and trithionate to sulfate (Schippers & Sand, 1999; Schippers et al., 1996; Sand et al., 2001).

In contrast to the thiosulphate pathway, the polysulphide pathway is associated with acid soluble metal sulphides such as chalcopyrite and pyrrhotite (Schippers & Sand, 1999; Schippers et al., 1996; Sand et al., 2001; Vera et al., 2013). In the polysulphide mechanism, metal sulphides are oxidised to elemental sulphur. The mechanism involves an iron (III) attack followed by the formation of polysulphide intermediates which progresses to elemental sulphur. Even though sulphur is reasonably stable, in the presence of sulphur-oxidising bacteria it is oxidised to sulphuric acid as indicated in Figure 4b.

a.

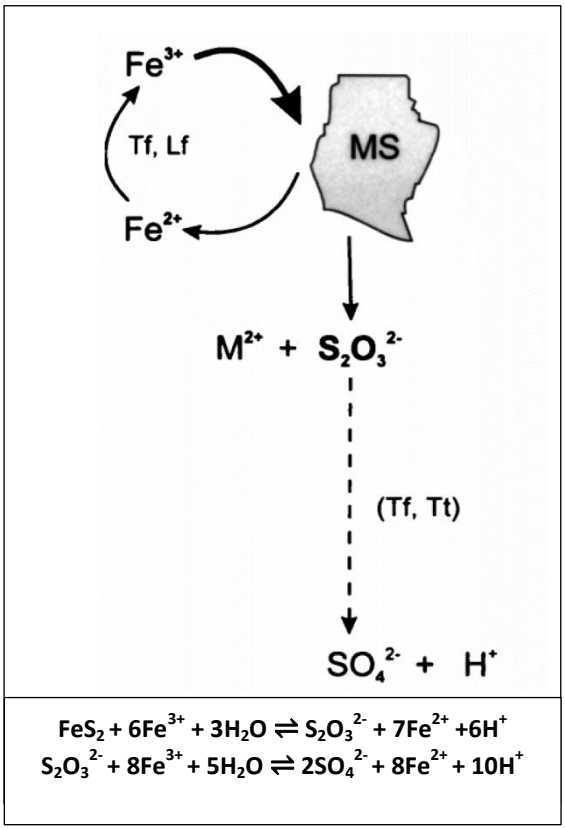

$FeS_2 + 6Fe^{3+} + 3H_2O \rightleftharpoons S_2O_3^{2-} + 7Fe^{2+} + 6H^+$

$S_2O_3^{2-} + 8Fe^{3+} + 5H_2O \rightleftharpoons 2SO_4^{2-} + 8Fe^{2+} + 10H^+$

b.

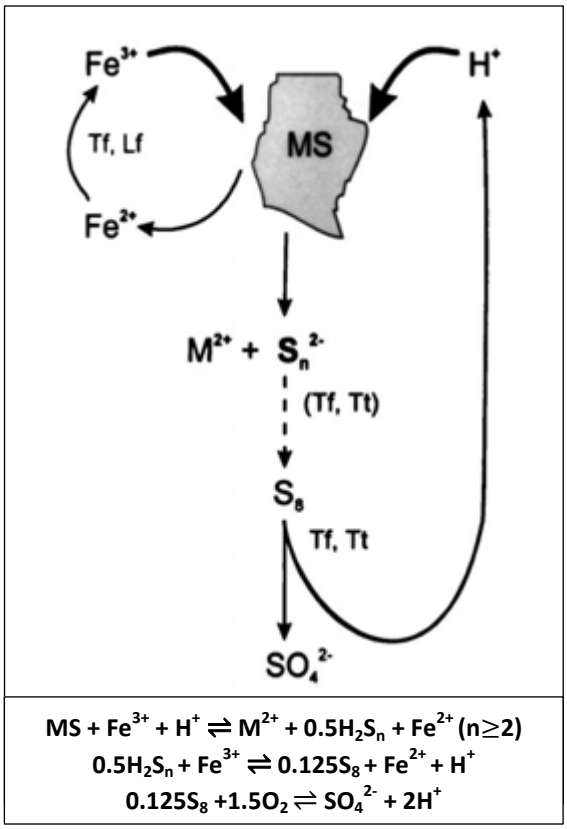

$MS + Fe^{3+} + H^+ \rightleftharpoons M^{2+} + 0.5H_2S_n + Fe^{2+}\ (n \geq 2)$

$0.5H_2S_n + Fe^{3+} \rightleftharpoons 0.125S_8 + Fe^{2+} + H^+$

$0.125S_8 + 1.5O_2 \rightleftharpoons SO_4^{2-} + 2H^+$

Figure 4: (a) Thiosulphate pathway and (b) polysulphide pathway (Schippers & Sand 1999; Schippers et al. 1996).

The dominance of BM as sulphide minerals in the PGM ore necessitates the need for a bioleach step. The bioleach carried out in the sequential heap leach by Mwase et al. (2014) utilised a pure culture of *Metallosphaera hakonensis*, a thermophile archeon known to be efficient at oxidising both iron and sulphur at high temperatures. Similarly, thermophiles are effective in the dissolution of Cu in chalcopyrite (main copper bearing mineral) in PGM ores, which does not respond to mesophilic bacteria; thus they were selected for their specific capabilities (Rawlings & Johnson, 2007).

The pre-treatment enables exposure of precious metals for extraction and limits reagent consumption during the subsequent cyanide leach (Mpinga et al., 2015). The possibility of employing a single cyanide leach step to recover both BM and PGMs exists, although it is not entirely feasible as reclamation of base metals from cyanide solution is not completely established. Furthermore, the removal of base metal sulphides prevents the formation of potential cyanicides (van der Merwe, 2012), which can be harmful if released into the environment.

2.3.2 Cyanide leach

For more than a century, cyanidation has been used for the recovery of gold from mineral resources. It has proven to be an effective and economical alternative for successful gold recovery (Habashi, 1999) and was thus selected for PGM leaching. Cyanide has a strong affinity for metals making it an ideal leaching reagent. It is capable of complexing with virtually any heavy metal at low concentrations (Young & Jordan, 2001). Platinum (II) and palladium (II) form relatively stable complexes with cyanide, specifically $[Pt(CN)_4]^{2-}$ and $[Pd(CN)_4]^{2-}$ (Kabesova & Gazo, 1980). This is indicated by the relatively high stability constants, 41 and 63 (Table 3) for Pt^{2+} and Pd^{2+} respectively.

The cumulative stability constants for the metal complex with cyanide are reported as β_n which is defined by complexation equation 1.

$$M^{m+} + nL^{-} \rightleftharpoons [M(L)]_n^{m-n} \qquad K = \frac{[M(L)_n^{m-n}]}{[M^{m+}][L^{-}]^{n}} \qquad \textbf{Equation 1}$$

$$\beta_n = K_1 \times K_2 \times K_3 \ldots\ldots K_n$$

Where M is the metal, L is the ligand, K is the formation constant and β_n is the cumulative stability constant.

Table 3: Overall stability constants of selected metal-cyano complexes

Metal ion	Cyanide complex	log β_n	Reference
Cu^{+}	$Cu(CN)_4^{3-}$	30.30	(Smith & Martell, 1976)
Ni^{2+}	$Ni(CN)_4^{2-}$	30.22	(Smith & Martell, 1976)
Fe^{2+}	$Fe(CN)_6^{4-}$	35.4	(Smith & Martell, 1976)
Fe^{3+}	$Fe(CN)_6^{3-}$	43.6	(Smith & Martell, 1976)
Au^{+}	$Au(CN)_2^{-}$	38.3	(Senyaka, 2004)
Au^{3+}	$Au(CN)_4^{-}$	85	(Senyaka, 2004)
Pt^{2+}	$Pt(CN)_4^{2-}$	41	(Muir & Ariti, 1991)
Pd^{2+}	$Pd(CN)_4^{2-}$	63	(Mountain and Wood, 1988)

PGM cyanidation occurs in a similar manner to gold, relating to similar chemical reactions. In the cyanide leach stage PGMs are solubilised as precious metal-cyanide complexes. The reactions that occur are known as the Elsener equations (Chen and Huang, 2006), which are listed in Table 4. The proposed chemical structures for platinum, $[Pt(CN)_4]^2$ and palladium, are square planar, $[Pd(CN)_4]^2$ whereas ruthenium is an octahedral complex, $[Ru(CN)_6]^{3-}$.

Table 4: PGM complexes formed during cyanidation process (Chen and Huang, 2006).

Platinum	$2Pt(s) + 8NaCN(aq) + O_2(g) + 2H_20(l) \rightleftharpoons 2Na_2[Pt(CN)_4](aq) + 4NaOH(aq)$
Palladium	$2Pd(s) + 8NaCN(aq) + O_2(g) + 2H_20(l) \rightleftharpoons 2Na_2[Pd(CN)_4](aq) + 4NaOH(aq)$
Ruthenium	$4Rh(s) + 24NaCN(aq) + 3O_2(g) + 6H_20(l) \rightleftharpoons 4Na_3[Rh(CN)_6](aq) + 12NaOH(aq)$

Cyanidation of PGMs conducted at room temperature has shown poor levels of recovery, averaging to 15% for Pt and 44% for Pd (Green et al., 2004). However, the study by Mwase et al. (2014) indicates that at increased operating temperature of 50^{o}C during the cyanidation stage, the rate of PGM dissolution substantially increases. In addition, cyanide is not selective towards PGMs, thus they require a pre-treatment to avoid complexation with BMs.

A further problem associated with this method is that the residual solids from the bioleach oxidative pre-treatment generally contain residual acid, whereas the cyanide leach process should be carried out at a pH of 9.31 and higher. At an optimum pH of 10.3, cyanide is still in the ionic form and prevents the formation of HCN, an extremely toxic gas. Therefore a caustic rinse of residual solids is required before entering the cyanidation step.

2.3.3 Findings

According to the findings obtained by Mwase et al. (2014), the bioleach conducted at 65°C achieved the best results for the -6+1mm Platreef ore sample compared to the -25+1mm sample. After 304 days, 93% Cu, 75% Ni and 53% Co were extracted. Subsequently, the cyanide leach conducted at 50°C achieved overall extraction of 57.8% Pt, 99.7% Pd and 90.3% Au after 60 days.

Even though the study showed promising results, two factors prevented further commercialisation of this process: a slow rate of platinum extraction and high cyanide consumption levels leading to thiocyanate formation.

The results obtained revealed that during the first 12 days, cyanide consumption was significant (Figure 5), which was accompanied by high levels of thiocyanate formation as seen in Figure 6. It is suspected that the incomplete sulfur oxidation in the bioleach stage led to the preferential reaction of reduced sulphur species with cyanide that formed thiocyanate. Furthermore, within this period the concentration of platinum extracted was at its highest, 340 µg/L in column 1 and 490 µg/L in column 2 over the first 4 days, as shown in Table 5. After 4 days platinum was the only metal being extracted, and leached at a much slower rate (Mwase et al., 2014).

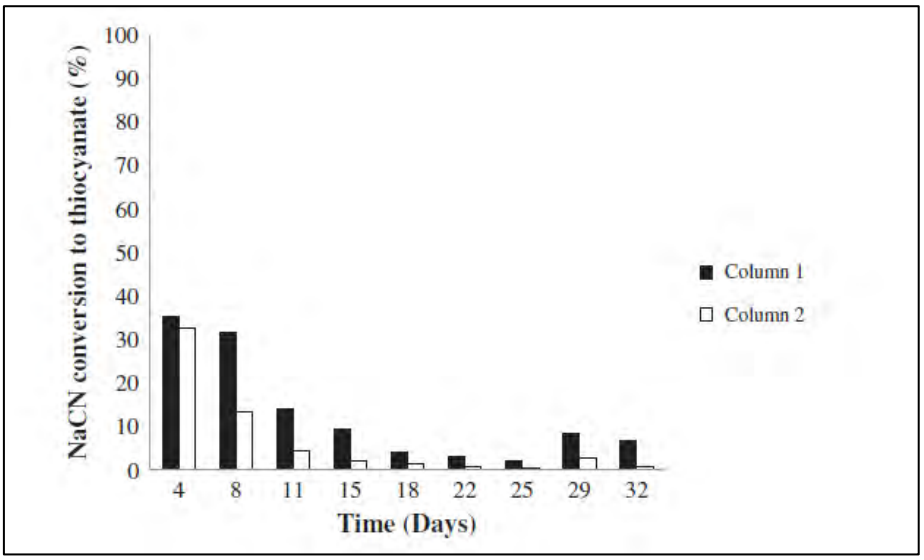

Figure 5: Percentage conversion of NaCN to thiocyanate. Column 1: -25+1mm, Column 2: -6+1mm: both columns leached at 5 L/m^2 with 5 g/L NaCN solution; aeration rate: 130 mL/min (Mwase et al., 2014).

Table 5: Concentration of Pt in solution (Mwase et al., 2014)

	4 days (µg/L)	Next 28 days (µg/L)	Last 28 days (µg/L)
Column 1 (-25 mm)	340	60	5-10
Column 2 (-6 mm)	490	60	5-10

The corresponding trends, observed between high levels of thiocyanate formation and elevated levels of platinum extraction within the first 4 days, implied that thiocyanate may have contributed positively to PGM extraction. However, this remained speculative, as to the author's knowledge thiocyanate leaching of PGMs has only been mentioned in one study by Kriek (2008) and thus further experimental work needs to be conducted to validate this theory. Also, the elevated level of thiocyanate conversion was an undesired side reaction and raised much concern in terms of cyanide consumption. The synthesis of thiocyanate is explored in the following section.

2.3.4 Thiocyanate conversion

The formation of thiocyanate during cyanide leaching is suggested to be the product of reaction between cyanide and reduced sulphur species (Botz, 2001). QEMSAN analysis of the bioleached residues leach confirmed the presence of sulphide minerals, pentlandite, pyrrhotite, chalcopyrite, pyrite and molybdenite (Mwase et al., 2014). LECO combustion analysis of bioleached residual ore showed minor traces of sulphide minerals and the absence of elemental sulfur. Furthermore, the results indicated that only 75% of the original total sulfur in the ore was oxidised in the bioleach process. During the bioleach sulphur species are generally oxidised to sulphate and sulphuric acid by the catalytic action of bacteria. It has been suggested by Mwase et al. (2014) that inconsistency in the sulfur content in bioleaching residue is due to incomplete biooxidation of sulphur in the bioleach stage.

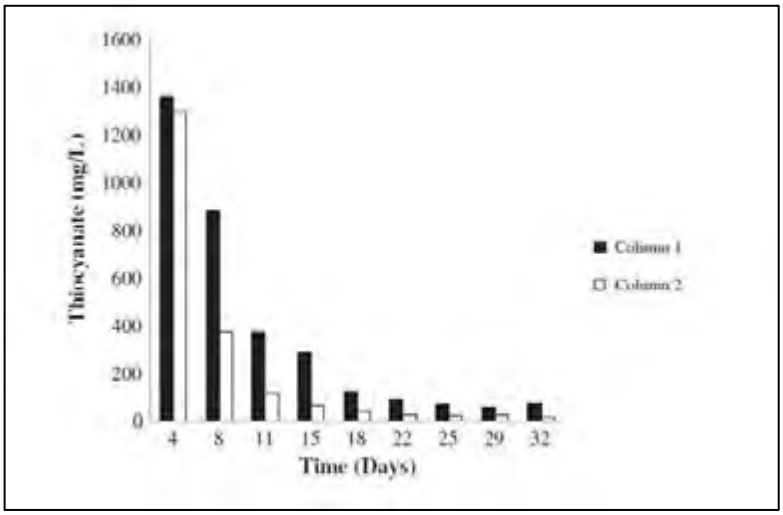

Figure 6: Thiocyanate in cyanide effluent solution. Column 1: -25+1mm, Column 2: -6+1mm: both columns leached at 5 L/m^2 with 5 g/L NaCN solution; aeration rate: 130 mL/min (Mwase et al., 2014).

Mwase et al. (2014) postulated that the reduced sulphur compounds liberated were presumably polysulphides, thiosulphates or polythionates. A paper by Luthy & Bruce (1979) highlights the potential reactions responsible for the synthesis of thiocyanate which are summarised in Section 2.4.2. Polysulphides are formed through successive combinations of neutral sulphur atoms with sulphide, whereas polythionates are produced by mixtures of thiosulphates (Koh, 1990). Although thermophiles were used in the course of the bioleach

step, the sulphur pathways followed and sulphur intermediates generated were expected to be similar to those known for mesophilic pathways, (Section 2.3.1).

Mwase et al. (2014) put forward the idea that the reduced sulphur species generated in the bioleach may have crystallised into precipitates or most probably co-precipitated onto jarosites which were later transferred to the cyanide leach (Mwase et al., 2014). These intermediate compounds are extremely reactive with cyanide (Luthy & Bruce, 1979), but were not detected by the mineral liberation analyser (MLA analysis). Even though polysulphides and polythionates were not detected, it is suspected that incomplete bio-oxidation of these species are responsible for increased levels of thiocyanate in the effluent (Mwase et al., 2014).

2.4 Thiocyanate formation

During gold mining operations, cyanide present in processing liquors is converted to several species which is largely dependent on the mineralogy of the ore, the chemical constituents of the system and lastly the operational parameters. The study by Mwase et al. (2013) speculated that the thiocyanate formed in his work was attributed to the reduced sulphur species generated in the bioleach; however his work did not focus on the mineralogy of the sample that may have influenced thiocyanate formation.

2.4.1 Chemistry of cyanide and sulphur species in pure minerals

Wilmot's (1997) study provides relevant insight relating to the chemistry of cyanide and metal sulphide interactions that generally occur in refractory ores. His study highlights the reactions that manifest at pure sulphidic mineral surfaces particularly focusing on elemental sulphur, pyrite, pyrrhotite and chalcopyrite, commonly associated with precious metal ores.

Elemental sulphur

The interaction between elemental sulphur and cyanide is one of the reactions that generate thiocyanate. In the past this reaction has been used as an analytical method to quantify sulphur. The chemistry of this particular reaction entails a strong nucleophilic attack by the cyanide anion on the strong sulphur-sulphur aromatic bond. Consequently, the sulphur ring is displaced which advances to further displacements of sulphur atoms.

$$S_8 + 8CN^- + \rightleftharpoons 8SCN^-$$

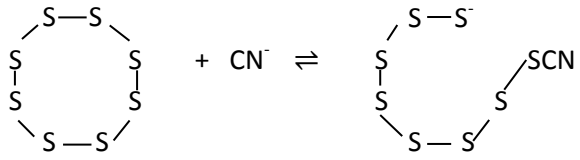

$$S\text{-}S_5\text{-}S\text{-}SCN + CN^- \rightleftharpoons S\text{-}S_4\text{-}S\text{-}SCN + SCN^-$$

$$S\text{-}S_X\text{-}S\text{-}SCN + CN^- \rightleftharpoons S\text{-}S_{X-1}\text{-}S\text{-}SCN + SCN^-$$

$$S\text{-}SCN + CN^- \rightleftharpoons 2SCN^-$$

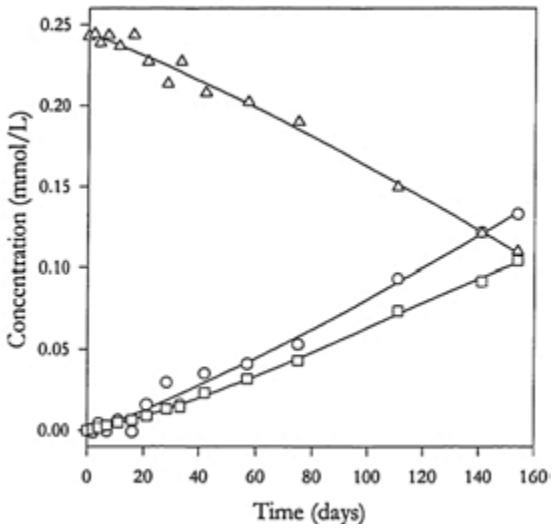

Wilmot (1997) investigated the reaction between Frasch sulphur and cyanide and established the reaction profiles. Figure 7 illustrates the decomposition of initial cyanide, the formation of thiocyanate and lastly the amount of free cyanide that reacted. From the 53.2% free cyanide reacted, 43.7% was attributed to thiocyanate conversion and 9.5% to cyanate formation, on a molar basis. The experiment ran for approximately 160 days and failed to reach completion within this time frame. Thus the reaction displayed fairly slow chemical kinetics and poor thiocyanate conversions.

Figure 7: Concentration profiles for the reaction of cyanide with a 10:1 excess of Frasch sulphur: ΔΔ CN^-_{WAD}, ○○ CN^-_{WAD} reacted, □□ SCN^- produced. Conditions for the experiment were: 0.0401g of Frasch sulphur in 0.50L of 0.25mM CN^- at 25°C (Wilmot, 1997).

Pyrite

The most abundant form of sulphide in the earth's crust is in the form of iron sulphide minerals with pyrite being the most common. Pyrite, FeS_2, is a cubic polymorph. Under aerated alkaline conditions the sulphur atom is released from the pyrite lattice as shown in the schematic below. In a cyanide leach circuit, the sulphide ion that is discharged is most likely to react with cyanide, producing thiocyanate in the process.

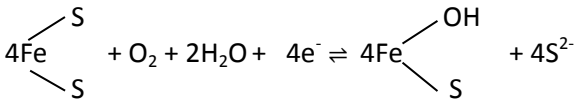

$$CN^- + S^{2-} \rightleftharpoons SCN^- + 2e^-$$

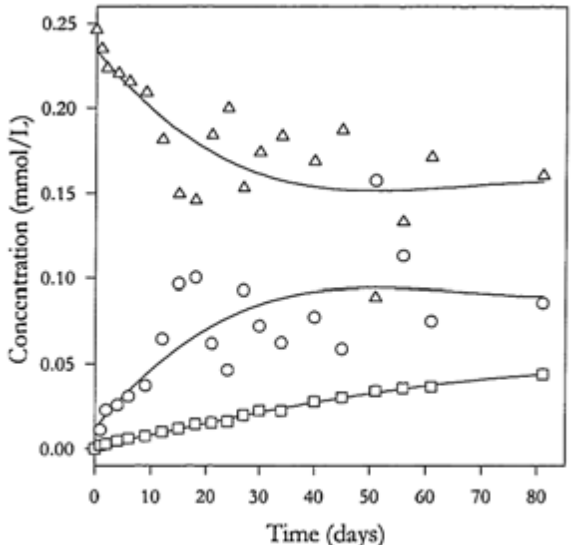

The results obtained for the pyrite-cyanide system were relatively inconsistent with no validation. After 80 days, the free cyanide reacted amounted to 35.2%. Both thiocyanate and cyanate conversion accounted for 18.3% and 4.6% respectively. It was believed that some of the cyanide loss, 12.3%, was due to cyanide fixation to pyrite.

Figure 8: Concentration profiles for the reaction of cyanide with a 10:1 excess of pyrite: ΔΔ CN^-_{WAD}, ○○ CN^-_{WAD} reacted, □□ SCN^- produced. Conditions for the experiment were: 0.0750g of pyrite in 0.50L of 0.25mM CN^- at 25°C (Wilmot, 1997).

Pyrrhotite

The chemistry related to pyrrhotite and cyanide interaction is slightly more complex in comparison to pyrite. Equally important, the mineralogy of pyrrhotite is inconsistent as it varies from Fe_5S_6 to $Fe_{16}S_{17}$. However, pyrrhotite is commonly referred to as the Fe_7S_8 composition. The additional sulphur atom present in the ferrous sulphide matrix is naturally reactive in most systems and presumed to be loosely held, leading it to react with cyanide as described below.

$$Fe_7S_8 + CN^- \rightleftharpoons 7FeS + SCN^-$$

The ferrous sulphide is further oxidised to ferrous sulphate and in the presence of excess free cyanide it forms a stable complex, hexacyano(II)ferrate as shown below. This becomes problematic in cyanide leach operations as large amounts of free cyanide are consumed during the production of hexacyano(II)ferrate.

$$Fe\,S + 2O_2 \rightleftharpoons FeSO_4$$
$$FeSO_4 + 6CN^- \rightleftharpoons [Fe(CN)_6]^{4-} + SO_4^{2-}$$

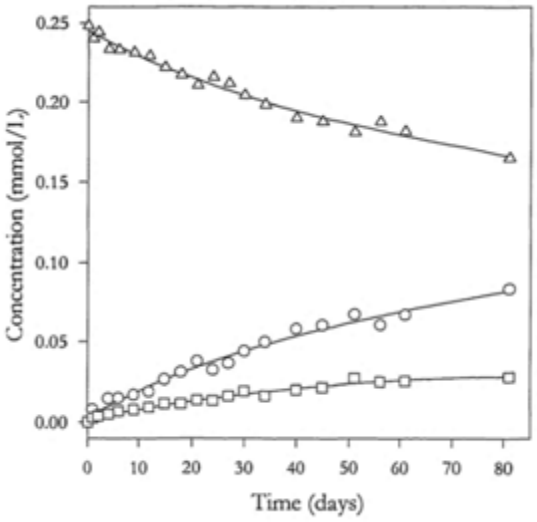

The pyrrhotite sample displayed reduced thiocyanate conversions, achieving a mere 11.2% within an 80 day period. Cyanate accounted for 11.35% of reacted free cyanide. However, the formation of hexacyano(II)ferrate is believed to be the main cause of cyanide loss which amounted to 12.99%.

Figure 9: Concentration profiles for the reaction of cyanide with a 10:1 excess of pyrrhotite: ΔΔ CN^-_{WAD}, ○○ CN^-_{WAD} reacted, □□ SCN^- produced. Conditions for the experiment were: 0.1040g of pyrrhotite in 0.50L of 0.25mM CN^- at 25°C (Wilmot ,1997).

Chalcopyrite

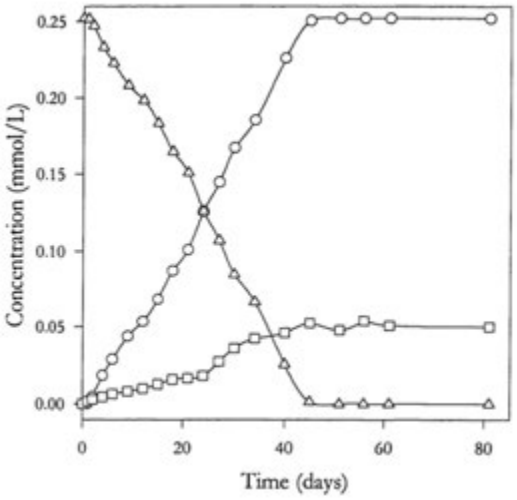

Chalcopyrite showed a strong tendency towards cyanide and demonstrated faster chemical kinetics in comparison to pyrite and pyrrhotite. By day 45 the reaction had reached completion with no free cyanide present in the solution. The production of cyanate was believed to be the main route of cyanide loss, which is described by the following equation:

$SCN^- + 5OH^- \rightarrow OCN^- + SO_4^{2-} + 5H^+ + 8e^-$.

This hydrolysis reaction may possibly be the cause of the irregularities observed in the results.

Figure 10: Concentration profiles for the reaction of cyanide with a 10:1 excess of chalcopyrite: ΔΔ CN^-_{WAD}, ○○ CN^-_{WAD} reacted, □□ SCN^- produced. Conditions for the experiment were: 0.1147g of chalcopyrite in 0.50L of 0.25mM CN^- at 25°C (Wilmot, 1997)

Wilmot's (1997) study provided significant data on the reaction profiles between cyanide and pure minerals as a function of time. However, he failed to establish the reaction rates and rate constants which may have assisted in validating the results achieved. The chemical reaction kinetics are further discussed in a comprehensive study by Luthy & Bruce (1979), their findings are presented in the following section.

2.4.2 Reaction kinetics of thiocyanate formation

In their work, Luthy & Bruce (1979) aimed to provide an improved understanding of the reaction kinetics involved in the interaction between cyanide and sulphide oxidation products. However, their study focused on pure (homogeneous) systems, thiosulphate and polysulphide and provided data on the initial rate kinetics.

Polysulphide reaction

The data gathered from the cyanide-polysulphide chemical kinetics revealed that the reaction was mixed order. The rate and reaction order varies according to the pH and therefore decreased with an increase in pH (Luthy & Bruce, 1979). For this reason, the overall reaction order decreased from 1.89 to 1.27 as the pH increased from 8.2 to 12.0. Equally important, the specific rate constant for the reaction decreased from 1.41 to 0.14 over the pH range 8.2 to 12. Luthy and Bruce (1979) concluded that the cyanide-polysulphide reaction proceeded fairly rapidly.

Thiosulphate reaction

The kinetics of the thiosulphate reaction was established by Bartlett & Davis (1958). The authors determined the reaction order to be second order at 25°C, with a reaction rate of 2.3×10^{-3} mol.L^{-1}.min^{-1} and an activation energy of 54.39kJ/mol (Bartlett & Davis, 1958).

Figure 11 presents the various reaction rates for thiocyanate formation for both the cyanide-polysulphide and cyanide-thiosulphate systems. The data indicates that the polysulphide reaction is virtually three orders of magnitude faster in relation to thiosulphate at pH 8.2. This suggests that the cyanide-polysulphide reaction is most likely to dominate with respect to the cyanide-thiosulphate pathway.

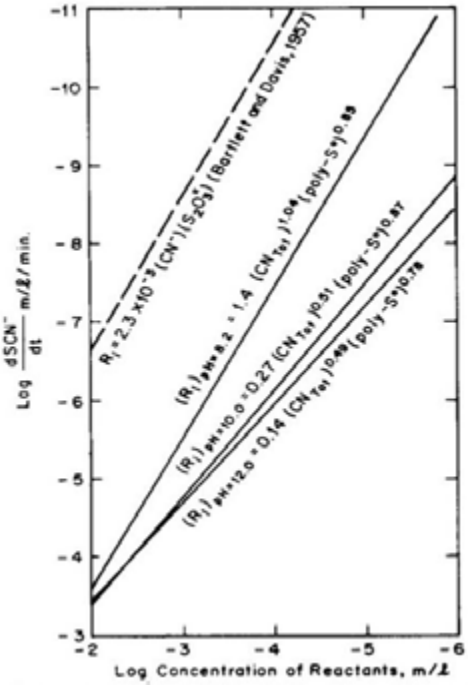

Figure 11: Comparison of production rates for formation of thiocyanate from reaction of equimolar concentrations of cyanide and polysulfide, and cyanide and thiosulfate (Luthy & Bruce, 1979).

Sulphur compounds formed are dependent on the system's pH. At high sulphide concentration, polysulphides are formed within the pH range of 6.5-8, where the principal polysulphides that dominate are S_4^{2-} and S_5^{2-} (Luthy & Bruce, 1979). However, thiosulphates are formed at a pH greater than 8. Thus by analysing the pH of the system, it may assist in possible classification of the sulphur compounds (Keller-Lehmann et al., 2007).

In summary the thiocyanate formation pathways are described in Figure 12 and the reactions are listed in Table 6 below.

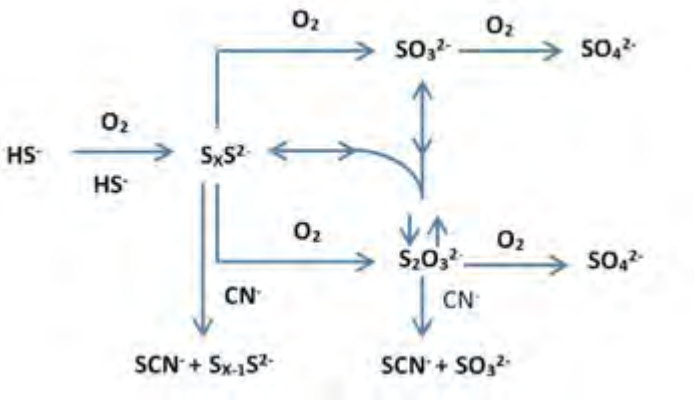

Figure 12: Possible reactions of cyanide with reduced sulfur species in aqueous solution to yield thiocyanate (Luthy & Bruce, 1979)

All sulphide minerals and partially oxidised sulphur intermediates have the ability to generate thiocyanate with an exception for lead sulphide. The production of thiocyanate is accelerated in low alkaline conditions with deficient aeration (Kuyucak & Akcil, 2013).

Table 6: Thiocyanate formation reactions (Luthy & Bruce, 1979; Wilmot, 1997).

Elemental sulphur	$S^0 + CN^- \rightleftharpoons SCN^-$
Sulphide	$S^{2-} + CN^- + H_2O + ½O_2 \rightleftharpoons SCN^- + 2OH^-$
Polysulphide	$S_xS^{2-} + CN^- \rightleftharpoons S_{x-1}S^{2-} + SCN^-$
Thiosulphate	$S_2O_3^{2-} + CN^- \rightleftharpoons SO_3^{-2} + SCN^-$
Polythionate	$S_xO_6^{2-} + (x-1)CN^- \rightleftharpoons SO_4^{2-} + (x-3)SCN^- + S_2O_3^{2-}$ (x=3, 4, 5 or 6)
Sulphite	$H_2O + 3SO_3^{2-} + CN^- \rightleftharpoons 2SO_4^{2-} + SCN^- + 2OH^-$

2.5 Thiocyanate hydrometallurgy

2.5.1 Chemical properties of thiocyanate

Thiocyanate ion is a widely studied ligand, which is known to complex with a variety of metals, particularly transition metals. The thiocyanate ion consists of a linear structure with a carbon atom positioned in the centre. It is present in compounds as either an anion or a ligand, due to its ability to form two resonance structures namely, thiocyanates/S-thiocyanate and isothiocyanates/N-thiocyanate (Kononova, 2005). Thus the chemistry of thiocyanate complexation is made more challenging as a result of its ambidentate nature.

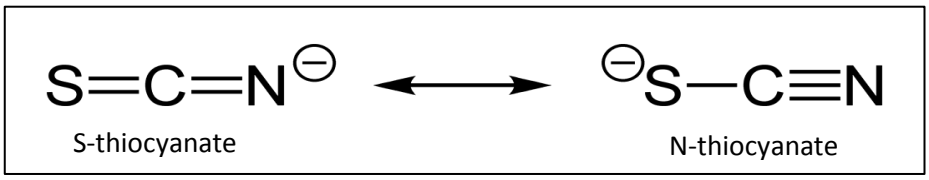

Figure 13: Resonance structures of thiocyanate (Li et al. 2012a)

Additionally, the two electron structures as shown in Figure 13, enables thiocyanate to act as a bridging ligand or a monodentate ligand, coordinated to sulphur or nitrogen (Kabesova & Gazo, 1980). These unique properties facilitate 10 potential bonding modes of thiocyanate. Thiocyanate combines with metals to produce metal-thiocyanate complexes given that it is a good ligand that readily forms complexes with transition metals (Gould et al., 2012).

2.5.2 Thermodynamics of thiocyanate leach systems

Metal dissolution is governed by the nature of the metal being leached and the degree of selectivity needed for metal recovery. Leaching of metals can be employed under varied conditions, such as acid or basic solutions and in the presence of oxidizing, neutral or even reducing agents.

As an alternative to cyanidation, the thiocyanate system has been extensively studied for the leaching of gold. Barbosa-Filho & Monhemius (1994) established that gold is successfully leached in thiocyanate solutions at 0.01-0.05M concentration, potentials around 0.6 -0.7 V and at an acidic pH of 1-3 in the presence of oxidants either, ferric ions (2-5g/L) or peroxide.

Li et al. (2012a) mapped out the E_h-pH diagrams and ion species distribution diagram for SCN–H_2O, Au–SCN–H_2O, Ag–SCN–H_2O, Cu–SCN–H_2O, and Fe–SCN–H_2O systems which assisted in predicting the behaviour of various metal ions in thiocyanate solution. Stability constant values obtained from Smith & Martell (1976) and Barbosa-Filho & Monhemius (1994) were used to calculate the free energy of formation (G_f), and prepare the E_h/pH diagrams using STABCAL software. The nature of the E_h/pH diagrams for various thiocyanate systems are discussed in the following section.

2.5.3 Au-SCN complexes

Thiocyanate forms stable and soluble complexes of aurothiocyanate, $Au(SCN)_2^-$ and aurithiocyanate, $Au(SCN)_4^-$ under appropriate leaching conditions. The E_h–pH diagram for the Au–SCN–H_2O system is presented in Figure 14 with an Au concentration of 2 mg/L, at free thiocyanate concentrations of, 0.5, 0.1 and 0.005 M at 25°C (Li et al., 2012a).

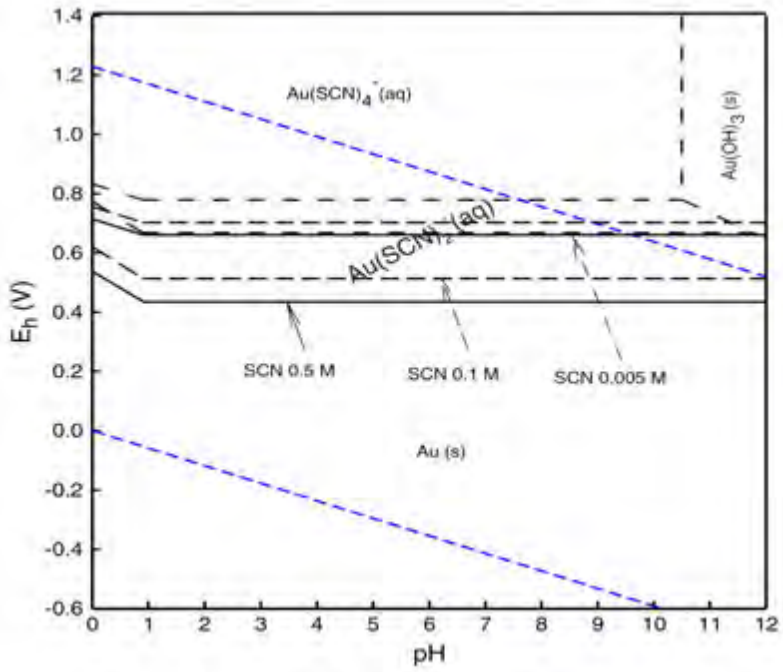

Figure 14: E_h-pH diagrams for the Au-SCN-H_2O system at SCN concentrations of 0.005, 0.1 and 0.5M, and Au concentration of 2mg/L at 25°C. Dashed lines indicate water stability (Li et al., 2012a)

Figure 14 indicates that gold leaching under conventional acid leach conditions of pH 1 to 2, requires a reasonably high oxidation potential, which is dependent on the thiocyanate concentration and that the $Au(SCN)_2^-$ complex dominates at lower oxidation potential.

Furthermore, the lowest potential for $Au(SCN)_2^-$ prevalence at pH 2 and SCN^- concentration of 0.5 M is 0.430 V, whereas at 0.005 M SCN^- concentration, the potential must be increased to 0.670 V for $Au(SCN)_2^-$ to stabilise. Hence at lower SCN^- concentrations a higher potential is imperative for $Au(SCN)_2^-$ to be stable in solution. Having established this, it is postulated that Au–SCN–H_2O leaching system should be controlled within a range of 0.6 to 0.7 V. Further, it should be noted that the position of the oxygen line suggests that metallic gold can be oxidised up to a pH of 12 (Li et al., 2012a).

The standard reduction potential for thiocyanate dissolution of gold are listed in the equations below, for aurous and auric complexes, respectively. Given that these potentials are lower than the reduction potential of oxygen gas and ferric ion, henceforth they can be employed as good oxidants.

$$2SCN^- + Au \rightleftharpoons Au(SCN)_2^- + e^- \qquad E^o = 0.691\ V$$
$$4SCN^- + Au \rightleftharpoons Au(SCN)_4^- + 3e^- \qquad E^o = 0.659\ V$$

2.5.4 Fe-SCN complexes

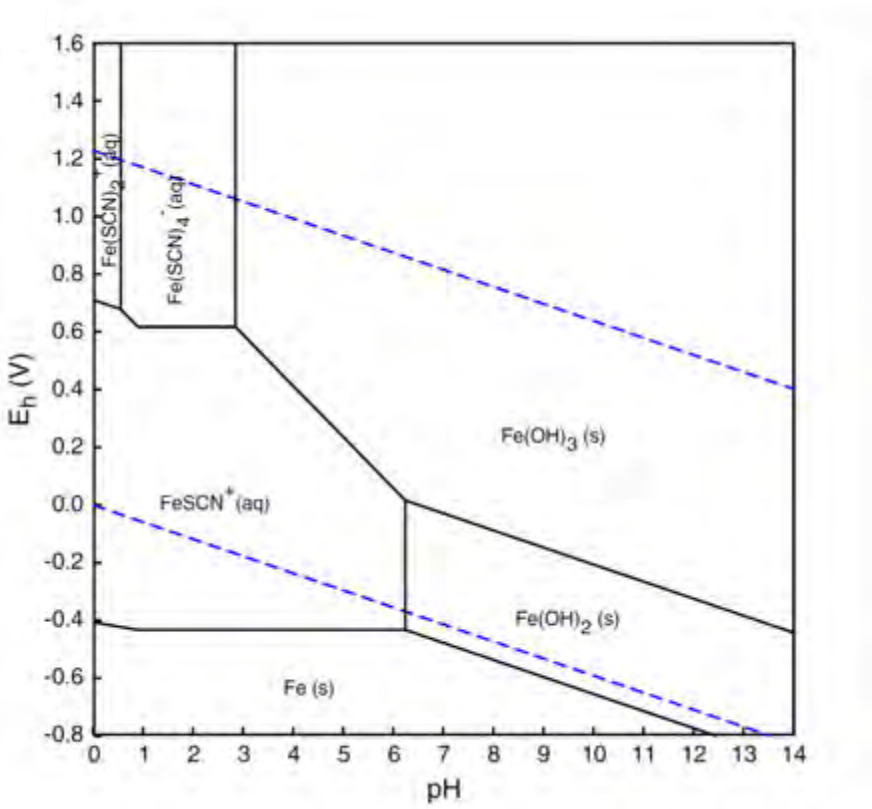

Figure 15: E_h–pH diagram for the Fe–SCN–H_2O system at Fe concentration of 0.1 M, SCN concentration of 0.1M at 25°C. Dashed lines indicate water stability limits (Li et al. 2012a).

Thiocyanate has the ability to complex with both ferrous and ferric ions. The complexation between ferrous and thiocyanate ions is relatively weak, which is indicated by the low stability constants, Table 7. In contrast, thiocyanate is known to form stable compounds with ferric salts, which contributes to increased leaching rates, as they act as potential oxidants. However, the formation of stable compounds could reduce the oxidizing potential of ferric ions and the concentration of free thiocyanate required for gold dissolution (Broadhurst, 1987).

$$Fe^{3+} + e^- \rightleftharpoons Fe^{2+} \qquad E^o = 0.77\ V$$
$$Fe(SCN)_2^+ + e^- \rightleftharpoons Fe(SCN)^+ + SCN^- \qquad E^o = 0.60\ V$$

Li et al. (2012a) went on to establish the E_h–pH diagrams for the Fe–SCN–H_2O system displayed in Figure 15. The system comprised of 0.1M Fe concentration and 0.1 M free thiocyanate concentration at 25 °C. The diagram suggests that at a pH of 2 at a relatively high thiocyanate concentration (0.1M), the ferric thiocyanate complex is stable within a leaching potential range of 0.6-0.7V. Consequently, if the free thiocyanate concentration is low (0.01M), then the ferrous–thiocyanate complex becomes the prevalent species, which has been established thermodynamically (Li et al., 2012a).

2.5.5 Cu-SCN complexes

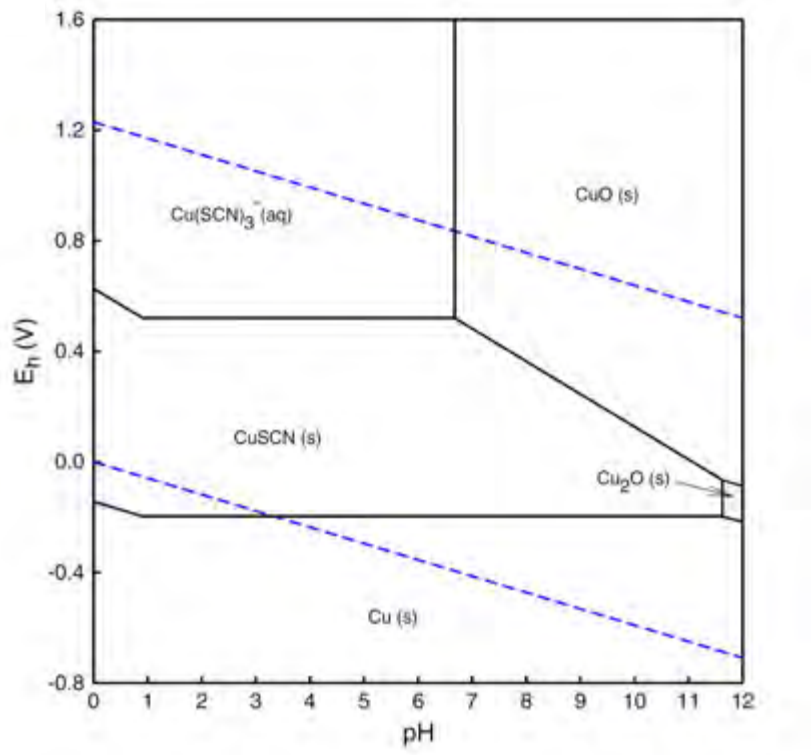

Figure 16: E_h–pH diagrams for the Cu–SCN–H2O system at Cu concentration of 0.2 g/L and SCN concentrations of 0.1M at 25 °C. Dashed lines show water stability limits (Li et al. 2012a).

Thiocyanate is classified as a pseudo-halide and thus capable of forming pseudo-halogen thiocyanogen $(SCN)_2$ and thiocyanic acid, HSCN (Gould et al., 2012). The pseudo-halide features are demonstrated by the ability of thiocyanate to form insoluble salts or complexes with mercury, lead, silver and copper ions under certain conditions, which is displayed in the E_h-pH diagram.

Generally, cuprous ion is not stable in aqueous solution and will eventually disproportionate to metallic copper or cupric ion; hence it requires a complexing agent. The E_h–pH diagram for the Cu–SCN–H_2O system is represented in Figure 16. The system contained a Cu concentration of 0.2g/L and a SCN^- concentration of 0.1M at 25°C. The reaction between thiocyanate and cuprous leads to the formation of an insoluble salt, CuSCN (s) with increased stability (log β = 13.08). Similarly the reaction with cupric ion forms a weak insoluble salt (log β = 3.66).

$$Cu^+ + SCN^- \rightleftharpoons CuSCN(s)$$

$$Cu^{2+} + 2SCN^- \rightleftharpoons CuSCN(s) + 0.5\ (SCN)_2$$

It can be concluded that if the concentration of the gold leaching system is controlled within the range of 0.05 – 0.1M, then the copper species should be soluble if the reduction potential is within the range of 0.6 and 0.7V.

2.5.6 Stability of thiocyanate

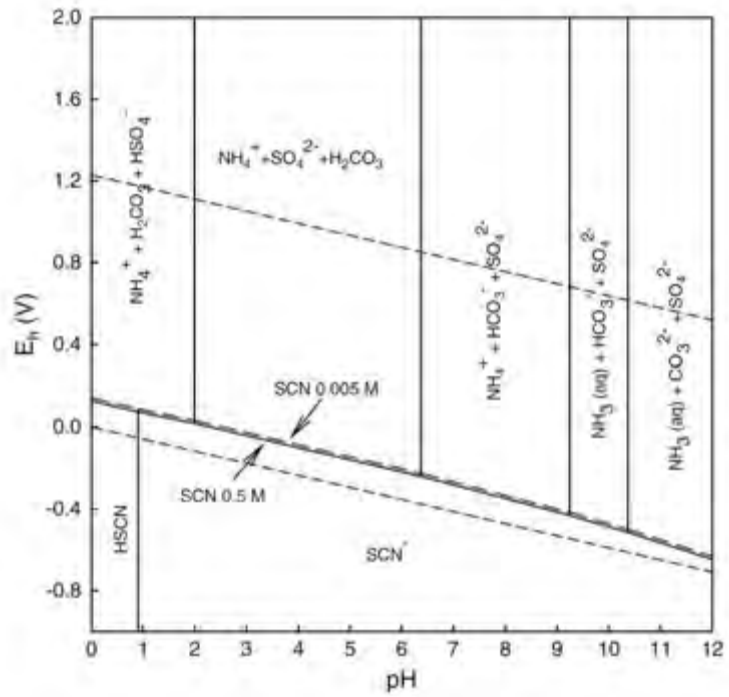

Figure 17: E_h–pH diagrams for the SCN–H2O system at SCN concentrations of 0.5 and 0.005 M at 25 °C. Concentration of all other dissolved species 0.1 M. Short dashed lines show water stability limits (Li et al., 2012a).

The stability of thiocyanate is largely governed by the oxidation potential and leaching conditions of the system (Li et al., 2012a). In order to reduce reagent consumption and improve metal recoveries during leaching, it is essential to understand the decomposition nature of the reagent. During gold leaching by thiocyanate, Fe(III) present in solution is reduced to Fe(II). This results in the oxidation of free thiocyanate to metastable intermediates thiocyanogen $(SCN)_2$ and trithiocyanate $(SCN)_3^-$ according to the following reactions:

$$(SCN)_2 + 2é \rightleftharpoons 2SCN^- \qquad E^o = 0.730\ V$$

$$(SCN)_3^- + 2é \rightleftharpoons 3SCN^- \qquad E^o = 0.650\ V$$

At relatively high concentrations of $(SCN)_2$ and $(SCN)_3^-$, these intermediate species are known to readily oxidise and dissolve gold in the process generating a high initial rate of gold dissolution (Barbosa-Filho & Monhemius, 1994). Thus $(SCN)_2$ and $(SCN)_3^-$, function as both oxidants and complexing reagent.

In addition, thiocyanate has proven to be thermodynamically unstable during the leaching of gold. It is also oxidised at a pH of 2-6.4 by ferric ion to sulphate, carbonate and ammonia, as shown in the equation below. It has been established by Dunne et al. (2009) that thiocyanate is much more stable in the leaching of oxide ores compared to sulphide ores due to the high iron content.

$$SCN^- + 7H_2O + 8Fe^{3+} \rightleftharpoons SO_4^{2-} + CO_3^{2-} + NH_4^+ + 10H^+ + 8Fe^{2+} \qquad E^0 = 141mV$$

Stability constants

The standard method for indicating the stability of a reaction product is the stability constant. Stability constants have been employed as an effective measure of affinity of a ligand for a particular metal ion in solution (Martell & Motekaitis, 1988). Extractive metallurgy generally involves the action of complexing agents and aqueous solutions on ores. Thus stability constants are needed to establish a complete understanding of the chemical reactions involved. Table 7 presents the stability constants of various thiocyanate complexes, which vary from very small to very large, depending on the metal ion complex (Union et al., 1999). It can be seen that thiocyanate forms a reasonably strong complex with auric ion, which is indicated by the $\log\beta_6$ value of 43.67 (Li et al., 2012a). In contrast, the formation of Pt and Pd, thiocyanate complexes are comparatively less stable with $\log\beta_4$ values of 33.6 for Pt and 27.42 for Pd, respectively.

The 'soft-soft' metal ligand interactions are favoured in thiocyanate and PGM complexation and hence Pt and Pd readily complex with soft ligands capable of covalent interactions. A complex with a low stability constant requires a high level of chemical control to equally enhance leaching and maintain the thiocyanate complex in solution once formed. Likewise, a system comprising of a less stable complex, the chemical equilibria dictates a high reagent concentration to retain the metal thiocyanate in solution.

Table 7: Stability constants for selected thiocyanate complexes

Metal ion	Thiocyanate complex		$\log\beta_n$	Reference
Au^{3+}	$Au(SCN)_4^-$	(aq)	β_4 = 43.66	(Barbosa-Filho & Monhemius, 1994)
	$Au(SCN)_5^{2-}$	(aq)	B_5 = 43.62	
	$Au(SCN)_6^{3-}$	(aq)	B_6 = 43.67	
Au^+	AuSCN	(aq)	β_1 = 15.19	(Barbosa-Filho & Monhemius, 1994)
	$Au(SCN)_2^-$	(aq)	β_2 = 19.17	
Pt^{2+}	$Pt(SCN)_4^{2-}$	(aq)	β_4 = 33.6	(Mountain & Wood, 1988)
Pd^{2+}	$Pd(SCN)^+$	(aq)	β_1 = 8.14	(le Roux et al., 2014)
	$Pd(SCN)_2$	(aq)	β_2 = 15.46	
	$Pd(SCN)_3^-$	(aq)	β_3 = 21.94	
	$Pd(SCN)_4^{2-}$	(aq)	β_4 = 27.42	
Cu^+	CuSCN	(s)	β_1 = 13.08	(Smith & Martell, 1976)
	CuSCN	(aq)	β_1 = 0	
	$Cu(SCN)_2^-$	(aq)	β_2 = 11	
	$Cu(SCN)_3^{2-}$	(aq)	β_3 = 10.89	
	$Cu(SCN)_4^{3-}$	(aq)	β_4 = 10.39	
Cu^{2+}	$CuSCN^+$	(aq)	β_1 = 2.33	(Smith & Martell, 1976)
	$Cu(SCN)_2$	(aq)	β_2 = 3.65	
	$Cu(SCN)_3^-$	(aq)	β_3 = 6.49	
	$Cu(SCN)_4^{2-}$	(aq)	β_4 = 6.53	
Fe^{2+}	$FeSCN^+$	(aq)	β_1 = 0.81	(Smith & Martell, 1976)
Fe^{3+}	$FeSCN^{2+}$	(aq)	β_1 = 2.30	(Smith & Martell, 1976)
	$Fe(SCN)_2^+$	(aq)	β_2 = 3.72	
	$Fe(SCN)_3$	(aq)	β_3 = 5.08	
	$Fe(SCN)_4^-$	(aq)	β_4 = 6.39	
	$Fe(SCN)_5^{2-}$	(aq)	β_5 = 6.27	
	$Fe(SCN)_6^{3-}$	(aq)	β_6 = 6.10	

Table 8: Stability constants for selected Pt and Pd complexes at 25°C (Mountain & Wood, 1988; le Roux et al., 2014)

Ligand	$Log\beta_4 (Pt)^{2+}$	$Log\beta_4 (Pd)^{2+}$
I^-	29.66	24.9
Cl^-	13.99	11.54
Br^-	15.4	14.9
SCN^-	33.6	27.42
CN^-	41.0	63

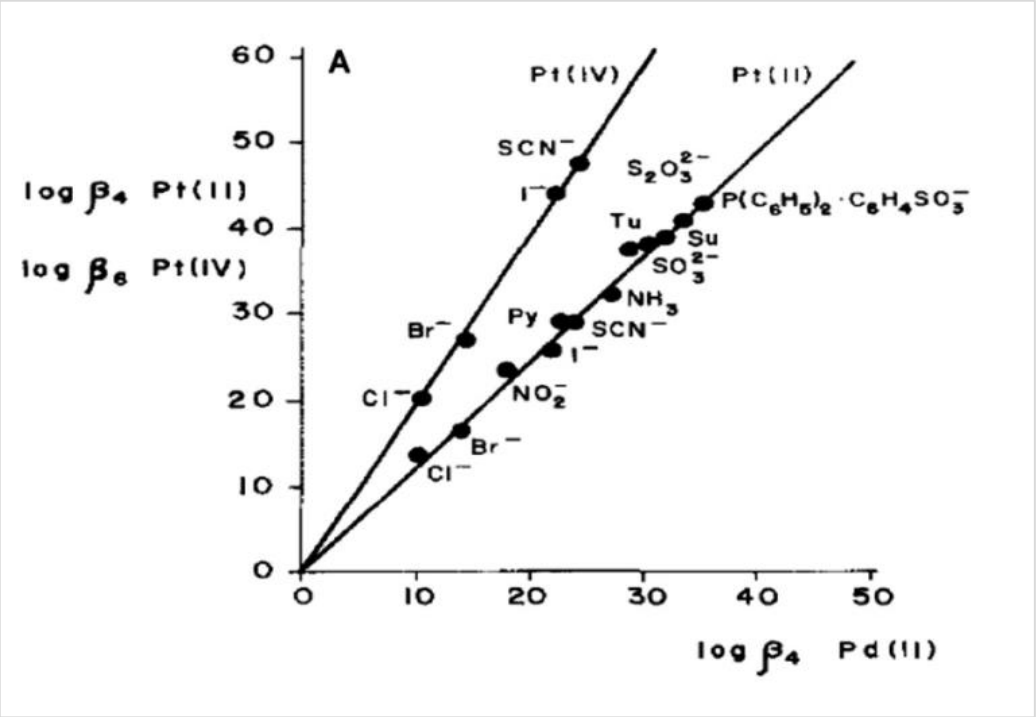

Figure 18: LFER for the formation constants of Pt(II) and Pt(IV) complexes against those for Pd(II) complexes. Tu = thiourea, Su = selenourea, py =pyridine.(Hancock et al. 1977)

The stability constants for various Pt(II) and Pd(II) complexes (β_4) are shown in Table 8. Evidently cyanide displays the highest stability with thiocyanate leading closely behind, while the stability constant for halide systems are several orders of magnitude less. Figure 18 presents the stability constants, $log\beta_4$ for Pt(II) and $log\beta_6$ for Pt(IV) complexes against the analogous $log\beta_4$ for Pd(II) complexes, also known as the linear free energy range (Hancock et al., 1977). This enables one to distinguish between relatively strong and weak complexes which further confirm the data presented in Table 8. Furthermore, the linear correlation of the stability constants further assists in establishing reliable thermodynamic data for Pt and Pd complexes in thiocyanate solution.

2.5.7 Thiocyanate complexation to Pt and Pd

Conventional PGM refining is based mainly on chloride chemistry. Hamacek & Havel (1999), identified thiocyanate to form extractable complexes with both platinum and palladium which displayed increased stability, when compared to chloro complexes. An extensive study by Elding (1978) concluded that Pt and Pd aqua complexes anation (replacement of a ligand by an anion) occur in the following kinetic trans-effect order: $H_2O<Cl^-<Br^-<I^-<SCN^-$. In view of Pt and Pd anation reactions, the rate of complexation for Pd(II) and Pt(II) are fairly different.

Both platinum (IV) and palladium (II) form complexes coordinating with the sulfur atom, leading to $Pt(SCN)_6^{2-}$ and $Pd(SCN)_4^{2-}$ complexes, as shown in Figure 19. In the presence of thiocyanate, Pd undergoes a substitution reaction instantaneously to form $Pd(SCN)_4^{2-}$. The rate of complexation for Pd is faster by a factor of 10^5-10^6 relative to Pt. However, complexation between Pt and thiocyanate is greatly dependant on acid and thiocyanate concentrations; which can be accelerated by heating or photochemically (Oleschuk & Chow, 1998). Furthermore, the rate of complexation is inversely proportional to the pH and results in complete inhibition at pH 7 (Al-bazi & Chow, 1984).

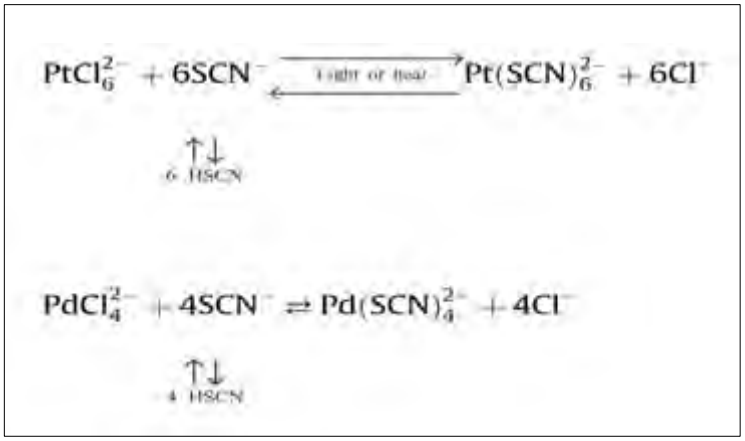

Figure 19: Reaction mechanisms for Pt and Pd complexes in thiocyanate solution

2.6 Leaching of precious metals in thiocyanate solutions - Dissolution rates

The use of thiocyanate as a lixiviant in PGM leaching remains unexplored, therefore literature is limited. Extensive research, numerous papers and reviews have been conducted on the thiocyanate dissolution of gold and hence will serve as a reference, which are discussed in this section.

Studies by Barbosa-Filho & Monhemius (1994) and Li et al. (2012b) investigated the leaching of gold in ferric thiocyanate solutions by a rotating disk technique at pH 1.5-2 under varied thiocyanate and ferric ion concentration. Barbosa-Filho & Monhemius (1994) were the only authors to investigate the effect of temperature (25°C-85°C) in order to quantify the activation energy as well as to determine the dissolution mechanism of the system.

Kholmogorov et al. (2002) explored the leaching of gold in thiocyanate solutions (0.01-0.5 M) relative to different complex forming reagents, (thiosulphate, thiocarbamide, sodium cyanide and sulphuric acid) from chemically prepared arsenopyrite, containing gold at 20°C in the presence of ferric sulphate (0.015M Fe^{3+}).

Kriek (2008) studied the effects of thiocyanate solution (0.3 and 0.6 M) on PGM recovery from virgin autocatalytic converters that were crushed and split into different sizes (+2mm, -2+1mm, and -1mm). Pt, Pd and Rh were present in the 0 oxidation state and were leached at 50°C, pH 1.24-1.28 in the presence of ferric sulphate (0.05-0.25M).

2.6.1 Effect of thiocyanate concentration on rate dissolution

Barbosa-Filho & Monhemius (1994) suggested that an increase in thiocyanate concentration from 0.050-0.50M led to an increase in both the rate of gold dissolution as well as the amount of gold dissolved (Table 9). There is no simple explanation for the relationship between the rate of gold dissolution and the corresponding thiocyanate concentration, however, it can be assumed that by increasing the thiocyanate concentration by a factor of 10, the dissolution rates are doubled (Barbosa-Filho & Monhemius, 1994). An increased thiocyanate concentration of 0.50 M, at 25°C amounted to highest gold dissolution rate of 13.1×10^{-10} mol $cm^{-2}s^{-1}$. Additionally, the authors indicated the gold dissolution rates decreased substantially after 1 hour as the rates are seemingly an order of a magnitude lower than the initial rates.

Table 9: Effect of thiocyanate concentration on the initial rate of gold dissolution (Barbosa-Filho & Monhemius, 1994)

SCN^- concentration ($mol.l^{-1}$)	Rate, *J*, mol $cm^{-2}s^{-1}$		Linear correlation coefficient, R^2, After 1 h
	Initial rate ($J \times 10^{-10}$)	After 1h ($J \times 10^{-11}$)	
0.050	6.30	6.96	1.00
0.10	7.78	8.08	1.00
0.75	9.91	7.63	0.98
0.50	13.1	13.5	1.00

Experimental conditions: initial Fe (III) = 0.055M, pH=1.5, 25°C; disk rotation speed, 720 rpm; atmosphere, N_2.

Further studies conducted by Li et al. (2012b) examined the effect of thiocyanate concentration between the range of 0.05-0.2M, on the rate of gold leaching. They concluded that, the initial rate of gold leaching is quite slow and virtually insensitive to thiocyanate concentration within the range of 0.05-0.2M (Table 10). Initial rates of gold dissolution were reported as mol $cm^{-2}.min^{-1}$ but were converted to mol $cm^{-2}.s^{-1}$ to easily compare findings with Barbosa-Filho & Monhemius (1994).

Table 10: Effect of thiocyanate concentration on the initial rate of gold dissolution (Li et al., 2012b)

SCN^- concentration ($mol.l^{-1}$)	Rate, *J*, mol $cm^{-2}.s^{-1}$
	Initial rate $J \times 10^{-10}$
0.050	5.07
0.10	6.33
0.25	5.90

Experimental conditions: initial Fe (III) = 0.2 g/L, pH=2, 25°C and disk rotation speed, 800 rpm

Kholmogorov et al. (2002) suggested that enhanced recovery of gold can be acquired within the range of 0.01-0.5M thiocyanate concentration. However, they proposed in weak acidic thiocyanate solutions at 0.4M concentration led to highest recovery of gold, totalling 89-93% recovery within 4-5 hours.

From the above findings it is expected that PGMs are more likely to exhibit enhanced recovery at similar or even higher thiocyanate concentrations. Kriek's (2008) study investigated the use of thiocyanate as a lixiviant in PGM recovery at 0.3 and 0.6M concentration. His results revealed that at 0.3M thiocyanate and 0.25M Fe^{3+} concentration, 92.06% Pt, 100.10% Pd and 32.66% Ru was recovered within a 24 hour period. Since Kriek (2008) only examined the effect for 2 different concentrations, it creates an opportunity to further investigate different concentrations. Table 11 summarises the above findings and highlights the main conclusions reached.

Table 11: Summary showing the effect of thiocyanate concentration on gold and PGM recovery

Author	**Barbosa-Filho & Monhemius (1994)**	**Li et al. (2012b)**	**Kholmogorov et al. (2002)**	**Kriek (2008)**
Metal	Gold	Gold	Gold	PGMs
SCN conc. range	0.05-0.5M	0.05-0.2M	0.01-0.5M	0.3 and 0.6M
Exp. conditions	Fe^{3+} = 0.055 M, pH = 1.5, 25°C, 720 rpm	Fe^{3+} = 0.2 g/l, pH = 1.5, 25°C, 800 rpm	Fe^{3+} = 0.015M pH = 2, 20°C, vigorous mixing	Fe^{3+} = 0.25M, pH = 1.28, 50°C, 300 rpm
Conclusions	At 0.5M displayed the highest: - Au dissolution - Au dissolution rate	Rate of Au leaching and Au dissolution insensitive to SCN concentration	At 0.4M displayed: - 89-93% recovery	At 0.3M displayed: -92.06% Pt, (0.58g/h) -100.10% Pd, (1.04g/h) -32.66% Ru, (0.34g/h)

Enhanced dissolution of metals cannot be achieved by focusing particularly on thiocyanate concentration alone, since different parameters work mutually to achieve an improved recovery rate. These parameters include oxidant concentration, pH and temperature which are focused on in the following sections.

2.6.2 Effect of oxidant concentration

Ferric ion (Fe(III)) is commonly used in acid leach systems as an oxidant due to its high solubility at pH<2 (Li et al., 2012a). The variation in ferric ion concentration has a substantial effect on dissolution of gold and PGMs. However, the need for an oxidant is only required in the conversion of an element from its metallic to a soluble species or liberation of a metal from a complex.

According to Barbosa-Filho & Monhemius (1994), their findings reported that the initial rate of gold dissolution increases with increased concentration of Fe(III) to a value of 0.055M (3g/L). However, further increasing the Fe(III) concentration to 0.100M, led to a decrease in gold dissolution and dissolution rate. Therefore a general increase in Fe(III) concentration will not result in the enhancement of gold dissolution but should be within the range of 0.055M to achieve this effect. At lower Fe (III) concentration (0.010 & 0.033M) the anionic complex $Fe(SCN)^{4-}$ dominates, whereas at higher Fe (III) concentration (0.055 & 0.100M) the cationic complex, $FeSCN^{2+}$ prevails (Barbosa-Filho & Monhemius 1994). The rates observed by Barbosa-Filho & Monhemius (1994) established that it was one order of magnitude lower compared to the rates observed during cyanide leaching which is typically in the range of 10^{-9} mol.cm^{-2}.s^{-1}.

Table 12: Effect of Fe (III) concentration on the initial rate of gold dissolution (Barbosa-Filho & Monhemius, 1994)

Fe^{3+} concentration (mol.l^{-1})	Rate, *J*, mol cm^{-2}s^{-1}		Rate, *J*, mol cm^{-2}s^{-1}
	Initial rate ($J \times 10^{-10}$)	Initial rate ($J \times 10^{-11}$)	
0.010	5.17	5.40	0.99
0.033	5.56	7.60	1.00
0.055	7.78	8.08	1.00
0.100	6.55	7.77	0.99

Experimental conditions: SCN^- = 0.10 M, pH = 1.5, 25°C; disk rotation speed, 720 rpm; atmosphere, N_2

Li et al. (2012b) examined the effect of Fe(III) concentration within the range of 0.1-1M on gold dissolution. They established that, the gold leaching rate is slightly sensitive to ferric ion concentration and high molar ratios of Fe(III)/SCN^- did not affect the initial rate of gold leaching (Table 13).

Table 13: Effect of Fe (III) concentration on the initial rate of gold dissolution (Li et al., 2012b)

Fe^{3+} concentration ($mol.l^{-1}$)	Rate, *J*, $mol\ cm^{-2}.s^{-1}$
	Initial rate $J\ x10^{-10}$
0.1	5.48
0.2	6.23
0.4	6.98
1.0	7.32

Experimental conditions: SCN^- = 0.1M, pH=2, 25°C and disk rotation speed, 800 rpm

A similar trend is expected to be seen in PGMs – a slight increase in metal dissolution with respect to an increase in Fe(III) concentration. This particular trend was reported in Kriek's (2008) study, where he examined the effect of Fe(III) concentration within the range of 0.05-0.25M. At 0.25M Fe^{3+}concentration, his findings displayed the highest recoveries which amounted to 90-92% Pt, 94-100%Pd and 31-32% Ru within 24 hour period. The results presented in Table 14 imply that varying the ferric (III) concentration has a minor effect on the rate of gold dissolution, which does not seem to be the case for PGMs.

Table 14: Summary showing the effect of Fe(III) concentration on gold and PGM recovery

Author	**Barbosa-Filho & Monhemius (1994)**	**Li et al. (2012b)**	**Kriek (2008)**
Metal	Gold	Gold	PGMs
Fe(III) conc. range	0.010-0.100 M	0.1 - 1M	0.05 and 0.25M
Exp. conditions	SCN^- = 0.10 M, pH = 1.5, 25°C, 720 rpm	SCN^- = 0.10 M, pH = 1.5, 25°C, 800 rpm	SCN^- = 0.3M, pH = 1.28, 50°C, 300 rpm
Conclusions	At 0.055M displayed the highest: - Au dissolution - Au dissolution rate	-Gold leaching rate is slightly sensitive to ferric ion concentration	At 0.25M displayed: -92.06% Pt, (0.58g/h) -100.10% Pd, (1.04g/h) -32.66% Ru, (0.34g/h)

2.6.3 Effect of temperature

Barbosa-Filho & Monhemius (1994) explored the effect of temperature on gold dissolution in thiocyanate/ferric systems. They established that by varying the temperature within the range of 25 to 85°C it had a significant effect on gold dissolution. Initial gold dissolution rates obtained at 25 and 85°C were of the order of 10^{-9} and 10^{-8} $mol\ cm^{-2}\ s^{-1}$, respectively. A 60°C temperature jump resulted in an increase in gold dissolution rate by magnitude of one order.

From the data presented in Table 15, the respective apparent activation energy for various thiocyanate concentrations are relatively similar. This conveys that the process of gold dissolution in the presence of thiocyanate is chemically controlled and that the very same

dissolution mechanism functions over the range of thiocyanate concentrations that were studied (Barbosa-Filho & Monhemius, 1994).

Table 15: Effect of temperaure on the rate of gold dissolution at 0.10 M SCN, 0.055M Fe(III), and at pH. 1.5 (Barbosa-Filho & Monhemius, 1994)

Temperature (°C)	Rate, J, mol $cm^{-2}s^{-1}$	
	Initial rate ($J \times 10^{-9}$)	After 1h ($J \times 10^{-10}$)
25	0.78	0.81
48	2.28	2.44
55	3.56	2.79
85	18.0	16.5

Experimental conditions: SCN^- = 0.10 M, Fe^{3+} = 0.055M, pH = 1.5, 25°C; disk rotation speed, 720 rpm; atmosphere, N_2

Table 16: Apparent activation energies for gold dissolution at 0.055M Fe (III), pH. 1.5(Barbosa-Filho & Monhemius, 1994)

Thiocyanate conc. (mol l^{-1})	Apparent E_a kJ mol^{-1}
0.050	42.9
0.100	46.6
0.275	44.6

Kriek (2008) suggests that by increasing the leaching temperature it significantly reduces the leaching time required for platinum and palladium dissolution. Additionally, the leaching temperature cannot be exceedingly high as it gives rise to side reactions, corrosion and potential PGM evaporation. The proposed optimum temperature for PGM leaching is within the range of 70 - 90°C. Kriek (2008) conducted all experiments at 50°C; with no variations within the temperature range to determine the effect it poses. Although, at 50°C it showed favourable findings, these results were governed by variation in other parameters. This creates an opening for further research to be conducted on this aspect.

2.6.4 Effect of pH

Thiocyanate is associated with an acid leach system, which enables the use of Fe(III) as an oxidising agent in acidic environments (Gould et al., 2012). To obtain enhanced leach performance, pH of thiocyanate leach solution is maintained within a narrow range of 1-4.

Gold leaching from products of chemically prepared arsenopyrite concentrates by SCN^- solutions (Kholmogorov et al., 2002) showed more than 95% gold recovery when conducted in a weak acidic conditions within the pH range of 2-5. Additionally, Kholmogrov (2002) established that introducing a more basic medium, the rate of gold dissolution diminishes which is evident in Figure 20 below.

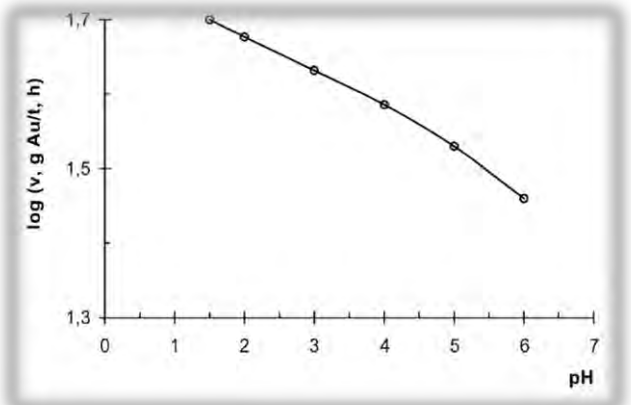

Figure 20: Dependence of leaching rate of gold from chemical product by KSCN solutions on pH value solution KSCN =0.4 M (Kholmogorov et al., 2002)

Further, Kriek (2008) showed promising results in experiments conducted at a pH of 1.24 and 1.28. Thus he verified the above statment that PGM dissolution is most likely to occur at highly acidic conditions. From the results above it is implied that the use of thiocyanate in the dissolution of PGMs compels the need for an acidic environment, due to Fe(III) hydrolysis. Since PGMs are relatively inert in comparison to gold, it is expected to display enhanced dissolution at a highly acidic pH.

In summary, all PGMs in solution are highly coordinated and complex. The increased inertness of PGMs dictates the conditions required for ligand substitution, which include high concentration reagents, high temperature and prolonged reaction times.

2.7 Research approach

The literature review presented in this chapter has highlighted the potential gaps concerning the use of thiocyanate leaching for PGM extraction in concentrate/ore. Researchers (Broadhurst, 1987; Kholmogorov et al., 2002) have investigated the speciation and kinetics of gold leaching in thiocyanate solutions. Further, Li et al. (2012a) has established the chemistry and thermodynamics associated with thiocyanate leaching, with particular focus on the construction of E_h/pH diagrams for various thiocyanate systems. In addition, thiocyanate leaching of PGMs from virgin catalytic converters has been briefly explored by Kriek (2008). However, the majority of work done has been on metallic gold with inadequate focus on either Au or PGMs in the context of natural minerals and ores.

The physical chemical characteristics as well as the thermodynamic analysis suggest that PGM elements are mobile in lixiviants such as thiocyanate, which are dependent on the ligand concentration, temperature and the pH of the system. Therefore, understanding the mechanism of thiocyanate formation as well as PGM-thiocyanate complexation, are essential to optimising the extraction of Pt and Pd in low grade concentrate. Based on the literature review presented in this chapter, the following hypotheses and key questions were formulated;

Hypothesis 1 and key questions

The interaction between residual sulphidic minerals (chalcopyrite, pyrite and pyrrhotite), including reduced sulphur species (polysulphide and thiosulphate), in combination with cyanide are accountable for generation of thiocyanate in cyanide leach circuits; based on the chemical kinetics, polysulphide is primarily responsible for thiocyanate generation.

- Is the generation of thiocyanate primarily influenced by interaction between cyanide and reduced sulphur species or by the direct interaction between cyanide and sulphidic minerals?
- What is the reaction order and activation energy associated with the thiosulphate, sulphite and polysulphide in cyanide systems?
- Does the experimental conditions at which high levels of thiocyanate generation is observed correlate with the conditions apparent in platinum leaching with cyanide?

Hypothesis 2 and key questions:

Pt and Pd extraction in low grade concentrate is promoted by thiocyanate leaching, attributed to the formation of highly stable and soluble complexes relative to conventional chloride-based lixiviants.

- Is the relationship between high levels of thiocyanate formation and increased recovery of PGM coincidental or beneficial?
- Considering that thiocyanate has been feasible in the recovery of gold; does thiocyanate leaching of PGMs produce commercially beneficial results?
- Thiocyanate is not selective towards PGMs, what is the most suitable method of pre-treatment?

- Does thiocyanate and cyanide act synergistically to promote the extraction of Pt and Pd?

3. Experimental materials and methods

This chapter presents the experimental procedure undertaken to investigate thiocyanate formation and thiocyanate leaching of PGMs. The experimental work serves to verify the proposed hypotheses and fulfil the study's objectives. This chapter consists of a description of the materials, methods and analytical techniques utilised. The experimental plan proceeded in 4 phases:

1. Chemical kinetics of thiocyanate formation
2. Preliminary test work on Platreef concentrate
3. Confirmatory test work on pure minerals
4. Final test work on Merensky concentrate

3.1 Materials

3.1.1 Platreef and Merensky concentrate

Batch samples of Platreef and Merensky concentrate were used during the course of the preliminary and final test work. Platreef contains a higher Pt and Pd content compared to Merensky (Table 17 & 18); therefore it was used as a proxy material in initial tests before moving on to Merensky concentrate. The concentrates used were sourced from the MF2 (float-mill-float) recovery process at Lonmin (PLC). Prior to leaching, both the Platreef and Merensky concentrate were subjected to a rigorous sample preparation process, which is described below.

Sample preparation

A 200 kg bulk sample was split into 10 kg samples by a 2-way-riffle splitter, to ensure that samples were homogenised and thoroughly mixed. The samples were further split by a Dickie and Stockler (Pty) 10kg rotary splitter into 4kg samples, followed by further sub-sampling into 2kg samples. To attain the required sample amount for leach tests, mineral analysis and size analysis, the 10 way-1kg rotary splitter and 8 way-Rotary micro riffler were used. This guaranteed homogeneity throughout and a correct representation of the bulk sample.

a. b. c.

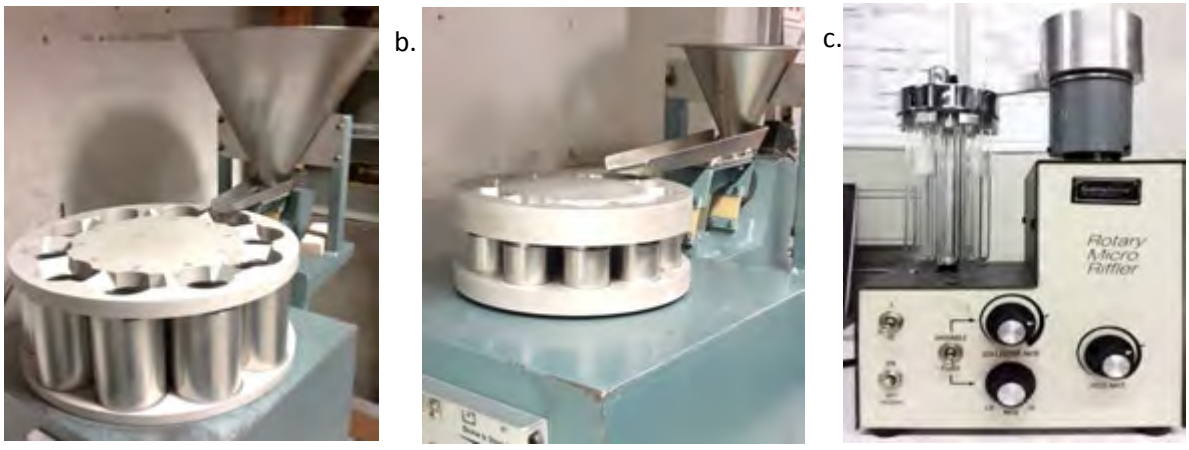

Figure 21: (a) Dickie and Stockler (Pty), (b) 10kg rotary splitter and (c) 1kg rotary splitter, Rotary micro riffler

Elemental analysis

Elemental analysis of Platreef and Merensky concentrate revealed the BM and PGM grade assays depicted in Table 17 and 18, respectively. Samples were analysed by UCT Chemical Engineering Analytical Lab and verified by ALS Geochemistry, an independent external laboratory. The analysis techniques used are comprehensively discussed in Section 3.4.

Table 17: Total BM and PGM analysis of Platreef concentrate

	Cu	Fe	Ni	Au	Pt	Pd
	%	%	%	ppm	ppm	ppm
ALS	2.04	14.55	2.94	3.19	22.3	23.8
UCT	2.23	15.62	3.21	3.25	21.2	27

Table 18: Total BM and PGM analysis of Merensky concentrate

	Cu	Fe	Ni	Au	Pt	Pd
	%	%	%	ppm	ppm	ppm
ALS	0.45	11.4	0.943	1.07	15	10.15
UCT	0.39	9.09	0.83	1.12	14.25	11.36

Size analysis

Size analysis of the concentrate was completed by using a Malvern Master Sizer Long Bench and standard vibrating wet screening tests. The size distributions for both Platreef and Merensky are displayed in Table 19, below.

Table 19: Size distribution analysis

Screen sizes (µm)	% passing	
	Platreef	Merensky
75	97%	97%
45	97%	97%
38	83%	88%

3.1.2 Pure minerals

Synthetic platinum (IV) sulphide (cooperite) and platinum sponge used in the confirmatory tests were manufactured by Alfa Aesar and supplied by Industrial Analytical. The certificate of analysis revealed that platinum (IV) sulphide consisted of 75.12% Pt with < 100 ppm total metallic impurities. Platinum sponge contained 99.998% Pt (metal basis) with <100 ppm total metal impurities. However, platinum arsenide (sperrylite) used in this study was in the natural form, sourced from the Sudbury deposit in Canada. SEM analysis revealed that natural sperrylite comprised of 55.13% Pt and 44.87% As.

3.1.3 Reagents

Various reagents were used throughout the study in line with the experimental plan. For the pre-treatment of Platreef concentrate, ammonium carbonate and aqueous 25% ammonia were utilised for the leaching of BMs. Additionally, ferrous sulphate and 98% sulphuric acid were used to make up the feedstock solution required for the bioleach. Sodium thiocyanate, sodium cyanide, ferric sulphate and potassium hexacyanoferrate(III), also known as potassium ferricyanide, were used in the extraction of PGMs in pure minerals and Merensky concentrate. Lastly, sodium sulphite, sodium thiosulphate and potassium polysulphide were used in the kinetic study. All reagents were acquired from Merck apart from ferricyanide and potassium sulphide which was acquired from Sigma Aldrich. The leaching solutions prepared comprised of known volumes and masses of reagents (reagent grade) in distilled water; this is described in further detail in the respective sections.

3.2 Equipment

3.2.1 Column reactors

Column reactors were used in this study specifically for the ammonia leach and bioleach pre-treatments as well as the final thiocyanate leach experiments. The advantage of using a column is the ability to simulate heap leaching as well as to generate large amounts of pre-treated concentrate that can be used in the secondary leach step, i.e. thiocyanate leach. The columns used in this study were 0.5m in height with a diameter of 0.09m. The columns were fitted with a heating coil in order to generate the desired temperature as well as a thermocouple to monitor the temperature within the ore bed. In addition, there was a feed inlet which allowed the flow-through of feed solution via a peristaltic pump and an outlet which enabled the collection of the pregnant leach solution (PLS). Lastly, the column comprised of a gas inlet and outlet which permitted the flow through of compressed air. A representation of the column and the experimental setup are shown in Figure 22.

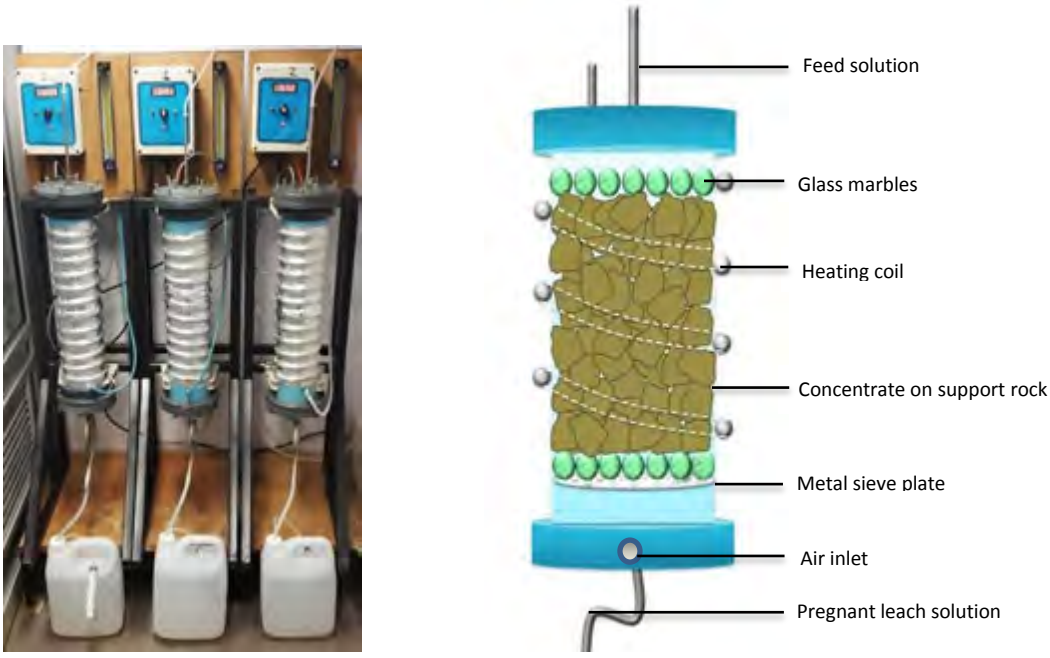

Figure 22: Schematic of column and experimental setup

GEOCOAT preparation

The GEOCOAT© process incorporates the coating of fine concentrate onto support media which is packed in a heap. This method of packing allows adequate inter-spatial channels within the heap and sufficient contact time between the concentrate and the solution (Mwase, Petersen & J J Eksteen, 2012).

For the GEOCOAT preparation, approximately 650g of concentrate was mixed with deionised water to form a slurry with a solid to liquid ratio of 5:3. The slurry was coated evenly onto 3.5kg granite pebbles (support rock) and packed in columns. The method used to determine the amount of concentrate added is further described in the Appendix A.

Figure 23: (a) Slurry coated onto support rock and (b) column packed with coated support rock.

Packing of columns

A 6cm layer of glass marbles was placed at the bottom of the column which permitted the distribution of air. On top of this, the column was loaded with the coated granite pebbles and packed to 2/3 of the column's height. The top layer was covered by an additional 6 cm layer of glass marbles which allowed for the even distribution of feed solution.

Pump calibration

The feed solution was supplied via a peristatic pump. The pump was calibrated to a feed rate of 1L/day. This slow rate enabled small quantities of feed solution to be transferred to the column to allow absorption onto the coated granite. The pump was calibrated using deionised water. To achieve a rate of 1L/day (3.5mL/5min), deionised water was pumped into a measuring cylinder for 5 minutes. The pump speed was adjusted to achieve the desired rate.

Recovery of concentrate

On completion of the column leach, the columns were unpacked to recover the concentrate for a second leach step as well as for analysis. The coated granite was released from the columns into a 20L bucket. The concentrate was washed off the granite and glass marbles. To ensure effective separation between the concentrate and support rock a

85µm sieve was used to wash the slurry from fine granite pebbles. The contents recovered were filtered using a pressure filter press. The filter cake obtained was dried, weighed and sampled for analysis.

3.2.2 Batch stirred tanks reactors

Batch reactors were used for experiments with a low solid loading, <10%. These reactors were specifically chosen for the preliminary thiocyanate leach, pure mineral leach and lastly the thiocyanate kinetics study. Two setups were adapted, for the preliminary thiocyanate leach, 1L jacketed reactors were used along with a 2 blade mechanical stirrer and Pyrex baffles. Whereas for the pure mineral leach and kinetic study, 500mL jacketed reactors were utilised. However, in these particular experiments magnetic stirrers, magnetic stirrer bars and Pyrex baffles were used to agitate the solution as it proved to be much more versatile as opposed to the mechanical stirrer. The desired temperature was maintained with a circulatory water bath. Likewise, the jacketed reactor enabled even distribution of heat. For the leaching experiments compressed air was sparged into the reactors, while N_2 gas was sparged into the reactors that were used in the thiocyanate kinetic study.

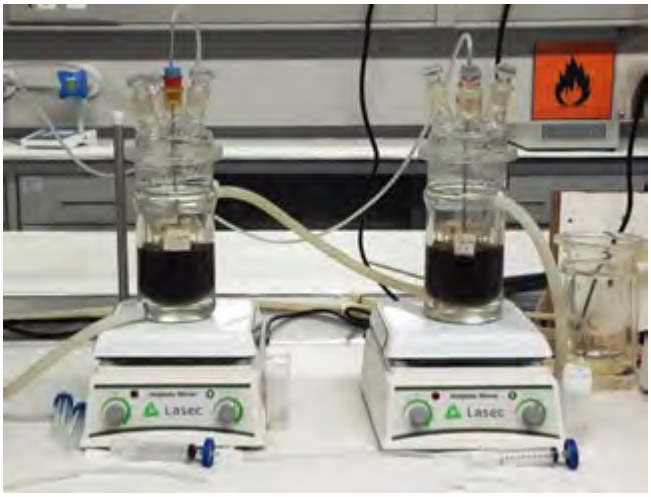

Figure 24: Experimental set-up of batch stirred tank reactors.

3.3 Methods

The general procedure undertaken in each experimental phase is described in the relevant sections. Section 3.3.1 provides the experimental plan carried out to investigate the chemical kinetics of thiocyanate formation, while Section 3.3.2 describes the preliminary thiocyanate leach experiments conducted on Platreef concentrate. To further validate the ability of thiocyanate to dissolve Pt and Pd, tests were conducted on pure minerals, demonstrated in Section 3.3.3. Having established the operational conditions leading to enhanced Pt and Pd recovery, final test work was carried out on Merensky concentrate, using dual lixiviant systems described in Section 3.3.4.

3.3.1 Phase 1: Chemical reaction kinetics of thiocyanate formation

The chemical reaction kinetics of cyanide and reduced sulphur species, namely thiosulphate, sulphite and polysulphide, in aqueous solution were investigated. The conditions used during these experiments were ideally adaptations of the conditions experienced within the column where thiocyanate formation was observed.

For this series of experiments, the concentration of the sulphur species was varied to establish the reaction order; similarly the temperature was adjusted to determine the activation energy. Known masses of the sulphur species and 1 g/L cyanide was added to a buffered solution comprising of 9.3 g/L sodium carbonate and 1g/L sodium bicarbonate (pH>10), with each experiment conducted in duplicate.

To prevent further oxidation of the sulphur species, nitrogen gas was gently sparged into the 500mL reactors. The temperature was maintained by means of a circulatory water bath, and all experiments were conducted in a fume hood to limit the exposure to cyanide. The experimental plan for the thiosulphate-cyanide system is listed in Table 20.

Table 20: Experimental plan used in determining the reaction order and activation energy in thiosulphate and cyanide reaction

	Mole ratio ($S_2O_3^{2-}$:CN^-)	Temperature
Reaction order	5:1	60°C
	3:1	60°C
	1:1	60°C
Activation energy	1:1	75°C
	1:1	60°C
	1:1	45°C

The initial experiments conducted on thiosulphate ran for approximately 4 hours. However to obtain a more accurate representation of the initial reaction rates, repeat experiments ran for only 2 hours, but were sampled much more frequently, at 20 minute time intervals.

According to the equations listed below, the formation of sulphite in the thiosulphate-cyanide system may possibly alter thiocyanate levels. As a result, the chemical kinetics between sulphite and cyanide were explored in 2 experiments at 1:1 and 5:1 molar ratio at 45°C.

$$S_2O_3^{2-} + CN^- \rightleftharpoons SO_3^{2-} + SCN^-$$

$$H_2O + 3SO_3^{2-} + CN^- \rightleftharpoons 2SO_4^{2-} + SCN^- + 2OH^-$$

Initial experiments carried out on polysulphide demonstrated extremely fast reaction kinetics under the similar conditions used for thiosulphate. Consequently, these operating conditions proved to be extremely challenging in terms of quantifying the rate and reaction orders involved. Hence the temperature and concentrations were lowered for the corresponding polysulphide experiments (Table 21).

Table 21: Experimental plan used in determining the reaction order and activation energy in polysulphide and cyanide reaction

	Mole ratio (S_2^-:CN^-)	Temperature
Reaction order	1.12:1	25°C
	0.56:1	25°C
	0.28:1	25°C
Activation energy	0.56:1	45°C
	0.56:1	35°C
	0.56:1	25°C

During the experimental sampling, the reaction was inhibited with the immediate addition of ferrous sulphate solution (0.5M) to the sample. The addition of ferrous sulphate to a cyanide containing solution, enables the immobilisation of free cyanide as an insoluble precipitate, $Fe_4[Fe(CN_6)]_3$ better known as Prussian blue (Adams, 1992):

$$7Fe^{2+}_{(aq)} + 18CN^-_{(aq)} + O_2 + 4H^+ \rightleftharpoons Fe^{III}_4[Fe^{II}(CN)_6]_3 + 2H_2O$$

Subsequently, the solution was filtered and analysed for thiocyanate using the ferric nitrate assay described in Section 3.4.

3.3.2 Phase 2: Preliminary test work on Platreef concentrate

This experiment explores the use of ammonia leaching to extract base metals, Cu and Ni followed by a thiocyanate leach to extract Pt and Pd. The presence of acid consuming gangue established the need for an acid wash before progressing to the thiocyanate leach. Thiocyanate leaches conducted in this phase was an adaptation of the experimental plans used for gold leaching described in Section 2.6. A general outline of the experimental procedure is depicted in Table 22.

Ammonia leaching

For the ammonia leach, approximately 600g of Platreef concentrate was packed into a column using the GEOCOAT method. A 6M ammonia solution was pumped into columns at a rate of 1L/day which continued for 40 days. The solution comprised of 1M $(NH_4)_2CO_3$ and 4M NH_4OH. Columns operated at 40^oC and compressed air was sparged in at a rate of 80mL/min. The pregnant leach solution was collected in a 5L container and recycled as feed within a period of 3 days. Thereafter the solution was replaced every 3 days after sampling. During this stage, base metals such as copper, nickel and cobalt were extracted. On completion, the concentrate was washed, filtered, split and subjected to a sulphuric acid leach.

Sulphuric acid wash

Pre-treated concentrate underwent a 1M sulphuric acid leach in batch reactors with a 10% solid loading, 100 g of concentrate in 1L solution. This ran at 45^oC and at 400 rpm for a period of 2-24 hours before advancing to the thiocyanate leach stage.

Thiocyanate leach

Thiocyanate leaching was conducted in batch stirred tank reactors. The batch reactors ran for approximately 8 days with a 10% solid loading, 100 g of concentrate in 1L solution. The system operated at a temperature of 50^oC, 400rpm and a pH of 2-4. The thiocyanate concentration was varied at 0.2M and 0.3 M, to establish which led to better recovery. Samples were taken within the first four hours and on a daily basis for a period of 8 days.

Table 22: General outline of preliminary test work on Platreef concentrate

Preliminary test	Ammonia leach • $(NH_4)OH$ (4M) • $(NH_4)_2CO_3$ (1M) • 40^oC • pH 9.6 -10.4 • 40 days	Sulphuric acid leach • H_2SO_4 (1M) • 50^oC • pH: 0.5-0.7	Thiocyanate leach • NaSCN (0.2 & 0.3M) • 50^oC • pH: 1.5-2.5 • 8 days
A	✓		✓
B	✓	✓ 1 hour	✓
C		✓ 24 hours	✓

3.3.3 Phase 3: Confirmatory test work

This phase of experimental work served to validate whether or not thiocyanate does indeed leach Pt as well as to identify the most suitable route for dissolving Pt. The experimental plan comprised of a thiocyanate leach, a cyanide leach and a mixed thiocyanate-cyanide system. In addition, the process conditions explored included the effect of pH, the oxidation state of Pt in the proxy material, the presence of chemical oxidisers as well as the influence of a mixed system as opposed to an individual system.

PGMs occur mainly in the form of sulphides, tellurides, arsenides and ferroalloys in concentrate. For this reason, high grade cooperite (Pt (IV) sulphide) and sperrylite were selected as a proxy material for confirmatory tests. Pt in synthetic cooperite occurs in the +4 oxidation state, while Pt is assumed to be in the +2 oxidation state in natural sperrylite. Therefore, to further investigate the influence of oxidation state on Pt extraction, Pt sponge was chosen accordingly as it occurs in the 0 oxidation state.

A series of small scale experiments were conducted in batch stirred tank reactors. For the confirmatory tests, 50mg of the pure mineral was added to 250mL of solution. The concentration and operating conditions are listed in Table 23, below. Thiocyanate experiments were performed in an acidic environment in the presence and absence of Fe as an oxidant, whereas all cyanide experiments were performed in an alkaline environment to prevent the formation of hydrogen cyanide. Fe precipitates under alkaline conditions and thus was omitted as an oxidiser in experiment 3 and 4. However, experiments 5 and 6 incorporated Fe in the form of ferricyanide, although its concentration was dictated by the concentration of cyanide. The pH of solutions were altered with sulphuric acid and in the case of alkaline experiments sodium carbonate (9.3g/L) and sodium bicarbonate (1g/L) were utilised. Each experiment ran for approximately 2 days. Samples were taken at 1, 2, 3, 4, 8, 24 and 30 hours.

Table 23: Experimental design used during the leaching of pure minerals

Confirmatory tests	SCN^-			CN^-		Mixed $SCN^-/CN^-/[Fe(CN)_6]^{3-}$
	1	2	3	4	5	6
pH.	1.5-1.6	1.5 – 1.6	10.5-10.6	10.6-10.7	10.6-10.7	10.6-10.7
Concentration	SCN^- =2g/L	SCN^- =2g/L	SCN^- =2g/L	CN^- = 2g/L	*CN^- = 2g/L	SCN^- = 1 g/L **CN^- = 1g/L
Temperature	50°C	50°C	50°C	50°C	50°C	50°C
Compressed air	✓	✓	✓	✓	✓	✓
Oxidiser	Fe^{3+} = 2g/l (ferric sulphate)	-	-	-	Fe^{3+} =0.4g/l (ferric cyanide)	Fe^{3+} = 0.2g/l (ferric cyanide)

* CN^- = 2g/L comprises of 1g/L CN^- from NaCN + 1g/L CN^- from ($K_3[Fe(CN)_6]$)

**CN^- = 1g/L comprises of 0.5g/L CN^- from NaCN + 0.5g/L CN^- from ($K_3[Fe(CN)_6]$)

3.3.4 Phase 4: Final test work on Merensky concentrate

After establishing the best route of extraction from the work conducted in Phase 2 and 3. It was proposed that a bioleach would be most suitable for base metal extraction, as it assisted in the removal of Cu, Ni and Fe. For PGM extraction, a dual lixiviant system (cyanide-thiocyanate) showed improved recoveries as opposed to individual systems and was thus chosen as an effective way of leaching PGMs.

Bioleach

This experiment aimed to extract the bulk of the base metals present in ore, which includes Cu, Ni and Fe. For this experiment, approximately 650g Merensky concentrate was packed into 3 separate column reactors, utilising the GEOCOAT method. Initially, the feed solution comprised of 30g/L sulphuric acid, which was fed to the column for 8 days at 50^{o}C. Thereafter, the columns were inoculated with a mixed thermophile culture at 65^{o}C. The feed solution was substituted with 10g/L sulphuric acid and 0.2g/L Fe^{2+}, in the form of ferrous sulphate. The columns were fed at a rate of 1L/day and aerated at 130mL/min. The bioleach ran for approximately 72 days. 15mL Samples were withdrawn every 3 days for AAS analysis. Upon completion the support rock was washed with deionised water to remove the concentrate. The wash water was filtered and the concentrate dried and split for the secondary leach.

Dual lixiviant system: Cyanide -thiocyanate leach

The dual lixiviant systems were used with the purpose of extracting both Pt and Pd. Once again, the 3 separate columns were packed with 400g of pre-treated concentrate using the GEOCOAT method. The feed solution was prepared by adding 9.3 g/L sodium carbonate and 1g/L sodium bicarbonate to deionised water to adjust the pH to above 10. Each column represented a varying sodium cyanide/sodium thiocyanate concentration, in the presence and absence of oxidant, potassium hexacyanoferrate(III). The concentrations are listed in Table 24. All columns operated at 50^{o}C, with a feed rate of 1L/day and aerated at 130mL/min. The columns ran for 60 days and 15 mL samples were withdrawn every 3 days for ICP-MS analysis.

Table 24: Cyanide-thiocyanate leach for Merensky ore

Reagent	Column 1 (SCN^-/CN^-)	Column 2 ($SCN^-/CN^-/[Fe(CN)_6]^{3-}$)	Column 3 ($CN^-/[Fe(CN)_6]^{3-}$)
NaSCN	1g/L SCN^-	1g/L SCN^-	
NaCN	1g/L CN^-	0.5g/L CN^-	1g/L CN^-
$K_3[Fe(CN)_6]$		0.5g/L CN^-	1g/L CN^-

3.4 Analysis techniques

3.4.1 pH and redox analysis

The pH of samples were measured using a standard CRISON pH meter. The probe was calibrated with three standard pH solutions, pH 4, 7 and 9 at the beginning of each day to ensure good precision among the readings obtained. The redox potential was measured using a Pt electrode attached to a calibrated Metrohm 827 Redox meter. The redox potential was measured with reference to a saturated Ag/AgCl electrode. The accuracy of the probe was verified against a standard redox buffer solution with a potential of 250mV at 25^{o}C (error < 1%).

3.4.2 Elemental analysis of solids

PGM analysis of the solid samples was determined by fire assay using nickel sulphide as a collector. The nickel sulphide was dissolved in aqua-regia followed by inductive coupled plasma atomic emission spectrometry (ICP-AES) to quantify the Pt, Pd and Au content with a method precision of ± 10%. Multi element analysis (Cu, Fe and Ni) was determined by sodium peroxide fusion and acid dissolution in aqua regia followed by ICP-AES analysis, with a method precision of ±7.5%. The analyses were conducted at ALS Geochemistry (Johannesburg).

3.4.3 Elemental analysis of solutions

The amount of BMs extracted in leach solutions were analysed through atomic absorption spectrometry (AAS) at UCT Analytical lab. Additionally, the PGM analysis of leached solutions was conducted at Stellenbosch University, Central Analytical Facilities using inductive coupled plasma mass spectrometry (ICP-MS). Given that the PGM extractions were relatively low, ICP-MS proved to be more beneficial in terms of analysing Pt and Pd as it has a minim detection limit of 0.02 µg/L for Pt and 0.002 µg/L for Pd. The error associated with ICP-MS analysis was reported to be 3.06% for Pt and 4.07% for Pd.

3.4.4 Thiocyanate analysis

Analysis on thiocyanate formation was determined through the use of spectrophotometry (Lahti, 2000). This technique exploits the chemical equilibrium between the thiocyanate ion (SCN^-) and the ferric ion (Fe^{3+}) which reacts to form thiocyanatoiron(III) ion ($FeSCN^{2+}$) described in Equation 2 below:

$$Fe^{3+}_{(aq)} + SCN^-_{(aq)} \rightleftharpoons FeSCN^{2+}_{(aq)} \qquad \textbf{Equation 2}$$

The formation of the $FeSCN^{2+}$ results in a deep blood-red colour which can be measured at 461nm on a spectrophotometer to quantify the concentration of thiocyanate present. For this assay a reagent comprising of 0.2M ferric nitrate, dissolved in 1M nitric acid reagent was prepared. A standard curve was generated by utilising standard SCN^- solutions comprising of 15, 25, 30, 50, 75 and 100 mg/L. To quantify the concentration of SCN^- in solution, the reagent was added to sample according to a 1:1 volume ratio. Prior to the application of this method the cyanide was removed by the addition of ferrous sulphate.

4. Results and discussion

This section presents the experimental results obtained for the respective phases of work carried out. It is aimed at developing some basic knowledge and understanding of thiocyanate formation and thiocyanate leaching of Pt in pure minerals and low grade concentrate, due to limited research in the area. It further highlights and discusses the key findings obtained.

4.1 Chemical kinetics of thiocyanate formation

An initial study was conducted on the chemical kinetics of thiocyanate formation in individual thiosulphate, sulphite and polysulphide systems to support the findings obtained in literature. This section analyses the initial kinetics, reaction orders and activation energies associated with thiocyanate formation for the relevant systems. The findings presented in this section were based on the experimental work and analyses carried out by Burcher-Jones and Lodewyk (2015) under the author's guidance.

In order to determine the reaction order and rate constant with respect to the sulphur source, the van't Hoff's differential method was used. For these experiments, the concentration of the sulphur source was varied at a fixed cyanide concentration and fixed temperature. This procedure was based on the following general kinetic equation:

$$\frac{d}{dt}\left[SCN^-\right] = r_{S_{source}} = k_{S_{source}}\,[S_{source}]^i \qquad \textbf{Equation 3}$$

The equations listed above can be rearranged to a logarithmic expression:

$$\ln\left(\frac{d}{dt}\left[SCN^-\right]\right) = \ln k_{S_{source}} + i\,\ln[S_{source}] \qquad \textbf{Equation 4}$$

Thus a plot of $\ln\left(\frac{d}{dt}\left[SCN^-\right]\right)$ vs. $i\,\ln[S_{source}]$ gives rise to a straight line where the gradient, i, is the reaction order and the y-intercept = $\ln k_{S_{source}}$ can be rearranged to determine the rate constant. $k_{S_{source}}$ is the specific rate constant $\left(hr^{-1}\right)$, i is the reaction order of the sulphur source, and $[S_{source}]$ = molar concentration of the sulphur source ($mol.L^{-1}$)

The activation energy, E_a, was established by varying the operational temperature at fixed molar concentration (sulphur source: cyanide). The E_a was calculated using the Arrhenius equation:

$$k_{S_{source}} = A_{S_{source}} \exp\{E_{a,S_{source}}/RT\} \qquad \textbf{Equation 5}$$

The logarithmic expression of the Arrhenius equation is as follows:

$$\ln\left(k_{S_{source}}\right) = -\frac{E_{a,S_{source}}}{R}\,\frac{1}{T} + \ln(A_{S_{source}}) \qquad \textbf{Equation 6}$$

Hence a plot of $\ln\left(k_{S_{source}}\right)$ vs $\frac{1}{T}$ will produce a gradient of $-\frac{E_{a,S_{source}}}{R}$ with a y-intercept of $\ln(A_{S_{source}})$. A is a pre-exponential factor, $E_{a,S_{source}}$ is the activation energy ($kJ.mol^{-1}$), R is the universal gas constant (8.314 $J.K^{-1}mol^{-1}$) and T is the temperature (K).

As previously mentioned a series of tests were conducted, in order to ascertain the influence of thiosulphate, polysulphide and sulphite on thiocyanate conversion. From Figure 25 it was apparent that an increase in thiosulphate molar ratio led to increased thiocyanate conversion. The 1:1, 3:1 and 5:1 molar ratio experiments obtained an average initial rate of $1.51x10^{-10}$, $5.08x10^{-10}$ and $6.81x10^{-10}$ $mol.L^{-1}.s^{-1}$, respectively. The error bars depicted on these curves is the error associated with spectrophotometric analysis, as samples were analysed in triplicates.

Sulphite is formed as a by-product during the reaction between thiosulphate and cyanide. Therefore, in order to determine the impact it has on thiocyanate levels, the reaction between sulphite and cyanide was studied. From the results presented in Figure 26 it can be seen that at different molar ratios there was no influence on thiocyanate formation as no measurable concentrations were obtained under the conditions studied. Therefore no further investigations to calculate the reaction order and reaction kinetics were conducted.

Polysulphide demonstrated extremely fast reaction kinetics (Figure 27), which proved to be challenging in terms of quantifying the reaction order and activation energy and hence was sampled more frequently. Therefore, the first 3 data points were used to establish the initial rates which created a high uncertainty in the gradient values obtained. An increase in polysulphide concentration was coupled with an increase in initial rates achieving $8.22x10^{-9}mol.L^{-1}.s^{-1}$ for the 0.28:1M and $2.53x10^{-8}mol.L^{-1}.s^{-1}$ for the 1.1M ratio.

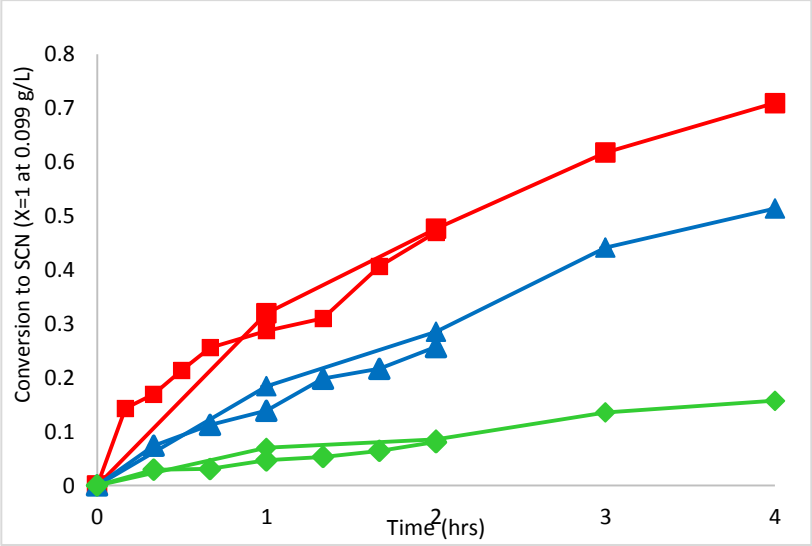

Figure 25: SCN^- concentration profile for the reaction of cyanide with ■ 5:1 ratio, ▲ 3:1 ratio, ◆ 1:1 excess thiosulphate at 60°C.

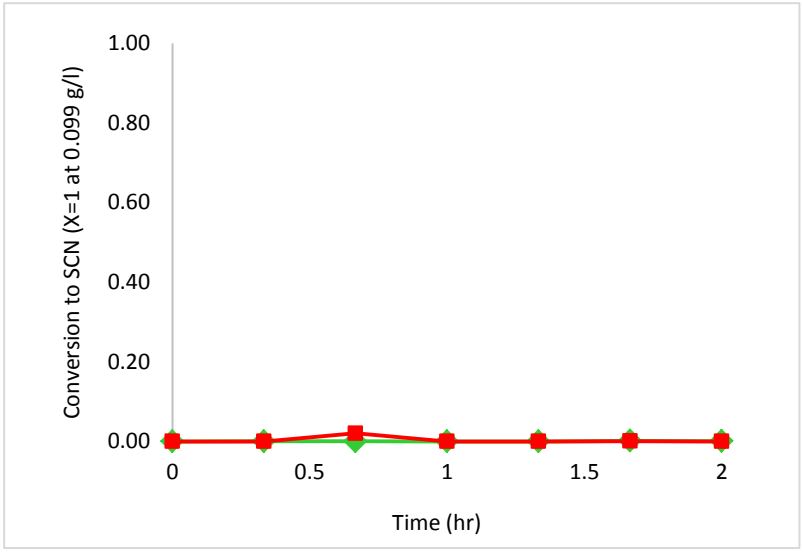

Figure 26: SCN^- concentration profile for the reaction of cyanide with ■ 5:1 ratio and◆ 1:1 ratio excess sulphite at 45°C.

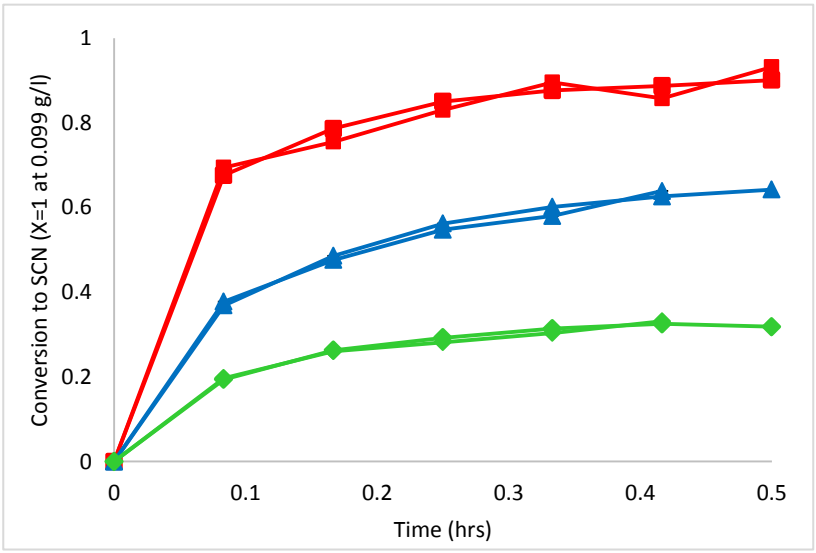

Figure 27: SCN^- concentration profile for the reaction of cyanide with polysulphide: ■ 1.12:1 ratio, ▲0.56:1 ratio, ◆ 0.28:1 ratio at 25°C.

Figure 28 displays the SCN^- concentration profile at varied temperature while maintaining a constant 1:1 molar ratio of thiosulphate to cyanide. The variation in temperature aided in determining the activation energy associated with various systems. Accordingly, there was a noticeable increase in initial rates associated with an increase in temperature. At 45°C a low initial rate for thiocyanate formation of 8.00×10^{-11} $mol.L^{-1}.s^{-1}$, was observed, whereas at 60°C and 75°C the rates were an order of a magnitude larger, achieving values of 1.81×10^{-10} and $3.94 \times 10^{-10} mol.L^{-1}.s^{-1}$, respectively. The 15°C jump in temperature resulted in the initial rates doubling.

The activation energy for polysulphide was measured at lower temperatures (25-45°C) with a 0.56:1 M ratio in excess cyanide. From the data gathered in Figure 29, it is apparent that at 25°C the reaction occurs fairly slowly with an initial rate of $1.53x10^{-8}$ $mol.L^{-1}.s^{-1}$. However, the initial rates for the 35 and 45°C experiment were $2.49x10^{-8}$ and $2.71x10^{-8}$ $mol.L^{-1}.s^{1}$, respectively which were relatively close. The reaction rates obtained for polysulphide were 2 orders of magnitude larger in comparison to thiosulphate.

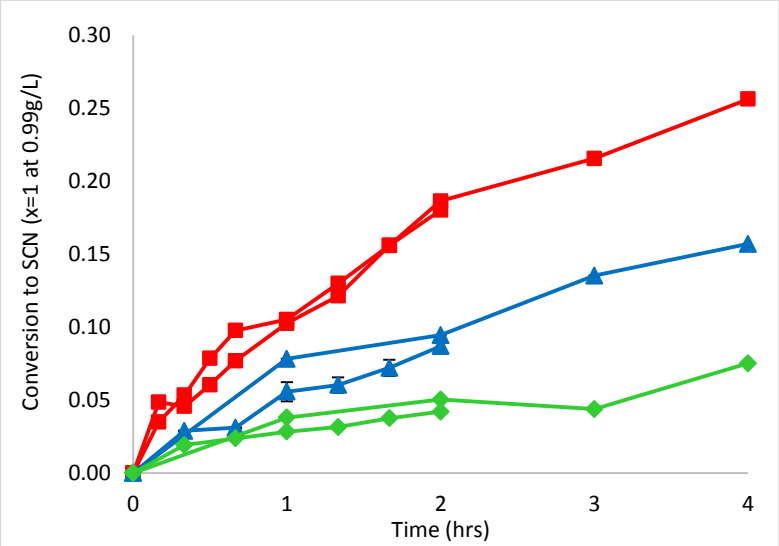

Figure 28: SCN^- concentration profile for the reaction of cyanide and thiosulphate with 1:1 M ratio at ■ 75°C, ▲ 60°C and ◆ 45°C.

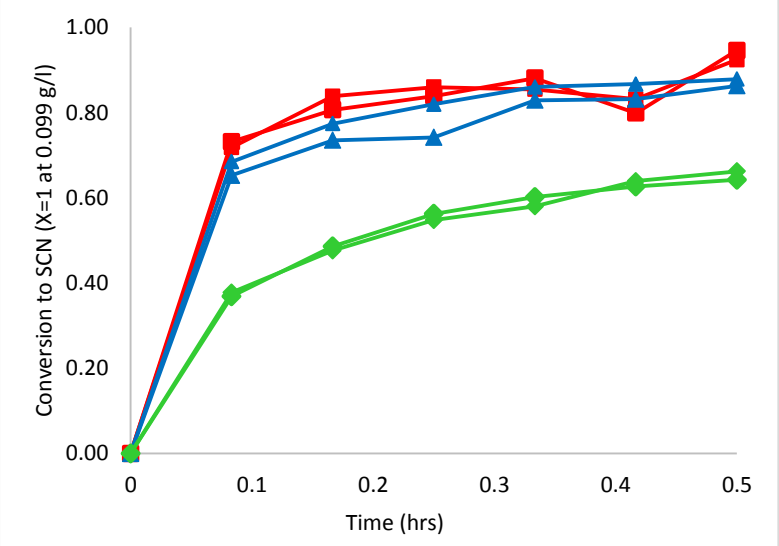

Figure 29: SCN^- concentration profile for the reaction of cyanide and polysulphide with 0.56:1 mol ratio at ■ 45°C, ▲ 35°C and ◆ 25°C.

The logarithmic plot shown in Figure 30 was used to establish the reaction order and the rate constant obtaining the equations displayed in Table 25. The reaction order of thiosulphate was determined to be 0.96 and 0.82 for polysulphide, therefore the assumption can be made that the reaction is first order with respect to these sulphur

species. A rate constant of 0.74h^{-1} was obtained for thiosulphate while polysulphide displayed a rate constant of 70.7hr^{-1}, indicating a significantly faster reaction rate.

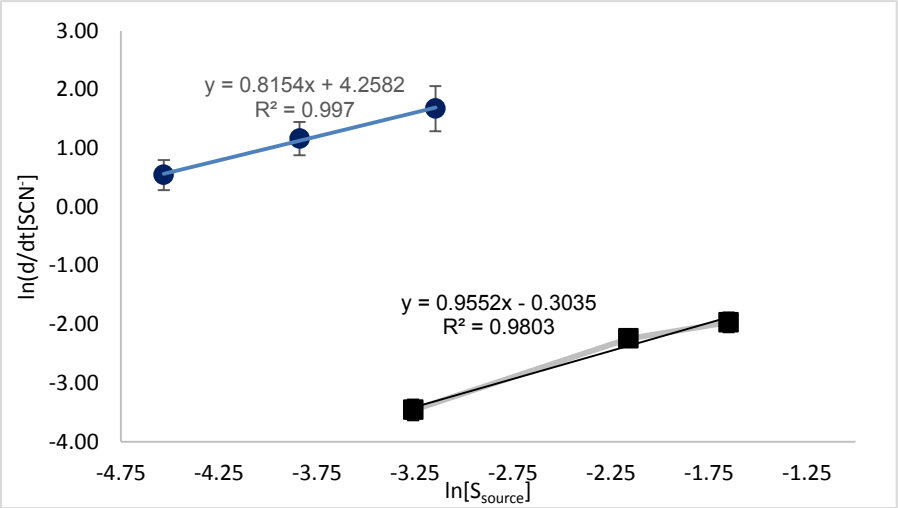

Figure 30: Initial rate kinetic data for the ■ thiosulphate-cyanide and ● polysulphide-cyanide reaction.

Table 25: Reaction rate equation for thiosulphate and polysulphide in cyanide systems

Thiosulphate	$r_{S_2O_3^{2-}}=(0.74\pm0.25)\left[S_2O_3^{2-}\right]^{(0.96\pm0.14)}$
Polysulphide	$r_{S_x^{2-}}=(70.7\pm12.4)\left[S_x^{2-}\right]^{(0.82\pm0.04)}$

Reaction rate expressed as (mol.L^{-1}.hr^{-1}) and rate constant expressed as (hr^{-1})

Using the Arrhenius equation the activation energy of thiosulphate was calculated to be 54.7kJ/mol with a pre-exponential factor of 12.3x10^{6}. Similarly, the activation energy for polysulphide was determined to be 17.8 kJ/mol with a pre-exponential factor of 2.83x10^{3}. The high uncertainty associated with this equation is primarily due to the similarities in the gradient.

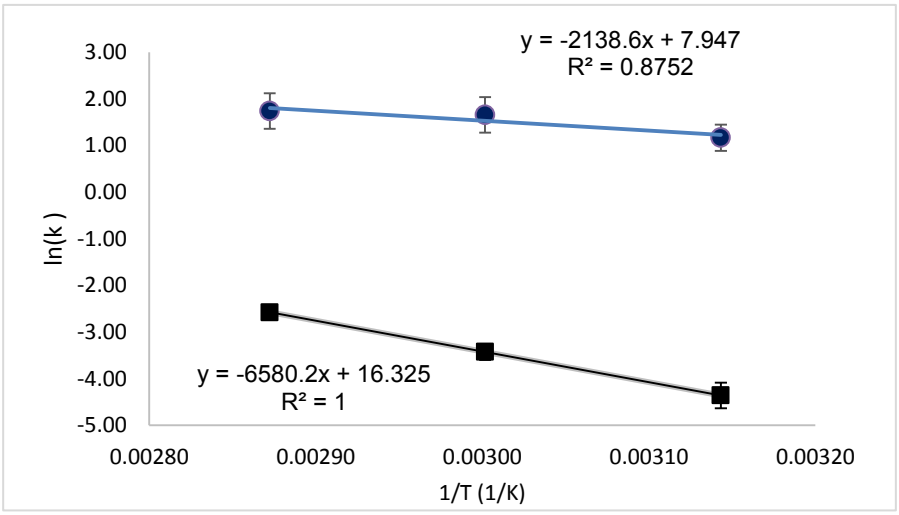

Figure 31: Linear plot of rates against the inverse of absolute temperature for ■ thiosulphate-cyanide and ● polysulphide-cyanide reaction.

Table 26: Activation energy equation for thiosulphate and polysulphide in cyanide systems

Thiosulphate	$k_{S_2O_3^{2-}}=(12.3\pm0.2\times10^6)\exp\left\{-\frac{(54.7\pm0.1)\text{kJ/mol}}{RT}\right\}$
Polysulphide	$k_{S_x^{2-}}=(2.83\pm31.8\times10^3)\exp\left\{-\frac{(17.8\pm6.7)\text{ kJ/mol}}{RT}\right\}$

Rate constant expressed as (hr^{-1}) and activation energy expressed as (kJ/mol)

Discussion

The main aim of this experiment was to explore the chemical reaction kinetics related to thiocyanate formation involving reduced sulphur species and cyanide. Generally, the trends observed for the rates of thiocyanate formation in individual thiosulphate and polysulphide systems were in agreement with literature (Luthy & Bruce, 1979). The cyanide-polysulphide system displayed the fastest reaction kinetics (Table 27) in relation to the thiosulphate-cyanide system. Additionally, sulphite exhibited no affinity for cyanide resulting in no measurable concentration of thiocyanate.

Table 27: Kinetic coefficients for thiosulphate-cyanide and polysulphide-cyanide systems

Compound	Formula	Rate constant (hr^{-1})	Reaction order	Activation energy (kJ/mol)
Thiosulphate	$S_2O_3^{2-}$	0.74	0.96	54.7
Polysulphide	S_XS^{2-}	70.7	0.82	17.8

The reaction rate constant for thiosulphate at 60°C was determined to be $0.74hr^{-1}$, while in a previous study (Bartlette and Davis, 1958) a rate constant of $1.058hr^{-1}$ was achieved at an increased temperature of 70°C. Similarly, an activation energy of 54.7 kJ/mol was achieved for thiosulphate, which was comparable to Bartlett & Davis's (1958) findings, who obtained an activation energy of 54.39kJ/mol at equimolar concentrations of thiosulphate and cyanide. From the experiments conducted, polysulphide revealed a reaction order of 0.82, while Luthy and Bruce (1979) achieved a reaction order of 0.87 at pH 10. Therefore the findings achieved in this study were in accordance with literature.

The different rates observed could be attributed to the different oxidation states that sulphur exists in the various species. For sulphite, sulphur is present in the +4 oxidation state, whereas for thiosulphate and polysulphide the terminal sulphur is present in the -2 oxidation state. Consequently a reduced sulphur species containing sulphur in the -2 oxidation is most likely to form thiocyanate (Botz, 2001) due to sulphur occupying the -2 oxidation state in thiocyanate (Table 28).

Table 28: Oxidation states of elements in thiocyanate related compounds

Compound	Formula	Element oxidation state			
		C	N	S	O
Thiosulphate	$S_2O_3^{2-}$	-	-	-2 and +6	-2
Sulphite	SO_3^{2-}	-	-	+4	-2
Polysulphide	S_XS^{2-}	-	-	-2	-
Thiocyanate	SCN^-	+4	-3	-2	-

Mwase et al. (2014) observed approximately 35-40% sodium cyanide conversion to thiocyanate within the first 4 days of the column leach. This behaviour was seen in both the 25 +1mm (column 1) and -6+1mm (column 2) sized ores they tested. It is believed that unreacted sulphidic minerals, especially pyrite, pyrrhotite and chalcopyrite, were not directly involved in the formation of thiocyanate. The kinetics associated with these systems is extremely slow, as discussed in Chapter 2.4.1. According to Wilmot (1997), these systems operated for approximately 80 days, with chalcopyrite being the only mineral that reacted completely with cyanide within 45 days. This serves to verify that reduced sulphur species generated during the bioleach were most likely responsible for SCN^- formation, and not the direct interactions between sulphidic minerals and cyanide.

From the results obtained it is postulated that the polysulphide-cyanide system dominates in the presence of other reduced sulphur species and hence is responsible for thiocyanate formation.

4.2 Preliminary test work: Platreef concentrate

4.2.1 Ammonia leaching

This experiment explores the use of ammonia leaching to extract base metals, Cu and Ni followed by a thiocyanate leach to extract Pt and Pd in Platreef concentrate (Table 17). An extensive study by Muzawazi (2013), on ammonia leaching of Platreef concentrate in columns showed favourable base metal recoveries, achieving 65% Ni and complete extraction of copper within a 40 day period. Ammonia leaching displays faster leaching kinetics, relative to a bioleach and was thus chosen for this particular reason.

Figure 32 (a) and (b) displays the Cu and Ni extractions obtained during the ammonia leach. The leach curves demonstrate that complete Cu extraction was achieved within a 40 day period, whereas the maximum Ni extraction obtained within this time frame was 65%. In Figure 32(b), there is an increased rate of Ni extraction within the first 12 days after which the maximum extraction was achieved. However, this behaviour is not seen with Cu as it displayed a continuous increase in extraction. The Cu and Ni extractions were in agreement with findings observed by Muzawazi (2013). The pH and ORP values of the system were in the range of 9.5-10.5 pH and 186-230mV respectively. This was in accordance with the expected range for the formation of Cu $(NH_3)_4^{2+}$on and the Ni $(NH_3)_5^{2+}$ ammine complexes (Muzawazi 2013). The pre-treated sample underwent a secondary thiocyanate leach, which is addressed in the following section.

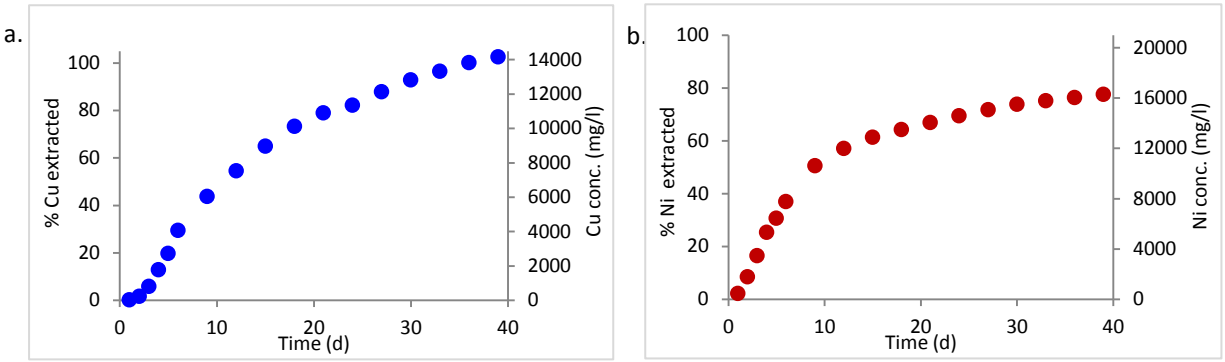

Figure 32: (a) Cu and (b) Ni extractions at 4M NH_4OH, 1M $(NH_4)_2CO_3$, 40°C, pH. 9.5-10.5 and aeration rate of 80mL/min.

4.2.2 Thiocyanate leaching

Figure 33 (a) and (b) represents the Pt extraction obtained at 0.2M and 0.3M SCN^- concentration, respectively. For the 0.2M SCN^- experiment, Sample A displayed relatively inconsistent behaviour. On day 1 the highest extraction of 0.73% was achieved followed by a decrease to 0.46% by day 4 before a further increase in extraction. During the thiocyanate leach, Sample A displayed highly unstable pH values within the first 2 days. It was expected to be within the range of 1-2.5 but displayed pH values of 5 and higher, thus the pH was adjusted regularly. It was established that the large amounts of Fe and acid consuming gangue present in concentrate were responsible for the rise in pH and prompted the need

for a sulphuric acid leach. Thus it was incorporated into experiments that followed. Sample B and C displayed a gradual increase in Pt extraction. An extraction of 0.1% was achieved in Sample B and Sample C achieved 0.08% Pt extraction by day 8.

To establish whether an increased concentration of thiocyanate led to increased Pt extraction, 0.3M SCN^- experiments were conducted. The Pt extraction improved marginally, however the same trends were displayed as the 0.2M SCN^- experiment. Once again, Sample A showed variable behaviour and Sample B and Sample C displayed a steady but slow increase. Sample A achieved the highest Pt extraction of 0.82%, Sample B obtained 0.3% and lastly Sample C obtained 0.2% by day 8

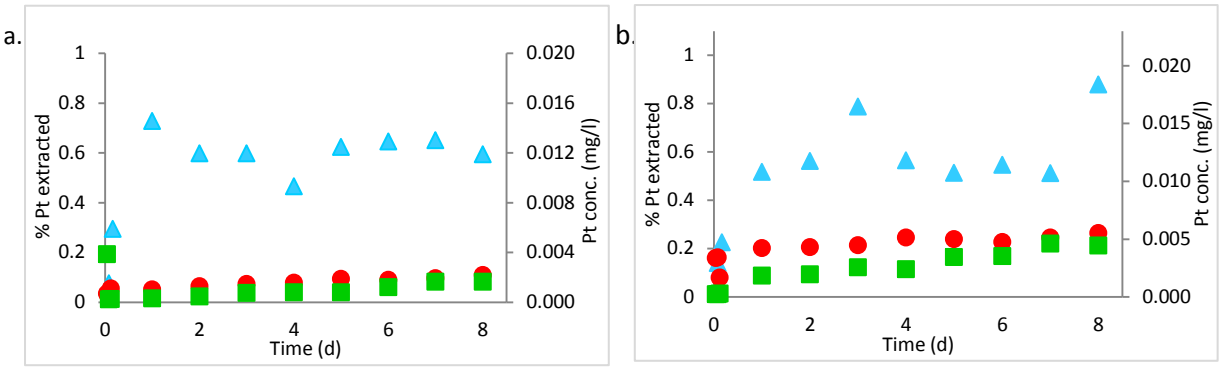

Figure 33: Pt extractions at (a) 0.2M and (b) 0.3M SCN^- concentration, 50°C, 500rpm, gentle air flow and pH. 1.5 – 2 using pre-treated concentrate: ▲ Sample A [6M NH_3] ● Sample B [6M NH_3 + 1M H_2SO_4 (1hr)] and ■ Sample C [1M H_2SO_4 (24 hrs)].

The Pd extractions achieved for the 0.2M and 0.3M SCN^- experiments are presented in Figure 34 (a) and (b). The Pd extractions were significantly higher in relation to Pt. Once more, Sample A exhibited the highest Pd extraction of 18% at 0.2M SCN^- concentration and 23% at 0.3M SCN^- concentration on day 1. After day 1 the Pd extraction decreased and by day 8 it had increased once again. The fluctuation in the results begs the question whether or not Pt and Pd may have precipitated in solution or whether they were competing with other metals to complex with thiocyanate. In contrast Sample B and C displayed minimal recoveries, achieving extractions below 15%.

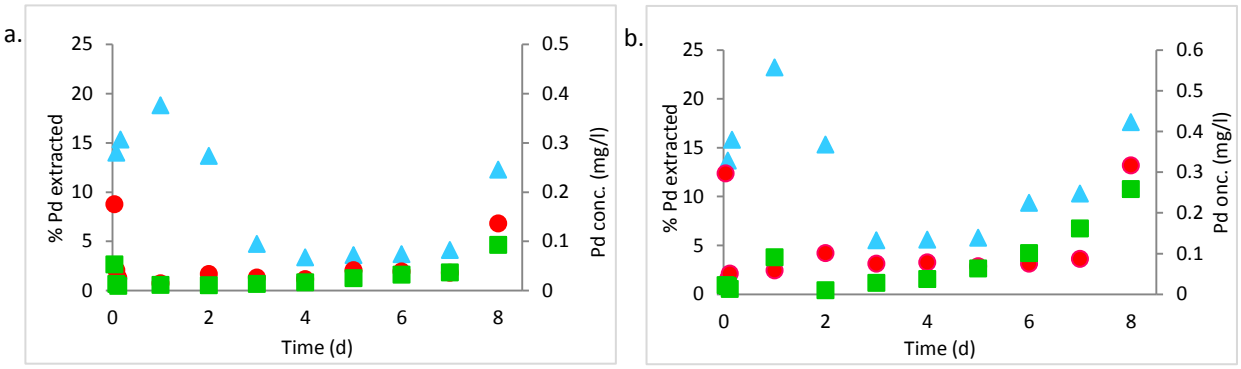

Figure 34: Pd extractions at (a) 0.2M and (b) 0.3M SCN- concentration, 50°C, 500rpm, gentle air flow and pH. 1.5 – 2 using pre-treated concentrate: ▲ Sample A [6M NH_3] ● Sample B [6M NH_3 + 1M H_2SO_4 (1hr)] and ■ Sample C [1M H_2SO_4 (24 hrs)].

4.2.3 Influence of base metal on thiocyanate consumption

The low Pt and Pd extractions may be attributed to the degree of base metal influence on thiocyanate consumption. Hence all thiocyanate samples (0.2M and 0.3M SCN^-) were analysed for Fe, Ni and Cu, which are shown in Figure 35, along with the extractions obtained during the relative pre-treatments.

Fe(III) is known to complex with thiocyanate (Li et al. 2012a) at highly acidic conditions (pH ≈ 2) and at high free thiocyanate concentrations (0.5M). It is evident that a substantial amount of the free thiocyanate was consumed by Fe(III). Approximately 5000ppm (33%) Fe(III) was extracted from Sample A, 4000ppm (25%) was extracted from Sample B and 4800 ppm (30%) in Sample C. In general, ferric that originates from sulphide mineral oxidation can be employed as an oxidant for PGM leaching. Thus ferric is known to act as complexant consuming SCN^- as well as an oxidant promoting PGM leaching.

In addition, the analysis showed high levels of Ni extraction. This confirms that, apart from the precious metals and Fe competing for thiocyanate complexation, Ni is another competitor and hence thiocyanate is not selective towards PGMs. Approximately 700ppm Ni was extracted from Sample A, 650-670ppm was extracted from Sample B. However Sample C showed significantly different Ni extractions, achieving 1764ppm and 2234ppm for 0.2M and 0.3M SCN^- concentration, respectively.

According to the results, Cu had a negligible effect on thiocyanate consumption. Sample A and B showed Cu extractions of 2ppm and 4ppm, respectively. One may argue that the bulk of Cu was removed during the ammonia leach which may have contributed to this; however, in Sample C which had not been subjected to an ammonia leach a similar trend was seen. Even though 90% of the Cu was still present in Sample C, the Cu concentrations totalled to 3ppm at 0.2M SCN^- concentration and 6ppm for 0.3M SCN^- concentration. Thiocyanate is capable of forming complexes with both cuprous (I) and cupric (II) ion which largely depends on the operating conditions. According to the E_h/pH diagram in Figure 16, the cuprous thiocyanate complex, CuSCN(s) dominates at pH 2 at a leaching potential of 0.4-0.6V. The pseudo halide feature of thiocyanate is demonstrated by the capability of forming an insoluble salt with cuprous ion and thus explains the low Cu extraction in all the Samples.

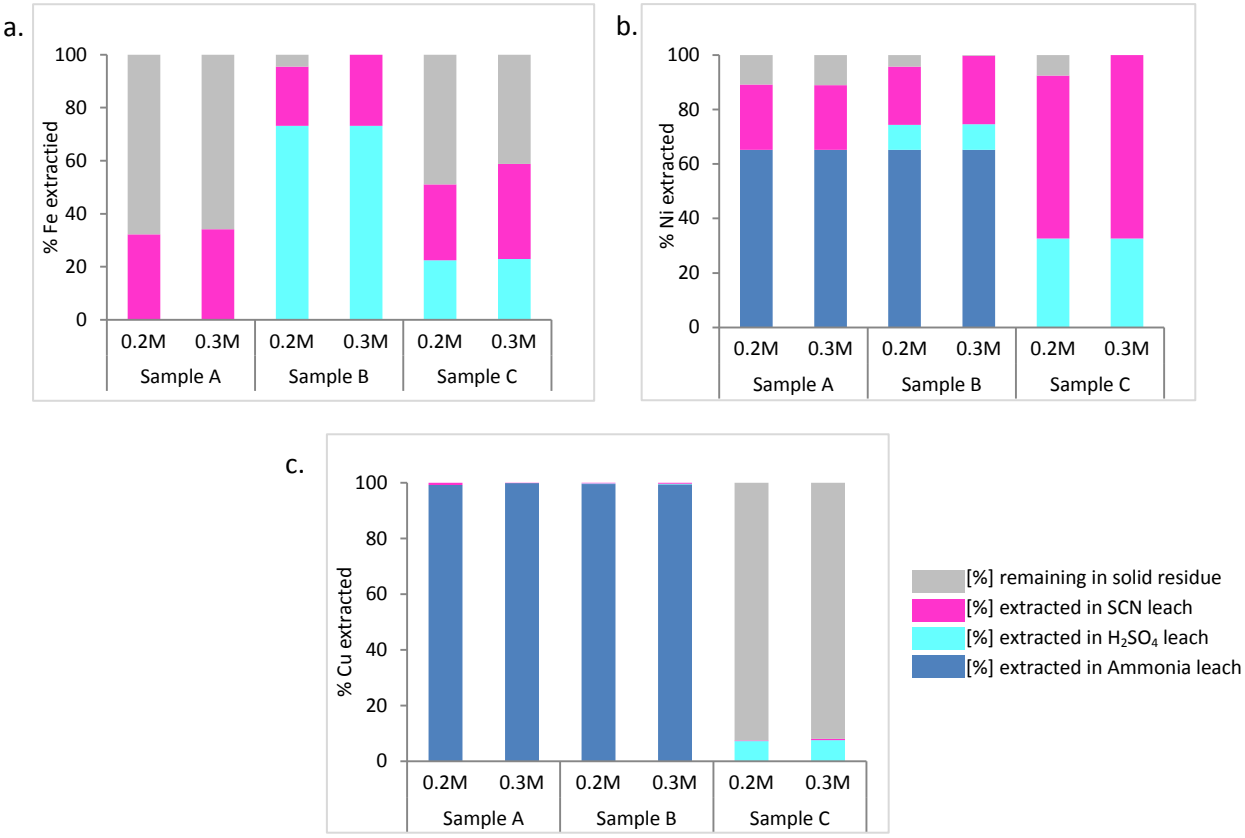

Figure 35: Stacked diagram showing the total base metal recoveries achieved during pre-treatment and thiocyanate leaching for (a) Fe (b) Ni and (c) Cu.

Discussion

In the preliminary experiments, factors such as the pre-treatment process and SCN^- concentration were investigated. From the pre-treatments that were studied, it was anticipated that Sample C would display the best results as it aided in the removal of Cu, Ni as well as Fe; however this was proven wrong as in fact Sample A demonstrated the highest extraction. More importantly, an increase in SCN^- concentration displayed improved Pt and Pd extractions, which was in agreement with the findings of Barbosa-Filho & Monhemius (1994) for gold.

Evidently the acidic thiocyanate solution in Sample A appeared to be blood red in colour. The addition of thiocyanate to ferric ions resulted in a dark red colour which reflects the formation of strong Fe^{3+}–SCN^- complexes (Dutrizac & Hardy, 1997). This reaction is described by the general equation (Lahti, 2000):

$$[Fe(H_2O)_6]^{3+} + nSCN^- = [Fe(SCN)_n(H_2O)_{6-n}]^{(3-n)} + H_2O \qquad \textbf{Equation 7}$$

However, the complex formed is largely dependent on the concentration of thiocyanate in conjunction with the solvent medium used. Some researchers suggest that a series of complexes is formed which are represented by the formula, $[Fe(SCN)_n]^{(3-n)}$ (where n= 1-6), although in dilute SCN^- solution only $[FeSCN^{2+}]$ is formed. Thiocyanate has a strong affinity

for ferric ions (Dutrizac & Hardy, 1997), this could have been a major contributing factor to low PGM extraction.

Likewise, the remaining BMs consumed a large portion of the free thiocyanate available for Pt and Pd extraction. High extractions of Ni were obtained during the thiocyanate leach, indicating a further reduced free thiocyanate concentration available for PGM leaching. With regards to Cu, it displayed a negligible behaviour on thiocyanate consumption. It is assumed that Cu-SCN forms an insoluble complex which poses a problem as this may result in loss of thiocyanate from the leach circuit due to precipitation.

The scatter in data obtained for Sample A suggests that the experiments need to be repeated to confirm the trends observed. This study provided relevant insight to base metal and thiocyanate interactions; however, no concrete conclusions were established in terms of Pt and Pd extraction. Thus several arguments were formulated to guide and further develop the existing experimental plan, as follows:

- Ammonia leaching is known to selectively extract Cu, Ni and Co (Muzawazi, 2013); however it is not capable of extracting Fe.
- Bioleaching aids in the removal of Fe which prevents consumption of free SCN^-, which may be a more suitable method of extracting BMs.
- Mwase et al. (2014) observed high Pt, Pd extractions and corresponding high thiocyanate levels in alkaline solution, therefore by adjusting the system to more alkaline pH this may possibly enhance the degree of Pt and Pd extraction.
- Pt and Pd were present as relatively low grades; the 100g solid sample used may have been too small and unrepresentative of the bulk sample.
- Samples were diluted prior to ICP-MS analysis; this could have possibly contributed to the fairly inconsistent data as it was an incorrect representation of the PLS.

4.3 Pure Mineral leach

The results gathered from the preliminary tests created an uncertainty as to whether thiocyanate is capable of leaching Pt. Therefore to further validate this thiocyanate leaching was conducted on pure minerals: cooperite, sperrylite and platinum sponge under various process conditions, described in Section 3.3.3. The use of pure minerals eliminated the interference of thiocyanate consumption by base metals and ideally allowed for studying the extraction with respect to Pt only.

4.3.1 Cooperite (platinum sulphide)

Figure 36 (a) displays the Pt extractions curves for synthetic cooperite under various thiocyanate and cyanide leach systems, while Figure 36 (b) particularly focuses on systems with lower recoveries. For both the acidic SCN^- systems, the trend displays a progressive increase with comparatively similar initial rate kinetics within the first 4 hours; however the extractions after 8 hours differ significantly. The acidic SCN^- system containing Fe^{3+} achieved a Pt extraction of 2.69%, while in the absence of Fe^{3+} an even lower extraction of 1.67% was achieved. This serves to validate that the presence of Fe^{3+} does in fact promote Pt extraction supporting the findings obtained in Section 4.2.2.

The extent of leaching observed for the alkaline SCN^-, CN^- and $CN^-/[Fe(CN)_6]^{3-}$ systems showed minimal Pt extractions. Both the alkaline CN^- and $CN^-/[Fe(CN)_6]^{3-}$ systems obtained extractions of 0.05%, the presence of hexacyanoferrate (III) as an oxidant failed to improve Pt extractions. However, the alkaline SCN^- system achieved a slightly higher extraction of 0.09%. This suggests that individual alkaline systems are not suitable for Pt dissolution.

Experiments conducted on cooperite established that the degree of extraction varies largely for the mixed ($SCN^-/CN^-/[Fe(CN)_6]^{3-}$) as opposed to individual systems. Moreover the mixed system showed the highest Pt extraction of 52.5%. Within the first 2 hours, 45% extraction was obtained, indicating extremely fast dissolution kinetics.

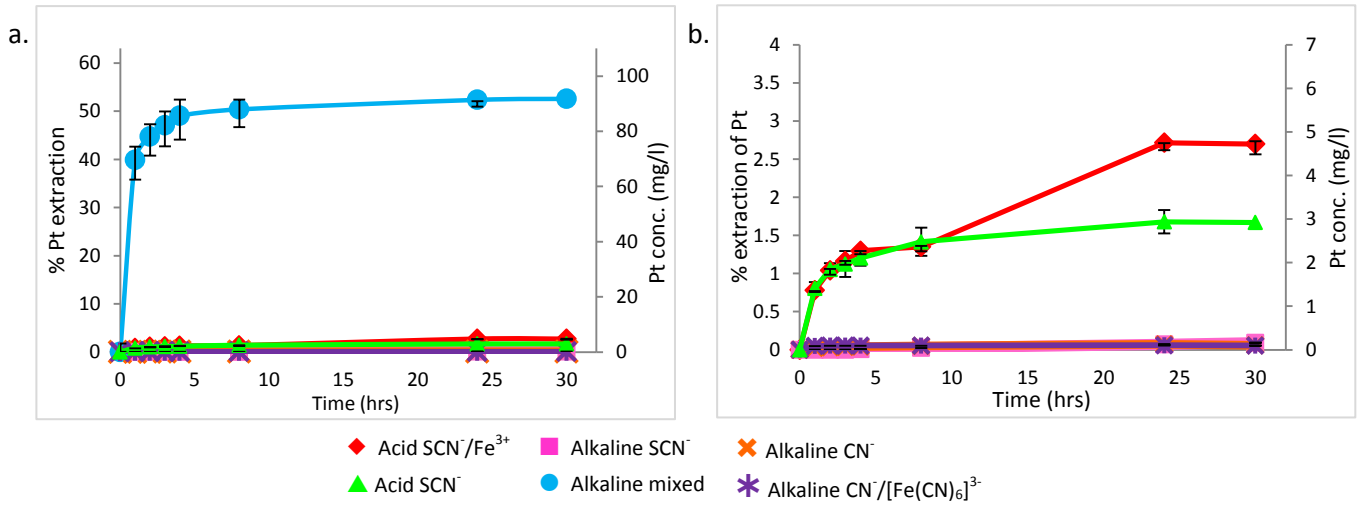

Figure 36: Pt extractions achieved for synthetic cooperite under varied conditions at 50°C and 500rpm

4.3.2 Sperrylite (platinum arsenide)

The Pt extraction curves for natural sperrylite under varied conditions are displayed in Figure 37. Sperrylite exhibits altered leaching behaviour in relation to cooperite which is apparent in the results obtained. Work done by Mwase et al. (2014) has confirmed that minerology of sperrylite may possibly be a limiting factor that contributes to extremely slow Pt leaching kinetics from Platreef ores; however he did not quantify the rates involved.

According to the results, the acidic SCN^- system comprising of Fe^{3+} obtained a negligible Pt extraction of 0.06% while in the absence of Fe^{3+}, 0.05% extraction was obtained. The alkaline SCN^- and alkaline CN^- system presented a minor increase achieving 0.13% and 0.73% Pt extraction, respectively. The trends for the above mentioned experiments were fairly linear and postulated to fit a first order rate.

The degree of Pt dissolution improved substantially for both the alkaline $CN^-/[Fe(CN)_6]^{3-}$ and the mixed ($SCN^-/CN^-/[Fe(CN)_6]^{3-}$) system. The leach trend for these systems illustrated rapid Pt extractions within the first four hours and then appeared to have reached maximum extraction after 25 hours. The use of hexacyanoferrate(III) as an oxidant proved to be advantageous in terms liberating Pt from refractory sperrylite. The $CN^-/[Fe(CN)_6]^{3-}$ leach system obtained 5.89% and the mixed alkaline system displayed the highest Pt extraction of 8.09%. Similarly, the mixed system displayed the same behaviour as observed for cooperite.

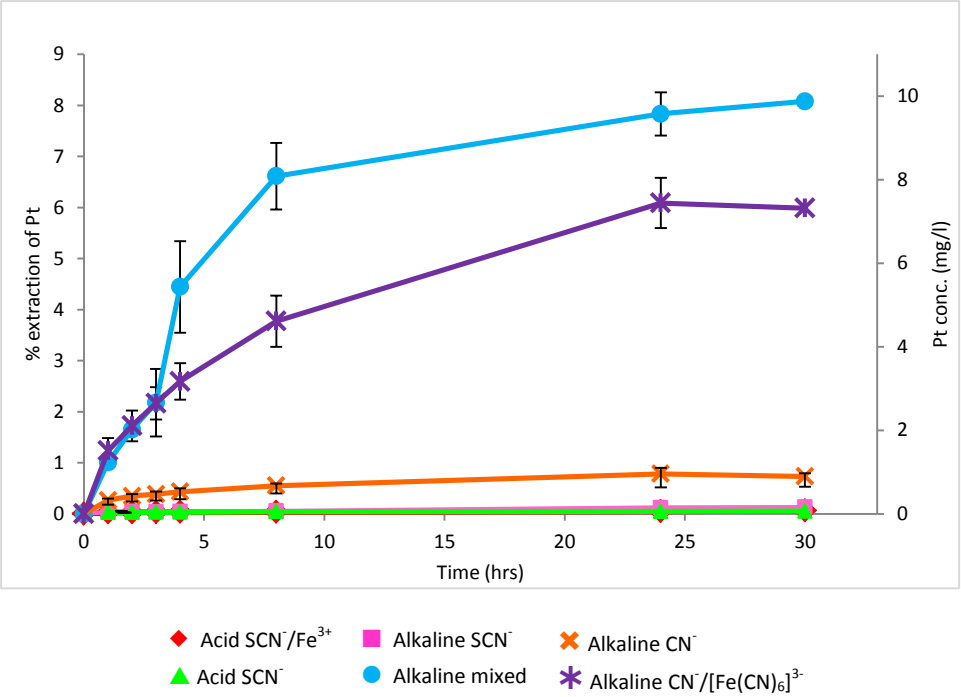

Figure 37: Pt extractions achieved for natural sperrylite under varied conditions at 50°C and 500rpm.

4.3.3 Platinum sponge

Pt occurs in the metallic state with an oxidation number of 0, in Pt sponge. Therefore it is required to be oxidised to transform from a metallic state to a soluble species. The results obtained for Pt sponge demonstrated fairly poor extractions and extremely slow leaching kinetics as presented in Figure 38.

There is a vast difference in extractions, amongst the systems containing an oxidant in comparison to systems excluding an oxidant. The acid SCN^- and alkaline SCN^- system achieved approximately 0.02% extraction whereas the alkaline CN^- system showed an extraction of 0.08%.

In contrast, the alkaline SCN^- and alkaline CN^- systems comprising of Fe^{3+} obtained extractions of 0.11%. Once again the best result was obtained for the mixed system with the highest extraction of 0.27%. These systems displayed increased extraction which is attributed to the presence of an oxidant. It is worth noting that the extractions were fairly close.

Metallic platinum has a relatively high standard reduction potential of E^o=1.118V ($Pt^{2+} + 2e^- \rightleftharpoons Pt$). Therefore Pt can only be oxidised with extremely strong oxidising agents with a reduction potential of up to 1.23V (Kriek, 2008), which is strong enough to oxidise PGMs but not water. However the oxidants used during the course of the experiments may not have been strong enough to induce a substantial amount of leaching, as the reduction potential of ferric and oxygen is relatively low. Kriek (2008) suggests that oxidants such as chlorine and hydrogen peroxide are possibly suitable for Pt^o dissolution as they have sufficiently high reduction potentials.

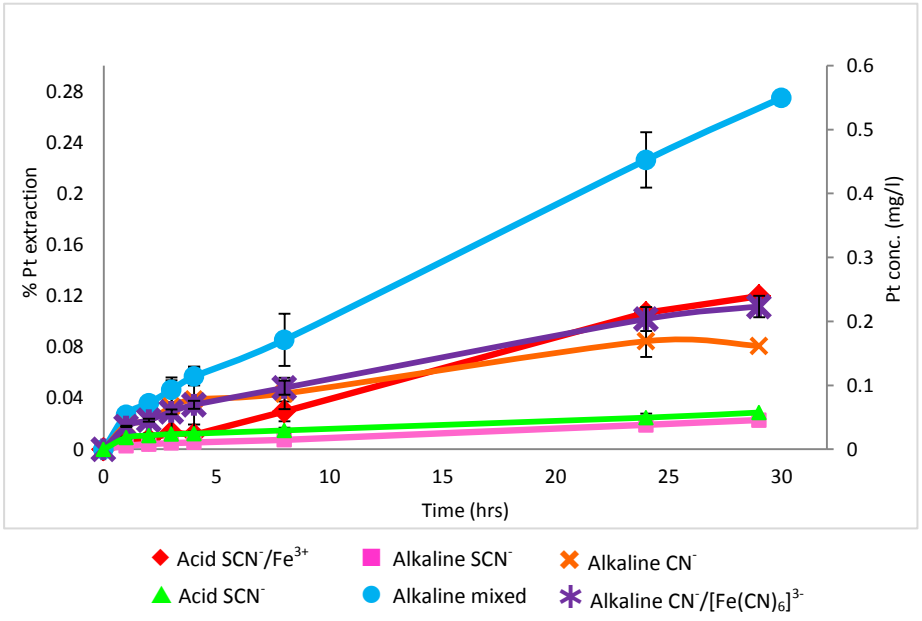

Figure 38: Pt extractions achieved for Pt sponge under varied conditions at 50°C and 500rpm.

4.3.4 ORP and pH

The ORP and pH values for the pure minerals leaches were measured to ensure that there were no substantial changes within the system. Furthermore, there are no established E_h/pH diagrams for the Pt-thiocyanate system; although Kriek (2008) has used the HSC Chemistry 6 software package developed by Outokumpu to illustrate a very basic E_h/pH diagram. Due to insufficient data on the software, the diagram was not comprehensive enough to distinguish between different complexes in the current systems and portray a realistic image of the stability regions. Figure 39 and 40 presents the pH values in both acidic and alkaline environments respectively, while Figure 41 presents the ORP values of the system.

Acid systems

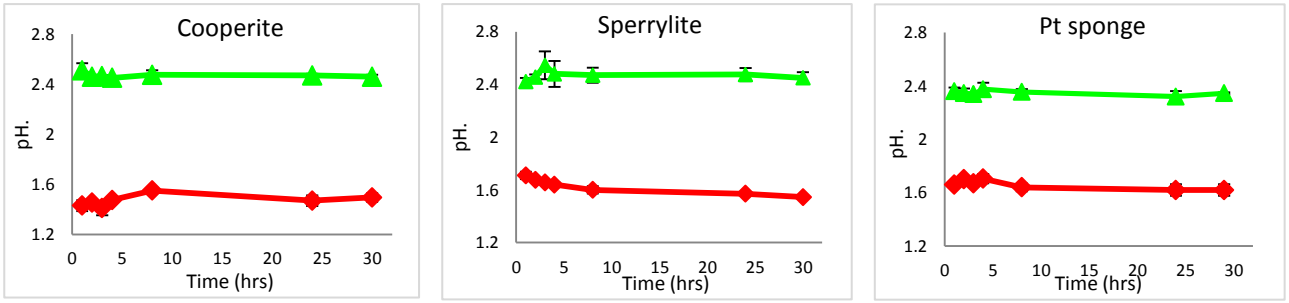

Figure 39: pH profile for cooperite, sperrylite and Pt sponge in ◆ acid SCN^-/Fe^{3+} and ▲ acid SCN^- systems.

Alkaline systems

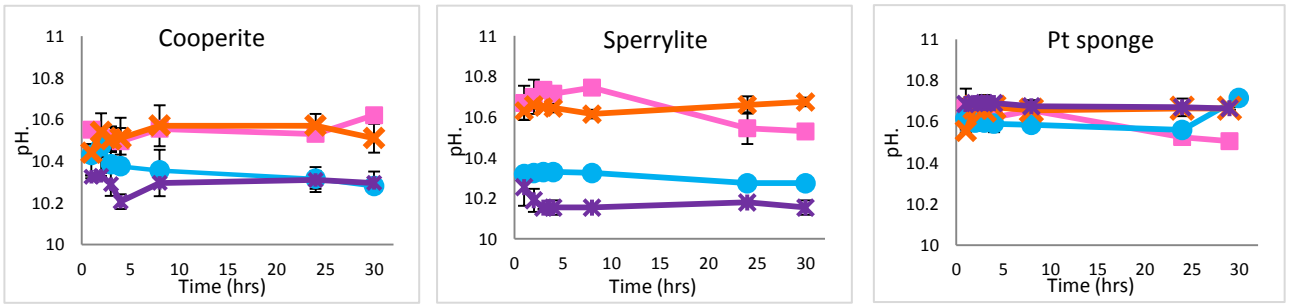

Figure 40: pH profile for cooperite, sperrylite and Pt sponge in ■ alkaline SCN^-, ● alkaline mixed, ✖ alkaline CN^- and ✱ alkaline $CN^-/[Fe(CN)_6]^{3-}$.

For the acid systems the pH was relatively consistent for all minerals. However, the system comprising of Fe^{3+} displayed lower pH values. The pH of alkaline systems was in the range of 10-11, significantly high enough to prevent the formation of hydrogen cyanide in cyanide systems. Sperrylite experiments showed a significant variation in pH values, whereas Pt sponge displayed very little difference in pH values amongst the systems studied.

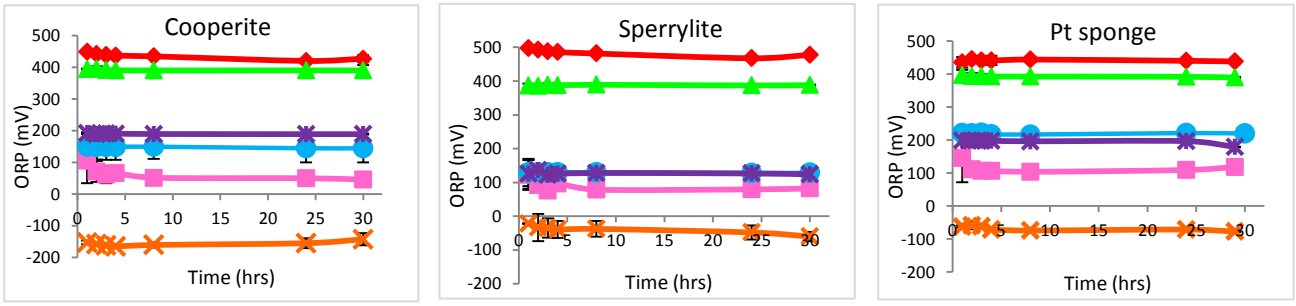

Figure 41: ORP profile for cooperite, sperrylite and Pt sponge in ◆ acid SCN^-/Fe^{3+}, ▲ acid SCN^-, ■ alkaline SCN^-, ● alkaline mixed, ✖ alkaline CN^- and ✱ alkaline $CN^-/[Fe(CN)_6$.

The leach systems operated at very different ORP levels, but these stayed more or less constant throughout the experiment in each mineral. Focusing particularly on the mixed system that obtained overall highest Pt extraction, cooperite displayed ORP values within the range of 145-150mV, while the ORP values ranged from 124-136mV for sperrylite. Lastly, the mixed system containing Pt sponge displayed ORP values between 216-220mV. The presence of ferric ion in a system increases the ORP, evidently, the systems that contained Fe^{3+} as an oxidant displayed higher ORP values in relation to those without an oxidant. The mixed alkaline system displayed improved Pt extraction coupled with intermediate ORP values whereas the SCN^-/Fe^{3+} system exhibited the highest ORP values coupled with minimal Pt extractions. It is evident that no conclusive findings could be deduced from the ORP values.

4.3.5 Reaction rates

Initial rates

The initial rates for Pt leaching in the respective systems were quantified using the first order reaction model (Table 29). The rates were calculated based on the slope of the conc. vs. time curves within the first 4 hours, applying the equation below:

$$\text{Initial rate} = \frac{\text{Slope}\left(\frac{mg}{L.s}\right)}{M_{Pt}} \times 10^{-3} \left(\frac{mol}{L.s}\right) \qquad \textbf{Equation 8}$$

where M_{Pt} is the molecular weight of platinum (195.08 g.mol^{-1}).

Table 29: Initial rate of Pt leaching in thiocyanate and cyanide solutions for cooperite, sperrylite and Pt sponge under different conditions

Experimental variable	Experimental conditions	Cooperite	Sperrylite	Pt sponge
		Initial rates (mol.L^{-1}s^{-1}) r x 10^{-10}		
Acid SCN^-/Fe^{3+}	[SCN^-]=2g/L, [Fe^{3+}]=2g/L, pH=1.5-1.6, 50°C	7.29	0.12	0.08
Acid SCN^-	[SCN^-]=2g/L, pH=1.5-1.6, 50°C	6.67	0.10	0.07
Alkaline SCN^-	[SCN^-]=2g/L, pH=10.6-10.7, 50°C	0.05	0.15	0.04
Alkaline mixed $SCN^-/CN^-/[Fe(CN)_6]^{3-}$	[SCN^-]=1g/L,*[CN^-]=1g/L, [0.2g Fe^{3+}], pH=10.6-10.7, 50°C	532.97	15.79	0.38
Alkaline CN^-	[CN^-]=2g/L, pH=10.6-10.7, 50°C	0.13	1.55	0.26
Alkaline $CN^-/[Fe(CN)_6]^{3-}$	**[CN^-]=2g/L, [0.4g Fe^{3+}], pH=10.6-10.7, 50°C	0.16	9.60	0.23

*CN^- = 1g/L comprises of 0.5g/L CN^- from NaCN + 0.5g/L CN^- from $K_3[Fe(CN)_6]$

** CN^- = 2g/L comprises of 1g/L CN^- from NaCN + 1g/L CN^- from $K_3[Fe(CN)_6]$

Overall cooperite displayed the fastest dissolution kinetics for the acid SCN^-/Fe^{3+}, acid SCN^- and the alkaline mixed system generating initial rates of 7.29x10^{-10}, 6.66x10^{-10} and 532.97x10^{-10} mol.L^{-1}.s^{-1}, respectively. According to the LFER (linear free energy relation for the formation of Pt (II)L and Pt(IV)L complexes) presented in Figure 18, Pt in the +4 oxidation state displays a higher stability constant of ≈57 when complexed with thiocyanate in comparison to Pt in the +2 oxidation state, which displays a stability constant of 33.6. The fact that Pt occurs in the +4 oxidation state in synthetic cooperite used in the experimental work, serves to explain the increased levels of extractions, as it forms relatively stable complexes with thiocyanate.

However, sperrylite dominated the cyanide systems producing initial rates of 1.55x10^{-10} and 9.60x10^{-10} mol.L^{-1}.s^{-1} for the alkaline CN^- and the alkaline $CN^-/[Fe(CN)_6]^{3-}$ systems, respectively. From this it can be assumed that thiocyanate and cyanide may possibly work synergistically to extract Pt in low grade concentrate. In other words, thiocyanate promotes the leaching of Pt from cooperite, whereas cyanide contributes to the leaching of Pt in sperrylite; this technique could be exploited to selectively dissolve Pt from both cooperite and sperrylite.

Dissolution mechanism

During the leaching process, the size of the solid mineral particles is reduced by either dissolution or reaction. Initially the reaction occurs at the outer skin of the particle. Subsequently, the zone of the reaction progresses into the solid, resulting in converted material and, in some cases, inert solid remains behind otherwise known as ash. An unreacted core of material is present that shrinks in size during the reaction (Levenspiel 1972).

In a scenario where chemical reaction occurs much faster than diffusion, the leaching process is presumed to be diffusion-controlled. This diffusion-controlled mechanism often applies when a porous layer coats the surface of the particle to be leached or leaching occurs from distinct mineral grains with an inert matrix. Consequently this results in a decrease in the extraction rate. However, as the core shrinks it gives rise to a thickening ash layer which lowers the rate of diffusion, a concept known as the shrinking core model. Resistance to diffusion through the ash layer controls the rate of reaction. For the shrinking core model particles are assumed to be spherical, the particle shrinks uniformly thus maintaining the spherical shape (Safari et al. 2009).

The shrinking sphere model constitutes a surface controlled reaction. For a chemical reaction controlled process, a concentration gradient exists within the particle. The rate of the reaction is directly proportional to the available surface of unreacted core and is unaffected by the presence of an ash layer (if there is one). The particle shrinks during the reaction over time (Lindsman & Simonsson 1978).

The data gathered from the pure mineral leach were modelled using 3 different models (Free 2013). Hence, if the model closely correlates to what essentially occurs in the system, the rate expressions obtained will be effective in predicting and describing the actual kinetics of the system.

Shrinking core model (SCM1): controlled by diffusion through inert layer

$$k_{app}t = 1 - 3(1-x)^{\frac{2}{3}} + 2(1-x) \qquad \textbf{Equation 9}$$

Shrinking sphere model (SSM2): surface chemical reaction controlled process

$$k_{app}t = 1-(1-x)^{\frac{1}{3}} \qquad \textbf{Equation 10}$$

Shrinking sphere model (SSM3): external diffusion controlled process

$$k_{app}t = 1-(1-x)^{\frac{2}{3}} \qquad \textbf{Equation 11}$$

Where x is the reacted particle and k_{app} is the apparent rate constant at time t in seconds.

The initial rates of Pt leaching for pure minerals, cooperite (PtS_2) and sperrylite ($PtAs_2$) are reported below; however these rates specify the leaching behaviour over the first four hours. Therefore, the shrinking core and shrinking sphere models were used to predict the dissolution mechanism occurring throughout the duration of the experiment (30 hours). The systems that showed overall best recoveries were modelled. The k_{app} and R^2 values for cooperite are listed in Table 30 while the values for sperrylite are listed in Table 32. In view of the fact that the shrinking core model showed the best fit in most cases, it was used as a means of comparing the k_{app} among the various systems.

From the data observed for cooperite in the acid SCN^-/Fe^{3+}, acid SCN^- and alkaline mixed ($SCN^-/CN^-/[Fe(CN)_6]^{3-}$) system it is postulated that the initial rates follow the first order rate mechanism; whereas the dissolution mechanism of the entire systems follows the shrinking core model which is verified by relatively high linear correlation coefficient (R^2) values.

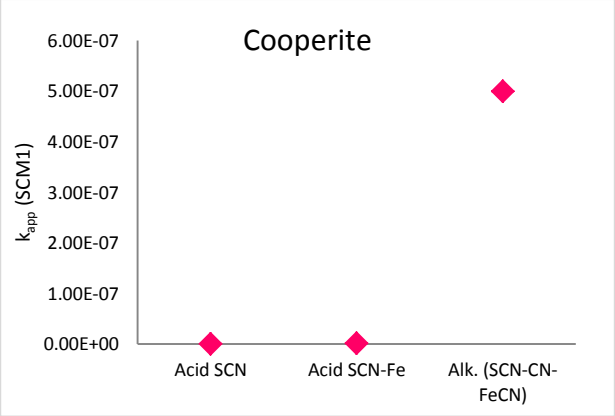

Figure 42: ◆ k_{app} using the SCM1 for cooperite

Table 30: Initial rates and k_{app} for cooperite

	1st order kinetics		SCM1		SSM2	
	r(mol/L•s) $rx10^{-10}$	R^2	k_{app} $kx10^{-10}$	R^2	k_{app} $kx10^{-10}$	R^2
Acid SCN^-	6.66	0.899	7	0.879	200	0.815
Acid SCN^-/Fe^{3+}	7.291	0.964	20	0.980	600	0.968
Alk. ($SCN^-/CN^-/[Fe(CN)_6]^{3-}$)	532.97	0.867	5000	0.934	3000	0.898

To develop an improved understanding of the trends observed, the different affinities of the anions present in the system are discussed. In addition, the possible speciation that may have occurred, are listed in Table 31 for acid SCN^- systems and Table 35 for the alkaline mixed system.

Several solution species are likely to form in the cooperite systems. However, the species formed are largely dictated by the operational conditions present in the system. In the acid SCN^-/Fe^{3+} system, the presence of ferric ions acts as an oxidant to improve the liberation of Pt from cooperite and hence an increased extraction was observed for this system. Although a minor increase was observed, it was established that $Fe_2(SO_4)_3$ was not a limiting reagent.

Initially, ferric complexes with thiocyanate which later dissociates to form platinum-thiocyanate complexes. Pt-SCN complexes are most likely to dominate in the presence of ferric ion as it displays enhanced stability.

For all acid systems it is highly unlikely for $Pt(SO_4)_3^{4-}$ species to form. Due to the soft nature of Pt, complexation with hard anions such as sulphate will demonstrate low stability, log *k* = 3.67 (Azaroual et al., 2001). Therefore it is highly improbable that sulphuric acid introduced to the system will interact significantly with dissolved platinum. Given that the leach curves for cooperite adheres to diffusion controlled mechanism, it is postulated that the formation of a passivation layer is primarily due to the hydrophobic coating of elemental sulphur.

Table 31: Chemical reactions involving cooperite in acid systems

	Acid SCN^-/Fe^{3+}	Acid SCN^-
Liberation (Cooperite)	$4Fe^{3+} + PtS_2 \rightleftharpoons Pt^{4+} + 4Fe^{2+} + 2S_0$ $4\ Fe^{2+} + O_2 + 4H^+ \rightleftharpoons 4Fe^{3+} + 2H_2O$ $2Fe(SCN)_4^- + PtS_2 \rightleftharpoons 2Fe(SCN)^- + Pt(SCN)_6^{2-} + 2S^0$ $Fe(SCN)_6^{3-} + PtS_2 \rightleftharpoons Pt(SCN)_6^{2-} + 2S^0 + Fe^{2+}$ $O_2 + 4H^+ + PtS_2 \rightleftharpoons 2H_2O + Pt^{4+} + 2S^0$	$O_2 + 4H^+ + PtS_2 \rightleftharpoons 2H_2O + Pt^{4+} + 2S^0$
Complexation	$Pt^{4+} + 6SO_4^{2-} \rightleftharpoons Pt(SO_4^{2-})_6^{2-}$ $Pt^{4+} + 6SCN^- \rightleftharpoons Pt(SCN)_6^{2-}$ $Fe^{3+} + 6SCN^- \rightleftharpoons Fe(SCN)_6^{2-}$ $Fe^{3+} + 4SCN^- \rightleftharpoons Fe(SCN)_4^-$ $H^+ + SCN^- \rightleftharpoons HSCN$	$Pt^{4+} + 6SO_4^{2-} \rightleftharpoons Pt(SO_4^{2-})_6^{2-}$ $Pt^{4+} + 6SCN^- \rightleftharpoons Pt(SCN)_6^{2-}$ $H^+ + SCN^- \rightleftharpoons HSCN$

Sperrylite showed improved dissolution in cyanide systems. Similarly, the initial rates of sperrylite followed the first order reaction mechanism and correlated closely to the shrinking core model for the alkaline CN^-, alkaline CN^-/Fe^{3+} and alkaline mixed system.

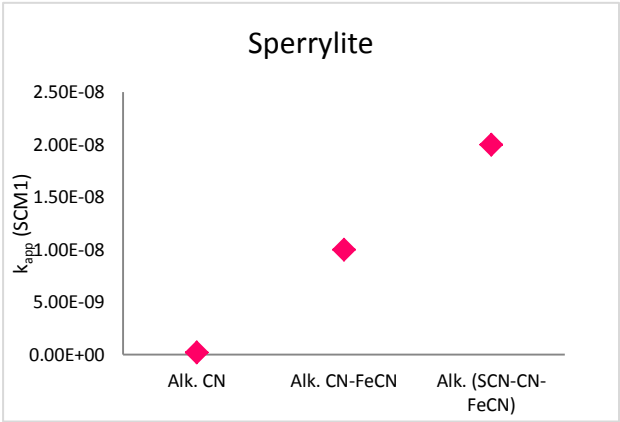

Figure 43: ◆ k_{app} using the SCM1 for sperrylite

Table 32: Initial rates and k_{app} for sperrylite

	1st order kinetics		SCM1		SSM2	
	r(mol/L•s) $rx10^{-10}$	R^2	k_{app} $kx10^{-10}$	R^2	k_{app} $kx10^{-10}$	R^2
Alk. CN^-	1.546	0.970	2	0.917	100	0.879
Alk. $CN^-/[Fe(CN)_6]^{3-}$)	9.599	0.936	100	0.967	2000	0.925
Alk. $(SCN^-/CN^-/[Fe(CN)_6]^{3-})$	15.794	0.919	200	0.828	2000	0.726

Sperrylite is relatively insoluble in relation to cooperite; this may be attributed to the strong bond shared between Pt and As. It requires harsh oxidising conditions to dissolve Pt; even though O_2 in the presence of H^+ was used as an oxidising agent with a high reduction potential of 1.23V, it did not significantly influence the Pt extractions.

Under alkaline systems the dissolution of Pt from sperrylite gives rise to various arsenic species, specifically $HAsO_2$ and AsO_2 (Table 33). The only difference amongst the Pt species in sperrylite and cooperite is the oxidation state. It can be assumed that Pt in the +4 oxidation state demonstrates little to no interaction with cyanide, but that Pt in +2 oxidation state is highly capable of forming complexes with cyanide, as seen with sperrylite.

Table 33: Chemical reactions involving sperrylite in alkaline cyanide systems

	Alkaline CN^-	**Alkaline $CN^-/[Fe(CN)_6]^{3-}$**
Liberation (Sperrylite)	$PtAs_2 + \frac{7}{2}O_2 + 5H_2O \rightleftharpoons 2(HAsO_2) + 8OH^- + Pt^{2+}$ $PtAs_2 + 4O_2 + 4H_2O \rightleftharpoons 2AsO_2 + 8OH^- + Pt^{2+}$	$PtAs_2 + \frac{7}{2}O_2 + 5H_2O \rightleftharpoons 2(HAsO_2) + 8OH^- + Pt^{2+}$ $PtAs_2 + 4O_2 + 4H_2O \rightleftharpoons 2AsO_2 + 8OH^- + Pt^{2+}$ $PtAs_2 + 4[Fe(CN)_6]^{3-} + 2O_2 \rightleftharpoons + Pt^{2+} + 4[Fe(CN)_6]^{4-} + 2AsO_2$
Complexation	$Pt^{2+} + CO^{3-} \rightleftharpoons Pt(CO_3)_4^{2-}$ $Pt^{2+} + HCO^{3-} \rightleftharpoons Pt(HCO_3)_4^{2-}$ $Pt^{2+} + 4OH^- \rightleftharpoons Pt(OH)_4^{2-}$ $Pt^{2+} + 4CN^- \rightleftharpoons Pt(CN)_4^{2-}$	$Pt^{2+} + CO^{3-} \rightleftharpoons Pt(CO_3)_4^{2-}$ $Pt^{2+} + HCO^{3-} \rightleftharpoons Pt(HCO_3)_4^{2-}$ $Pt^{2+} + 4OH^- \rightleftharpoons Pt(OH)_4^{2-}$ $Pt^{2+} + 4CN^- \rightleftharpoons Pt(CN)_4^{2-}$

Since the mixed system demonstrated the best recoveries by far, the respective activation energies associated with cooperite and sperrylite were further explored. Experiments conducted at different temperatures were used to construct the Arrhenius plots depicted in Figure 45 which yielded the activation energies given in Table 34.

$$\ln\left(k_{S_{source}}\right) = -\frac{E_{a,S_{source}}}{R}\ \frac{1}{T} + \ln(A_{S_{source}})$$

Hence a plot of $\ln\left(k_{S_{source}}\right)$ vs $\frac{1}{T}$ will produce a gradient of $-\frac{E_{a,S_{source}}}{R}$ with a y-intercept of $\ln(A_{S_{source}})$. A is the pre-exponential factor, $E_{a,S_{source}}$ is the activation energy ($kJ.mol^{-1}$), R is the universal gas constant ($8.314\ J.K^{-1}mol^{-1}$) and T is the temperature (K).

There was a noticeable increase in the rates of dissolution for both cooperite and sperrylite (Figure 45) with increased temperature. Evidently, extraction of sperrylite is strongly dependent on temperature as opposed to cooperite. At 65°C, the initial rates observed for sperrylite at 0.5g/L SCN^-/CN^- was $13.36x10^{-10}$ $mol.L^{-1}.s^{-1}$ compared to $17.07x10^{-10}$ $mol.L^{-1}.s^{-1}$ at 2g/L SCN^-, CN^- concentration, indicating that they were comparable. The respective activation energies listed in Table 34 indicates that cooperite has a lower activation energy, virtually half that of sperrylite.

The activation energy for cooperite at 0.5g/L SCN^-, CN^- was 26.68 kJ/mol whereas at 2g/L SCN^-, CN^- a value of 23.37kJ/mol was obtained. In contrast, sperrylite revealed an activation energy of 41.37 kJ/mol at 0.5g/L SCN^-, CN^- while at 2g/L SCN^-, CN^- a value of 44.60kJ/mol was observed. The activation energies obtained for Pt dissolution from cooperite suggest that it is diffusion controlled as the values are in close proximity of 20kJ/mol (Crundwell, 2013). Furthermore, this is validated by the passivation layer formed by elemental sulphur. Evidently, Pt dissolution from sperrylite is chemically controlled as activation energies are above 40kJ/mol (Crundwell, 2013) and the same mechanism is operative under varied SCN^-, CN^- concentration investigated, as the figures are relatively close.

The resulting activation energies reported for sperrylite are essentially similar to those reported for gold dissolution (Section 2.6.3) performed under similar conditions using the rotating disk technique (Barbosa-Filho & Monhemius 1994). Due to time constraints only 2 tests were conducted and the activation energy calculated only from interpolation rather than regression.

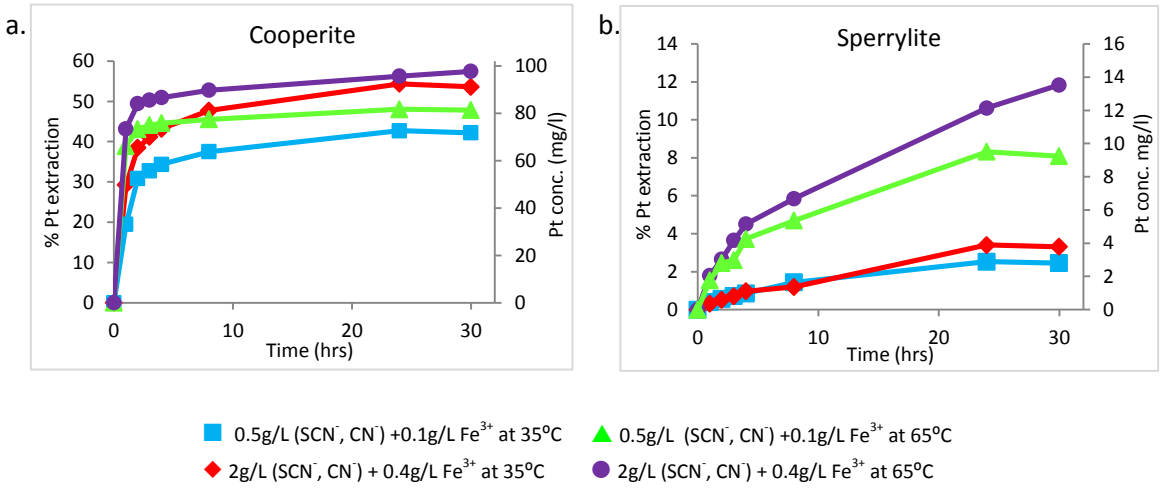

Figure 44: Platinum extractions achieved for (a) cooperite and (b) sperrylite under varied conditions at 500rpm

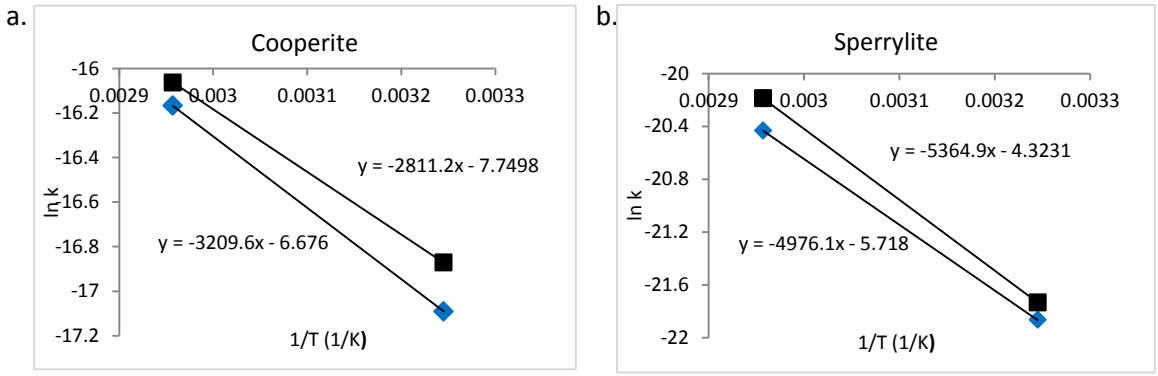

Figure 45: Linear plot of initial rates against the inverse of absolute temperature for (a) cooperite and (b) sperrylite at ◆0.5g/L (SCN^-,CN^-) and ■ 2g/L (SCN^-,CN^-) concentration

Table 34: Pt dissolution rates and apparent activation energies observed at varied temperature and SCN^-, CN^- concentrations

Mineral	Concentration	Temperature	Rate(mol/L•s) $rx10^{-10}$	R^2	E_a (kJ/mol)	A
Cooperite	0.5g/L (SCN^-, CN^-)	35°C	377.68	0.978	26.68	0.00126
		65°C	951.58	0.999		
	2g/L (SCN^-, CN^-)	35°C	470.31	0.917	23.37	0.00043
		65°C	1056.52	0.999		
Sperrylite	0.5g/L (SCN^-, CN^-)	35°C	3.19	0.939	41.37	0.00328
		65°C	13.36	0.937		
	2g/L (SCN^-, CN^-)	35°C	3.64	0.992	44.60	0.01325
		65°C	17.07	0.974		

Several complexes are formed in the mixed system compared to the individual alkaline SCN^- system. It is proposed that increased Pt extraction for both cooperite and sperrylite is due to improved liberation by ferricyanide and possibly the formation of a SCN^-, CN^- mixed ligand complex which is further discussed in Section 4.4.2. Additionally, hard carbonate anions introduced as buffers are highly unlikely to form stable complexes, due to the soft nature of Pt.

Table 35: Chemical reactions involving cooperite and sperrylite in alkaline mixed system ($SCN^-/CN^-/[Fe(CN)_6]^{3-}$)

	Cooperite	Sperrylite
Liberation	$PtS_2 + 4[Fe(CN)_6]^{3-} \rightleftharpoons Pt^{4+} + 4[Fe(CN)_6]^{4-} + 2S^0$ $O_2 + 2H_2O + PtS_2 \rightleftharpoons Pt^{4+} + 2S^0 + 4OH^-$	$PtAs_2 + \frac{7}{2} O_2 + 5H_2O \rightleftharpoons 2(HAsO_2) + 8OH^- + Pt^{2+}$ $PtAs_2 + 4O_2 + 4H_2O \rightleftharpoons 2AsO_2 + 8OH^- + Pt^{2+}$ $PtAs_2 + 4[Fe(CN)_6]^{3-} + 2O_2 \rightleftharpoons + Pt^{2+} + 4[Fe(CN)_6]^{4-} + 2AsO_2$
Complexation	$Pt^{4+} + 6CO^{3-} \rightleftharpoons Pt(CO_3)_6^{2-}$ $Pt^{4+} + 6HCO^{3-} \rightleftharpoons Pt(HCO_3)_6^{2-}$ $Pt^{4+} + 6OH^- \rightleftharpoons Pt(OH)_6^{2-}$ $Pt^{4+} + 6SCN^- \rightleftharpoons Pt(SCN)_6^{2-}$ $Pt^{4+} + 6CN^- \rightleftharpoons Pt(CN)_6^{2-}$	$Pt^{2+} + CO^{3-} \rightleftharpoons Pt(CO_3)_4^{2-}$ $Pt^{2+} + HCO^{3-} \rightleftharpoons Pt(HCO_3)_4^{2-}$ $Pt^{2+} + 4OH^- \rightleftharpoons Pt(OH)_4^{2-}$ $Pt^{2+} + 4SCN^- \rightleftharpoons Pt(SCN)_4^{2-}$ $Pt^{2+} + 4CN^- \rightleftharpoons Pt(CN)_4^{2-}$

In summary, the overall extractions obtained for cooperite and sperrylite were significantly low with an exception for the mixed systems. For dissolution mechanism models, the true difference between good and bad fit models only becomes apparent at extractions above 50%. In addition, the shrinking core and shrinking sphere models are strictly valid for single particle sizes – if the size distribution among the particles is too large errors are bound to occur. Therefore, conclusive findings were drawn from the activation energy analysis rather than the models. The activation energy values of 23-26kJ/mol obtained for cooperite, suggest that it is most likely diffusion controlled which is further explained by the passivation layer formed by elemental sulphur. However, sperrylite is presumably chemically controlled as activation energies of >40 kJ/mol were obtained (Crundwell, 2013).

4.4 Final test work on Merensky concentrate: dual lixiviant system

The final test work on Merensky ore is an adaptation of the experimental work explored in the preliminary tests and pure mineral leach, aimed at maximising overall enhanced extractions of BMs, Pt and Pd. The preliminary test work revealed that thiocyanate is not selective towards PGMs and hence a pre-treatment step is required. A thermophilic leach, comprising of both sulphur and iron oxidizing micro-organisms were used to aid in the extraction of BMs, Cu, Ni and Fe. The dual lixiviant system (cyanide-thiocyanate) showed improved recoveries as opposed to individual systems and was thus chosen as an effective way of leaching Pt and Pd.

4.4.1 Bioleach

The column bioleach runs were conducted in triplicate to generate a sizeable amount of pre-treated concentrate which could then be used in the secondary leach stage. The trends observed amongst the columns for Cu, Ni and Fe extractions differed to a certain degree. In the respective leach curves depicted in Figure 46, an average of 64.70±2.77% Fe, 80.44±1.41% Cu and 92.35±7.15% Ni was extracted over a period of 80 days. Cu and Fe displayed a small deviation amongst the extractions achieved, whereas Ni displayed a substantial variation at a standard deviation of 7.15%. Evidently, Ni demonstrated the fastest dissolution kinetics, achieving an average initial rate of 4.60×10^{-10} mol.L^{-1}.s^{-1} (Table 36) within the first 15 days, followed by Fe and Cu with average initial rates of 3.57×10^{-10} and 2.74×10^{-10} mol.L^{-1}.s^{-1}, respectively.

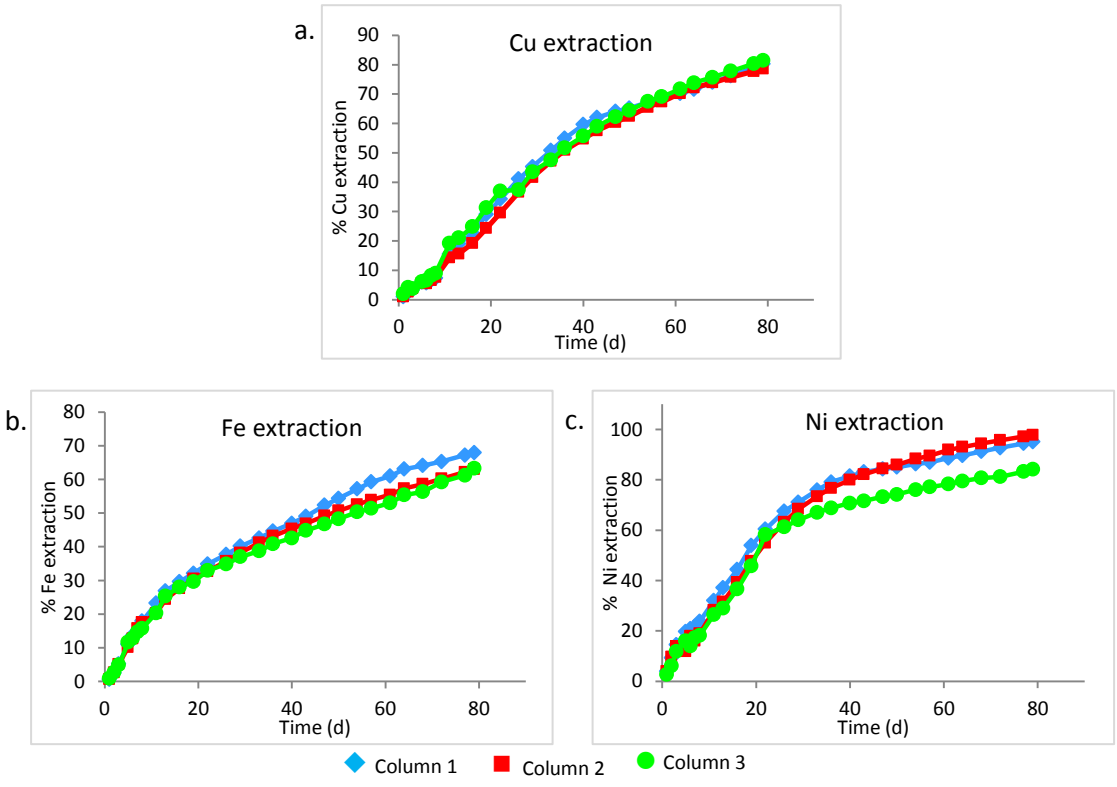

Figure 46: (a) Cu, (b) Fe and (c) Ni extractions achieved during bioleach process at 10g/L H_2SO_4, 0.2g/L Fe^{2+}, 65°C and aeration rate of 130mL/min.

Table 36: Initial rates and k_{app} for the bioleach process

	1st order kinetics		SCM1		SSM2	
	r(mol/L•s) $rx10^{-10}$	R^2	k_{app} $kx10^{-10}$	R^2	k_{app} $kx10^{-10}$	R^2
Cu	2.74	0.974	600	0.993	600	0.991
Fe	3.57	0.964	300	0.995	400	0.973
Ni	4.60	0.988	1000	0.989	800	0.963

Initially, a sulphuric acid leach was carried out within the first 8 days to dissolve as much acid soluble BM minerals as possible, prior to the bioleach. Consequently during this period, there was a fluctuation in the pH (Figure 47, a) rising from <1 to 2.5 ~ 3 as a result of the acid consuming gangue and dissolution of already oxidised BM minerals.

The redox potential provides a measure of the ferric to ferrous iron ratio, as the key redox couple in the system. A lower redox potential is indicative of a lower ferric iron to the ferrous iron concentration. During the bioleaching mechanism the ferric iron attacks the mineral sulphide releasing the ferrous iron into the solution, while the microorganisms convert the released ferrous iron to ferric iron. Therefore the high ORP value indicates high microbial activity. The redox potential (Figure 47, b) was relatively low during the sulphuric acid leach (≤ 8 days). Subsequently, the inoculation of microorganisms in columns led to a gradual increase in redox potential from 405-661mV over 80 days in Column 3, indicating that the microorganisms were becoming increasingly effective in converting ferrous to ferric ion. Column 2 showed moderate microbial activity, achieving redox potentials of 403-548mV by day 80 whereas the microbial activity in column 1 only became apparent after day 60, where redox potentials ≈495-520mV were obtained. It should be noted that BM extractions among the columns indicated marginal differences, and hence the redox potential is a mere indicator, specifically in thermophile systems where Fe (III) precipitation influences the redox reading.

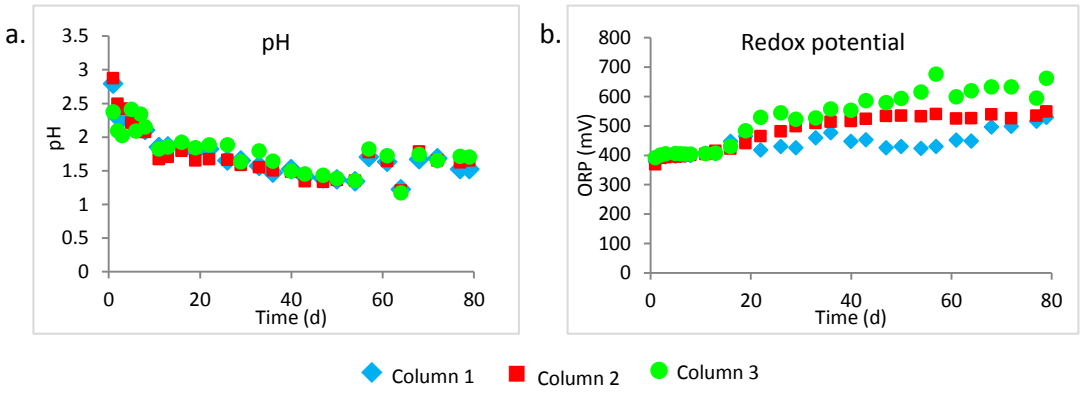

Figure 47: (a) pH and (b) ORP achieved during bioleach process at 10g/L H_2SO_4, 0.2g/L Fe^{2+}, 65°C and aeration rate of 130mL/min

Fairly low Fe extractions obtained suggested that the iron may have been leached and precipitated out immediately resulting in jarosite formation. Additionally, jarosite formation can cause loss of ferric ion, clogging of pore spaces and impede the flow of solution (Mwase et al. 2014). The leaching of Cu, Fe and Ni was diffusion controlled through an inert layer.

This was verified by the high R^2 values (Table 36) obtained using the shrinking core model. Formation of a passivation layer due to jarosites and polysulphides prevents the bacterial attachment to the EPS layer and inhibits the leaching process. Furthermore obtaining a high Fe extraction was crucial, as proceeding into the dual lixiviant system at increased pH may result in the further passivation due to the formation of iron hydroxides.

4.4.2 SCN-CN leach

The mixed systems displayed significant extractions for both Pt and Pd. Figure 48 shows that Column 1, using SCN^- and CN^-, reached a Pt extraction of 42.9%. Once again, Column 2 demonstrated the same trend observed in the pure mineral leaches achieving the highest extraction of 47.1%. Lastly, Column 3 comprising of CN^- and $[Fe(CN)_6]^{3-}$ showed a poor extraction of 35.6%. Even though Pt extractions were not exceedingly high, it should be noted that the reaction had not completely stopped but continued to leach at a slow rate, indicating that higher extractions could still be achieved.

Pd demonstrated an initial faster rate followed by a slower rate. All 3 systems demonstrated remarkable palladium recoveries, achieving ≈100% extraction. Unquestionably, Column 2 exhibited the fastest dissolution kinetics obtaining an initial rate of $0.155x10^{-10}$ $mol.L^{-1}.s^{-1}$.

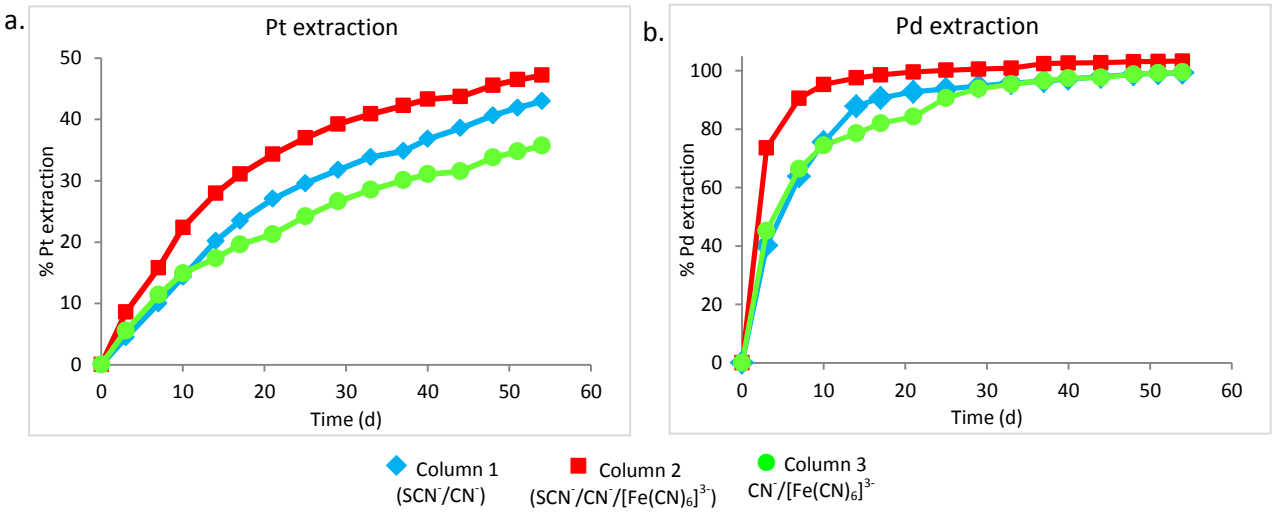

Figure 48: (a) Pt and (b) Pd extractions achieved for mixed systems at 50°C and aeration rate of 130mL/min.

Table 37: Initial rates and k_{app} for Pt in mixed systems

	1st order kinetics		SCM1		SSM2	
	r(mol/L•s) $rx10^{-10}$	R^2	k_{app} $kx10^{-10}$	R^2	k_{app} $kx10^{-10}$	R^2
C1	0.032	0.996	200	0.995	300	0.957
C2	0.041	0.982	200	0.979	400	0.894
C3	0.029	0.991	100	0.996	300	0.952

Table 38: Initial rates and k_{app} for Pd in mixed systems

	1st order kinetics		SCM1		SSM2	
	r(mol/L•s) $rx10^{-10}$	R^2	k_{app} $kx10^{-10}$	R^2	k_{app} $kx10^{-10}$	R^2
C1	0.145	0.914	2000	0.888	1000	0.857
C2	0.155	0.742	6000	0.917	5000	0.861
C3	0.124	0.876	2000	0.969	2000	0.936

Very little is known about the coordination chemistry regarding palladium-thiocyanate complexation. However, a study by le Roux et al. (2014) has revealed that palladium (II) complexation with thiocyanate exists in 5 different modes. These complexes are generally accepted to be square planar. However, the addition of the 5th ligand leans towards square pyramidal geometry with enhanced stability.

In a previous study, Yang et al. (2011) investigated the use of dual lixiviants, thiocyanate and thiourea in leaching of gold. They concluded that small concentration of thiourea added to thiocyanate ferric solution resulted in a synergistic effect on gold dissolution. Findings suggested that the rate of dissolution was significantly higher for mixed systems compared to individual systems at the same concentration. The authors attributed the increased dissolution to the formation of a mixed ligand complex $Au(TU)_2SCN$ confirmed by FTIR analysis.

Similarly, it is postulated that some interaction occurred amongst thiocyanate, cyanide and ferricyanide which led to enhanced Pt and Pd extraction. Ferric cyanide mainly functions as an oxidant while cyanide and thiocyanate operates as a complexing agent. From the results observed it is theorised that apart from homogenous ligand complexes that form, heterogeneous (mixed ligand) complexes are key factors influencing the enhanced extraction. Table 39 lists the various homogenous and heterogeneous complexes that are capable of forming.

Table 39: Homogenous and heterogeneous, Pt and Pd complexes, adapted from Kabesova & Gazo (1980).

Octahedral complex Coordination Type: 6 M= Pt^{4+} & Pd^{4+}	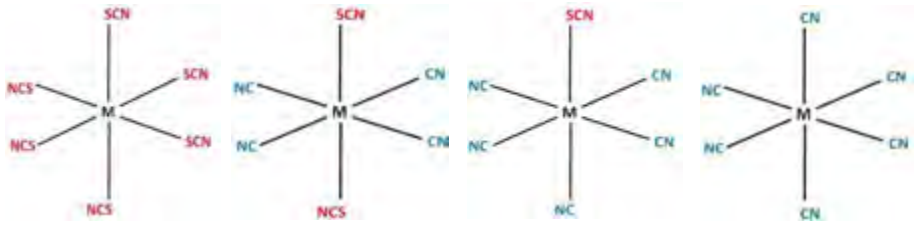
Square planar complex Coordination Type: 4 M= Pt^{2+} & Pd^{2+}	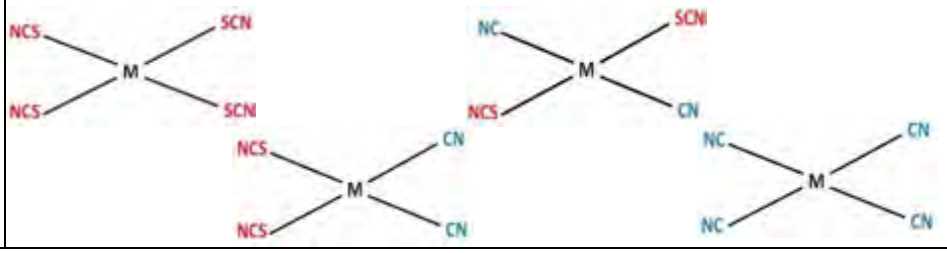

The coordination mode of thiocyanate ligands in complexes depends largely on the properties of the central atom and on properties of other ligands in the coordination sphere. Among heterogeneous thiocyanate complexes, a maximum of two S-bonded thiocyanate ligands can be present while for N-bonded ligands the maximum is 5. Owing to low ionisation energy and high polarizability of the sulphur atom, it has the greater ability to affect the oxidation, reduction properties of the central atom, as opposed to the nitrogen

atom (Kabesova & Gazo 1980). Therefore various Pt and Pd complexes can form which contributes to improved dissolution. Based on the individual systems studies conducted on pure minerals, it is speculated that the mixed ligand complexes exhibit higher stability as opposed to homogenous complexes, this behaviour is manifested in the increased initial rates and extractions.

Pearson (1963) has stated that the simultaneous co-ordination of various ligands to one metal ion gives rise to mixed complexes which are favoured when both ligands are hard or soft Lewis bases (Wanninen, 1977). As a result, bonding with ligands belonging to the same group, (soft or hard Lewis bases) the mixed complexes obtained are generally more stable. Likewise cyanide and thiocyanate are classified as soft Lewis bases and hence likely to form more stable complexes.

With specific reference to concentrate, another key factor that possibly influenced the trends observed was the diverted interaction of residual base metals with cyanide. Given that cyanide forms exceptionally stable complexes with Cu, Ni and Fe (Table 3), it is proposed that a high concentration of free thiocyanate was available for Pt and Pd extraction. Additionally, the adherent film formation of polysulphides across the mineral particle surface most likely interacted with available free cyanide, generating an increased concentration of thiocyanate available for complexation.

5. Conclusions and recommendations

This study was set out to explore an alternate lixiviant to treat PGM bearing ores to simplify the overall process, with the purpose of providing a route that is economical and environmentally more acceptable. Further, this research is an initial attempt to investigate the effectiveness of thiocyanate leaching in low grade concentrate, as well as to determine whether thiocyanate and cyanide act synergistically to promote the dissolution of Pt and Pd. The experiments conducted investigated the kinetics of thiocyanate formation in thiosulphate, sulphite and polysulphide systems. This was followed by thiocyanate leaching of Pt and Pd, initially explored in Platreef low-grade concentrate and then in pure minerals, cooperite, sperrylite and platinum sponge. Having established the conditions aimed at maximising overall Pt and Pd extraction, final test work was carried out on Merensky low-grade concentrate.

Based on the experimental work conducted the following conclusions have been reached:

- The polysulphide-cyanide system dominates in the presence of other reduced sulphur species and is primarily responsible for thiocyanate formation in bioleaching residues.
- Unreacted sulphidic minerals, specifically pyrite, pyrrhotite and chalcopyrite, were not directly involved in the formation of thiocyanate as a result of slow reaction kinetics.
- The presence of base metals in low-grade ore significantly influences thiocyanate consumption, particularly Fe (under acidic conditions) and Ni which demonstrates an increased affinity for thiocyanate, as opposed to copper which shows negligible effect.
- Synthetic cooperite displayed the fastest Pt dissolution kinetics under acid SCN^-, acid SCN^-/Fe^{3+} and alkaline mixed ($SCN^-/CN^-/[Fe(CN)_6]^{3-}$) conditions, while sperrylite exhibited the fastest Pt dissolution kinetics under alkaline CN^- and alkaline $CN^-/[Fe(CN)_6]^{3-}$ conditions.
- The activation energies, 23-26kJ/mol obtained for platinum dissolution from cooperite suggests that it is diffusion controlled. It suspected that the formation of elemental sulphur is responsible for the passivation layer formed in pure minerals.
- For Pt dissolution from sperrylite, activation energies of >40kJ/mol were obtained which implied that it is chemically controlled.
- A 3-component system comprising of SCN^-, CN^- and $[Fe(CN)_6]^{3-}$ displayed enhanced Pt and Pd extraction in Merensky low-grade concentrate, in relation to a 2 component consisting of either CN^- and SCN^- or CN^- and $[Fe(CN)_6]^{3-}$.
- It is postulated that cyanide and thiocyanate act synergistically to promote the dissolution of Pt and Pd through a mixed ligand complex, while the presence of ferricyanide enhances rate of extraction through its role as oxidant.

Recommendations:

The following recommendations are suggested for future work:

Further experiments should be conducted to explore the extent of Pt extraction from pure minerals under SCN^-/CN^- and $SCN^-/[Fe(CN)_6]^{3-}$ conditions to positively confirm that cyanide and thiocyanate act synergistically to promote the dissolution of Pt.

Having established that the mixed system displays improved Pt and Pd extraction, additional experiments should be conducted at increased temperature and reagent concentrations to identify the optimum conditions for leaching.

This research specifically explored the extraction of Pt and Pd. Therefore the pregnant leach solution should also be analysed for Rh, Ru, Ir and Os to evaluate the effectiveness of thiocyanate and cyanide as lixiviants for these metals.

In order to validate that formation of mixed ligand complex, FTIR analysis of the pregnant leach solution should be performed to affirm the presence of homogenous and heterogeneous complexes.

The ability of a lixiviant to dissolve precious metal is significantly important in PGM extraction, however equally important is the further reclamation of the PGMs from solution. This can be achieved through precipitation, solvent extraction or ion exchange which requires further investigation for thiocyanate-cyanide solutions.

6. References

Adams, M.D., 1992. The removal of cyanide from aqueous solution by the use of ferrous sulphate. *Journal of South African Institue of Minerals and Metallurgy*, 92(1), pp.17–25.

Al-bazi, S. & Chow, A., 1984. Platinum metals-solution chemistry and separation methods (ion-exchange and solvent extraction). *Talanta*, 31(10A), pp.815–836.

Anglo American Platinum. *Integrated report*, 2014.

Archer, K., 1997. *Potential of themophilic bioleaching, effect of temperature on the process perfomance*. MSc (Eng) thesis, University of Cape Town.

Azaroual, M., Romand, B., Freyssinet, P., & Disnar, J., 2001. Solubility of platinum in aqueous solutions at 25 ° C and pHs 4 to 10 under oxidizing conditions. *Geochimica et Cosmochimica*, 65(24), pp.4453–4466.

Barbosa-Filho, O. & Monhemius, A., 1994. Leaching of gold in thiocyanate solutions - Part : rates and mechanism of gold dissolution. *Mineral processing and extractive metallurgy*, 103, pp.117–125.

Bartlett, P. & Davis, R., 1958. Reactions of elemental sulfur. II. The reaction of alkali cyanides with sulfur, and some single-sulfur transfer reactions. *Am. Chem. Soc.*, 80, pp.2513.

Botz, M., 2001. Process for the regeneration of cyanide from thiocyanate. *Minerals and Metallurgical Processing*, 18(3), pp.126–132.

Broadhurst, J., 1987. *The chemistry of the dissolution of gold in aqueous thiocyanate medium*. MSc thesis, University of Port Elizabeth.

Burcher-Jones, C. & Lodewyk, S., 2015. *Conversion kinetics of cyanide to thiocyanate in the presence of sulphur, polysulphide , sulphite and thiosulphate*. BSc (Hons) thesis, University of Cape Town.

Cawthorn, G., 2010. The platinum group element deposits of the Bushveld complex in South Africa. *Platinum metals,* 4(54), pp.205-215.

Chen, J and Huang, K., 2006. A new technique for extraction of platinum group metals by pressure cyanidation. *Hydrometallurgy in China Journal*, 82(3-4), pp.164–171.

Crundwell, F. K., 2013. Hydrometallurgy The dissolution and leaching of minerals Mechanisms , myths and misunderstandings. *Hydrometallurgy*, 139, pp.132–148.

Crundwell, F., Moats, M., Ramachandran, V., Robinson, T. & Davenport, W., 2011. *Extractive Metallurgy of Nickel, Cobalt and Platinum-Group Metals*, Elsevier Ltd.

Dunne, R., Levier, M., Acar, S. & Kappes, R., 2009. Newmount's contribution to gold technology. In *The Southern African Institute of Mining and Metallurgy*.

Dutrizac, J.E. & Hardy, D.J., 1997. The behaviour of thiocyanate and cyanate during jarosite precipitation. *Hydrometallurgy*, 45, pp.83–95.

Ferron, C.J., Hamilton, C.C. & Valeyev, O., 2006. The effect of the mineralogy of the platinum group metals on their leachability during the Plastol leach process. *SGS Minerals Services*, 3, pp.1–8.

Free, M., 2013. *Hydrometallurgy: Fundamentals and Applications*, Hoboken, New Jersey: John Wiley and Sons.

Glaister, B.J. & Mudd, G.M., 2010. The environmental costs of platinum – PGM mining and sustainability: Is the glass half-full or half-empty ? *Minerals Engineering*, 23(5), pp.438–450.

Gould, W., King, M., Mohapatra, B., Cameron, R., Kapoor, A. and Koren, D., 2012. A critical review on destruction of thiocyanate in mining effluents. *Minerals Engineering*, pp.38–47.

Green, B., Smit, D., Maumela, H. and Coetzer, G., 2004. Leaching and recovery of platinum group metals from UG-2 concentrates. *The Journal of the South African Institute of Mining and Metallurgy*, pp.323–332.

Habashi, F., 1999. *Textbook of Hydrometallurgy* Second edi., Canada: Metallurgie Extractive Quebec.

Hamacek, J. & Havel, J., 1999. Determination of platinum (II, IV) and palladium (II) as thiocyanate complexes by capillary zone electrophoresis analysis of carboplatin and similar drugs. *Chromatography*, A(834), pp.321–327.

Hancock, R.D., Finkelstein, N.P. & Evers, A., 1977. A linear free-energy relation involving the formation constants of platinum (II) and pladiuM (II). *Inorganic Nuclear Chemistry*, 39, pp.1031–1034.

Jones, R., 1999. Platinum smelting in South Africa. *South African Journal of Science*, 95, pp.525–534.

Jones, R.T., 2005. An overview of Southern African PGM smelting. In *44th Annual Conference of Metallurgists*. pp. 147–178.

Kabesova, M. & Gazo, J., 1980. Structure and classification of thiocyanates and the mutual influence of their ligands. *Chem. zvesti*, 34(6), pp.800–841.

Keller-Lehmann, B., Corrie, S., Ravn, R., Yuan, Z. and Keller, J., 2007. Preservation and Simultaneous Analysis of Relevant Soluble Sulfur Species in Sewage Samples.

Kholmogorov, A., Kononova, O., Pashkov, G. and Kononov, Y., 2002. Thiocyanate solutions in gold technology. *Hydrometallurgy*, 64, pp.43–48.

Koh, T., 1990. A Review Chemistry of Polythionates Thiosulfate. *Analytical Sciences*, pp.3–14.

Kononova, O.N., 2005. Sorption of gold and silver on carbon adsorbents from thiocyanate solutions. *Carbon*, 43, pp.17–22.

Kriek, R., 2008. *Leaching of selected PGMs: A thermodynamic and electrochemical study employing less aggressive lixiviants*. MSc(Eng) thesis, University of Cape Town.

Kuyucak, N. & Akcil, A., 2013. Cyanide and removal options from effluents in gold mining and metallurgical processes. *Minerals Engineering*, 50-51, pp.13–29.

Lahti, M., 2000. Spectrophotometric Determination of Thiocyanate in Human Saliva. *Journal of Chemical Education*, 76(3), pp.1281–1282.

le Roux, C.J., Gans, P. & Kriek, R.J., 2014. Complexation of palladium (II) with thiocyanate – a spectrophotometric investigation. *Journal of Coordination Chemistry*, 67(9), pp.1520–1529.

Levenspiel, O., 1972. *Chemical Reaction Engineering*, New York: Wiley & Sons.

Li, J., Safarzadeh, M., Moats, M., Miller, J., Levier, K., Dietrich, M. and Yu, R., 2012a. Hydrometallurgy Thiocyanate hydrometallurgy for the recovery of gold . Part I : Chemical and thermodynamic considerations ☆. *Hydrometallurgy*, 113-114, pp.1–9.

Li, J., Safarzadeh, M., Moats, M., Miller, J., Levier, K., Dietrich, M. and Yu, R., 2012b. Hydrometallurgy Thiocyanate hydrometallurgy for the recovery of gold . Part II : The leaching kinetics ☆. *Hydrometallurgy*, 113-114, pp.10–18.

Lindsman, N. & Simonsson, D., 1978. On the application of the shrinking core model to liquid-solid reactions. *Chemical Engineering Science*, 34(6), pp.31–35.

Luthy, R. & Bruce, S., 1979. Kinetics of Reaction of Cyanide and Reduced Sulfur Species in Aqueous Solution. *Environ.Sci.Technol*, 13(12), pp.1481–1487.

Martell, A. & Motekaitis, R., 1988. *The determination and use of stability constants*, New York: VCH Publishers, Inc.

Mountain, B. & Wood, S., 1988. Chemical controls on the solubility, transport, and decomposition of platinum and palladium in hydrothermal solutions: a thermodynamic approach. *Eco. Geol.*, 83, pp.492–510.

Mpinga, C., Eksteen, J., Aldrich, C. and Dyer, L. 2015. Direct leach approaches to Platinum Group Metal (PGM) ores and concentrates : A review. *Minerals Engineering*, 78, pp.93–113.

Mpinga, C., Bradshaw, S., Akdogan, G., Snyders, C. and Eksteen, J., 2014. The extraction of Pt, Pd and Au from an alkaline cyanide simulated heap leachate by granular activated carbon. *Minerals Engineering*, 55, pp.11–17.

Muir, D. & Ariti, J., 1991. Studies on the dissolution of platinum and palladium from low grade ores and by-products. *Extractive Metallurgy Conference*, Perth

Muzawazi, C., 2013. *Base metal heap and tank leaching of a Platreef flotation concentrate using ammonical solutions*. MSc(Eng) thesis, University of Cape Town.

Mwase, J.M., Petersen, J. & Eksteen, J.J., 2012a. A conceptual flowsheet for heap leaching of platinum group metals (PGMs) from a low-grade ore concentrate. *Hydrometallurgy*, 111-112, pp.129–135.

Mwase, J.M., Petersen, J. & Eksteen, J.J., 2012b. Assessing a two-stage heap leaching process for Platreef flotation concentrate. *Hydrometallurgy*, 129-130, pp.74–81.

Mwase, J.M., Petersen, J. & Eksteen, J.J., 2014. A novel sequential heap leach process for treating crushed Platreef ore. *Hydrometallurgy*, 141, pp.97–104.

Nair, R., Fatman, D., Chinemberi, E., Montmasson-Clair, G., Ryan, G., & Nyakabawo, W., 2014. *The impact of electricity price increases on the competitiveness of selected mining sector and smelting value chains in South Africa (Commissioned for the Economic Development Department, EDD),* pp. 5–63. Pretoria.

Ngoma, E., 2015. *Investigating the effect of acid stress on selected mesophilic bioleaching microrganisms*. Mtech thesis, Cape Peninsula University of Technology.

Oleschuk, R.D. & Chow, A., 1998. The separation of platinum and palladium by selective extraction of $H_2Pt(SCN)_6$ and $H_2Pd(SCN)_4$ using a polyTHF-impregnated filter. *Talanta*, 45, pp.1235–1245.

Pearson, R.G., 1963. Hard and soft acid and bases. *Journal of the American Chemical Society*, 85(3), pp.3533–3539.

Rao, C.R.M. & Reddi, G.S., 2000. Platinum group metals (PGM); occurrence , use and recent trends in their determination. *Trend in Analytical Chemistry*, 19(9), pp.565–586.

Rawlings, D. & Johnson, D., 2007. *Biomining*, Berlin Heidelberg: Springer.

Safari, V., Arzpeyma, G., Rashchi, F. and Mostou, N., 2009. A shrinking particle — shrinking core model for leaching of a zinc ore containing silica. *Int. J. Miner. Process*, 93, pp.79–83.

Sand, W., Gehrke, T., Jozsa, P. and Schippers, A., 2001. (Bio) / chemistry of bacterial leaching—direct vs. indirect bioleaching. *Hydrometallurgy*, 59, pp.159–175.

Schippers, A., Jozsa, P. & Sand, W., 1996. Sulfur Chemistry in Bacterial Leaching of Pyrite. *Applied and Environmental Microbiology*, 62(9), pp.3424–3431.

Schippers, A. & Sand, W., 1999. Bacterial Leaching of Metal Sulfides Proceeds by Two Indirect Mechanisms via Thiosulfate or via Polysulfides and Sulfur. *Applied and Environmental Microbiology*, 65(1), pp.319–321.

Schouwstra, B.R.P. & Kinloch, E.D., 2000. A Short Geological Review of the Bushveld Complex. *Platinum Metals Rev.*, 44(1), pp.33–39.

Senyaka, G., 2004. Gold leaching in non-cyanide lixiviant systems: critical issues on fundamentals and applications. *Minerals Engineering*, 17, pp.785–801.

Shamaila, S. & Connor, C.T.O., 2008. The role of synthetic minerals in determining the relative flotation behaviour of Platreef PGE tellurides and arsenides. *Minerals Engineering*, 21, pp.899–904.

Smith, R. & Martell, A., 1976. *Critical stability constants. Inorganic Complexes*, New York and London: Plenum Press.

Tributsch, H., 2001. Direct versus indirect bioleaching. *Hydrometallurgy*, 59, pp.177 – 185.

Union, I., Pure, O.F. & Chemistry, A., 1999. Critical surevy of stability constants of complexes of thiocyanate ion. *Pure & Applied Chemistry*, 69(7), pp.1489–1548.

Van der Merwe, W., 2012. *The development of an online amperometric technique to measure free and WAD cyanide in gold plant leach liquors and effluent streams*. MSc (Eng) thesis, University of Cape Town.

Vera, M., Schippers, A. & Sand, W., 2013. Progress in bioleaching : fundamentals and mechanisms of bacterial metal sulfide oxidation — part A. *Appl Microbiol Biotechnol*, 97, pp.7529–7541.

Wanninen, E., 1977. *Analytical Chemistry*, Pergamon Press Ltd.

Wilmot, J.C., 1997. *The chemistry of cyanide in the presence of reduced sulphur sources*. PhD thesis, University of Nebraska.

Yang, X., Moats, M., Miller, J., Wang, X., Shi, X. and Xu, H., 2011. Hydrometallurgy Thiourea – thiocyanate leaching system for gold. *Hydrometallurgy*, 106, pp.58–63.

Young, C.A. & Jordan, T.S., 2001. Cyanide remediation: Current and past technologies. In *Proceedings of the 10th Annual Conference on Hazardous Waste Research*. Department of Metallurgical Engineering, Montana Tech, pp. 104–129.

7. Appendices

Appendix A: Raw Data

Ferric ion standard curve

Spectrophotometric determination of thiocyanate was measured using ferric nitrate assay. The standard curve was generated using triplicate samples of standard thiocyanate solutions using the spectrophotometer.

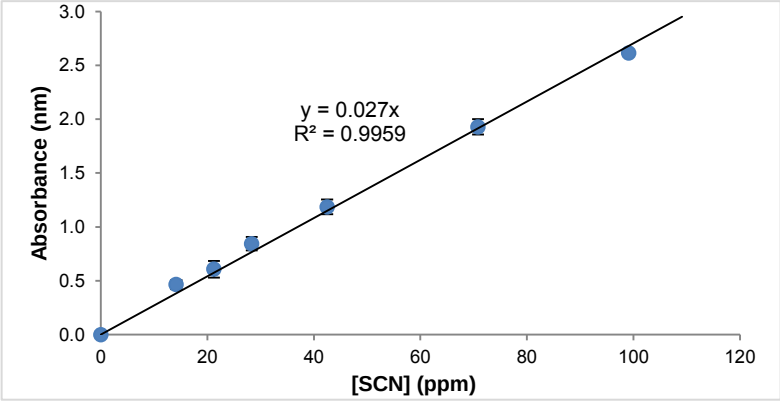

Figure 49: Ferric nitrate standard curve

Table 40: Thiosulphate raw data at varied concentration

Source	Thiosulphate					
Mole ratio	1:1		3:1		5:1	
Temp	60 °c					
m:	0.0313	0.0319	0.1105	0.1024	0.1690	0.1116
c:	0.0142	0.0324	0.0371	0.0942	0.1198	0.2421
St. error	0.0030	0.0027	0.0061	0.0094	0.0108	0.0128
R^2:	0.9653	0.9796	0.9878	0.9754	0.9763	0.9620

Table 41: Thiosulphate raw data at varied temperatures

Source	Thiosulphate					
Mole ratio	1:1					
Temp	45 °c		60 °c		75 °c	
m:	0.0136	0.0120	0.0358	0.0292	0.0742	0.0780
c:	0.0145	0.0226	0.0140	0.0439	0.0333	0.0250
St. error	0.0005	0.0030	0.0035	0.0021	0.0049	0.0036
R^2:	0.9954	0.8397	0.9627	0.9855	0.9745	0.9871

Table 42: Polysulphide raw data at varied concentration

Source	Polysulphide					
Mole ratio	0.28:1		0.56:1		1.12:1	
Temp	25 °c					
m:	1.7270	1.7241	3.2185	3.1913	5.3973	5.2905
st. error	0.2123	0.2258	0.4272	0.4743	0.9607	1.0760

Table 43: Polysulphide raw data at varied temperatures

Source	Polysulphide					
Mole ratio	**0.56:1**					
Temp	**25 °C**		**35 °C**		**45 °C**	
m:	3.2185	3.1913	5.0954	5.3599	5.6271	5.7474
St. error	0.4272	0.4743	0.9679	1.0100	1.1151	1.0141
R^2:	0.9660	0.9577	0.9327	0.9337	0.9272	0.9414
R^2:	0.9707	0.9668	0.9660	0.9577	0.9404	0.9236

Concentrate used in columns:

The actual mass of concentrate packed into columns was calculated using the method described below. An empty bucket was weighed. Concentrate and water was added into the bucket to form slurry (solid:liquid ratio of 5:3) and weighed once again. This was followed by the addition of granite pebbles to the slurry which was mixed thoroughly to ensure that it was coated evenly coated. After packing the column, the empty bucket with mud residue was weighed.

Concentrate	C
Bucket	B
Slurry	S
Mud (residue in bucket)	M
Water used	W
Liquid: solid ratio	X
Actual mass of slurry coated on media	M_1
Actual mass of concentrate packed in column	M_2

Water used $W = S - C$

Liquid: solid ratio $X = \frac{W}{S}$

Actual mass of slurry coated on media $M_1 = (S + B) - (B + M)$

Actual mass of concentrate packed in column $M_2 = M_1 - (M_1 \times X)$

% extraction achieved in leach curves

Metals leached in solution were reported in ppm for AAS analysis and ppb for ICP-MS analysis. The amount of metal dissolved during the leach tests were calculated as follows:

$$\text{Metal dissolved (mg)} = \text{ppm } (\tfrac{mg}{L}) \times \text{effluent (L)}$$

$$\% \text{ Metal dissolved} = \frac{\text{Metal dissolved}}{\text{Total metal in head sample}} \times 100$$

Appendix B: Material safety data sheet

Sodium thiocyanate

ScienceLab.com
Chemicals & Laboratory Equipment

Health	2
Fire	1
Reactivity	0
Personal Protection	E

Material Safety Data Sheet
Sodium thiocyanate MSDS

Section 1: Chemical Product and Company Identification

Product Name: Sodium thiocyanate

Catalog Codes: SLS3931, SLS1711

CAS#: 540-72-7

RTECS: XL2275000

TSCA: TSCA 8(b) inventory: Sodium thiocyanate

CI#: Not available.

Synonym:

Chemical Formula: NaCNS

Contact Information:

Sciencelab.com, Inc.
14025 Smith Rd.
Houston, Texas 77396

US Sales: **1-800-901-7247**
International Sales: **1-281-441-4400**

Order Online: ScienceLab.com

CHEMTREC (24HR Emergency Telephone), call:
1-800-424-9300

International CHEMTREC, call: 1-703-527-3887

For non-emergency assistance, call: 1-281-441-4400

Section 2: Composition and Information on Ingredients

Composition:

Name	CAS #	% by Weight
Sodium thiocyanate	540-72-7	100

Toxicological Data on Ingredients: Sodium thiocyanate : ORAL (LD50): Acute: 764 mg/kg [Rat]. 362 mg/kg [Mouse].

Section 3: Hazards Identification

Potential Acute Health Effects:
Very hazardous in case of ingestion. Hazardous in case of skin contact (irritant), of eye contact (irritant), of inhalation. Slightly hazardous in case of skin contact (permeator).

Potential Chronic Health Effects:
CARCINOGENIC EFFECTS: Not available. MUTAGENIC EFFECTS: Not available. TERATOGENIC EFFECTS: Not available. DEVELOPMENTAL TOXICITY: Not available. Repeated or prolonged exposure is not known to aggravate medical condition.

Section 4: First Aid Measures

Eye Contact:
Check for and remove any contact lenses. Immediately flush eyes with running water for at least 15 minutes, keeping eyelids open. Cold water may be used. Do not use an eye ointment. Seek medical attention.

Skin Contact:
After contact with skin, wash immediately with plenty of water. Gently and thoroughly wash the contaminated skin with running water and non-abrasive soap. Be particularly careful to clean folds, crevices, creases and groin. Cold water may be used. Cover the irritated skin with an emollient. If irritation persists, seek medical attention. Wash contaminated clothing before reusing.

Serious Skin Contact:
Wash with a disinfectant soap and cover the contaminated skin with an anti-bacterial cream. Seek immediate medical attention.

Inhalation: Allow the victim to rest in a well ventilated area. Seek immediate medical attention.

Serious Inhalation: Not available.

Ingestion:
Do not induce vomiting. Examine the lips and mouth to ascertain whether the tissues are damaged, a possible indication that the toxic material was ingested; the absence of such signs, however, is not conclusive. Loosen tight clothing such as a collar, tie, belt or waistband. If the victim is not breathing, perform mouth-to-mouth resuscitation. Seek immediate medical attention.

Serious Ingestion: Not available.

Section 5: Fire and Explosion Data

Flammability of the Product: May be combustible at high temperature.

Auto-Ignition Temperature: Not available.

Flash Points: Not available.

Flammable Limits: Not available.

Products of Combustion: Some metallic oxides.

Fire Hazards in Presence of Various Substances: Not available.

Explosion Hazards in Presence of Various Substances:
Risks of explosion of the product in presence of mechanical impact: Not available. Risks of explosion of the product in presence of static discharge: Not available.

Fire Fighting Media and Instructions:
SMALL FIRE: Use DRY chemical powder. LARGE FIRE: Use water spray, fog or foam. Do not use water jet.

Special Remarks on Fire Hazards: Not available.

Special Remarks on Explosion Hazards: Not available.

Section 6: Accidental Release Measures

Small Spill:
Use appropriate tools to put the spilled solid in a convenient waste disposal container. Finish cleaning by spreading water on the contaminated surface and dispose of according to local and regional authority requirements.

Large Spill:
Use a shovel to put the material into a convenient waste disposal container. Finish cleaning by spreading water on the contaminated surface and allow to evacuate through the sanitary system.

Section 7: Handling and Storage

Precautions:
Keep away from heat. Keep away from sources of ignition. Empty containers pose a fire risk, evaporate the residue under a fume hood. Ground all equipment containing material. Do not ingest. Do not breathe dust. Wear suitable protective clothing in

p. 2

Sodium cyanide

ScienceLab.com
Chemicals & Laboratory Equipment

Material Safety Data Sheet
Sodium Cyanide MSDS

Section 1: Chemical Product and Company Identification

Product Name: Sodium Cyanide

Catalog Codes: SLS2314, SLS3736

CAS#: 143-33-9

RTECS: VZ7525000

TSCA: TSCA 8(b) inventory: Sodium Cyanide

CI#: Not available.

Synonym:

Chemical Name: Sodium Cyanide

Chemical Formula: NaCN

Contact Information:

Sciencelab.com, Inc.
14025 Smith Rd.
Houston, Texas 77396

US Sales: **1-800-901-7247**
International Sales: **1-281-441-4400**
Order Online: ScienceLab.com

CHEMTREC (24HR Emergency Telephone), call:
1-800-424-9300

International CHEMTREC, call: 1-703-527-3887

For non-emergency assistance, call: 1-281-441-4400

Section 2: Composition and Information on Ingredients

Composition:

Name	CAS #	% by Weight
Sodium Cyanide	143-33-9	100

Toxicological Data on Ingredients: Sodium Cyanide: ORAL (LD50): Acute: 6.44 mg/kg [Rat]. DERMAL (LD50): Acute: 10.4 mg/kg [Rabbit].

Section 3: Hazards Identification

Potential Acute Health Effects:
Very hazardous in case of skin contact (irritant), of eye contact (irritant), of ingestion, of inhalation. Hazardous in case of skin contact (permeator). Corrosive to eyes and skin. The amount of tissue damage depends on length of contact. Eye contact can result in corneal damage or blindness. Skin contact can produce inflammation and blistering. Inhalation of dust will produce irritation to gastro-intestinal or respiratory tract, characterized by burning, sneezing and coughing. Severe over-exposure can produce lung damage, choking, unconsciousness or death. Inflammation of the eye is characterized by redness, watering, and itching. Skin inflammation is characterized by itching, scaling, reddening, or, occasionally, blistering.

Potential Chronic Health Effects:
CARCINOGENIC EFFECTS: Not available. MUTAGENIC EFFECTS: Not available. TERATOGENIC EFFECTS: Not available. DEVELOPMENTAL TOXICITY: Not available. The substance may be toxic to skin, eyes, central nervous system (CNS). Repeated or prolonged exposure to the substance can produce target organs damage. Repeated exposure of the eyes to a low level of dust can produce eye irritation. Repeated skin exposure can produce local skin destruction, or dermatitis. Repeated inhalation of dust can produce varying degree of respiratory irritation or lung damage. Repeated exposure to a highly toxic material may produce general deterioration of health by an accumulation in one or many human organs.

p. 1

Section 4: First Aid Measures

Eye Contact:
Check for and remove any contact lenses. In case of contact, immediately flush eyes with plenty of water for at least 15 minutes. Cold water may be used. Get medical attention immediately.

Skin Contact:
In case of contact, immediately flush skin with plenty of water for at least 15 minutes while removing contaminated clothing and shoes. Cover the irritated skin with an emollient. Cold water may be used.Wash clothing before reuse. Thoroughly clean shoes before reuse. Get medical attention immediately.

Serious Skin Contact:
Wash with a disinfectant soap and cover the contaminated skin with an anti-bacterial cream. Seek immediate medical attention.

Inhalation:
If inhaled, remove to fresh air. If not breathing, give artificial respiration. If breathing is difficult, give oxygen. Get medical attention.

Serious Inhalation:
Evacuate the victim to a safe area as soon as possible. Loosen tight clothing such as a collar, tie, belt or waistband. If breathing is difficult, administer oxygen. If the victim is not breathing, perform mouth-to-mouth resuscitation. WARNING: It may be hazardous to the person providing aid to give mouth-to-mouth resuscitation when the inhaled material is toxic, infectious or corrosive. Seek immediate medical attention.

Ingestion:
If swallowed, do not induce vomiting unless directed to do so by medical personnel. Never give anything by mouth to an unconscious person. Loosen tight clothing such as a collar, tie, belt or waistband. Get medical attention immediately.

Serious Ingestion: Not available.

Section 5: Fire and Explosion Data

Flammability of the Product: May be combustible at high temperature.

Auto-Ignition Temperature: Not available.

Flash Points: Not available.

Flammable Limits: Not available.

Products of Combustion: Some metallic oxides.

Fire Hazards in Presence of Various Substances: Slightly flammable to flammable in presence of acids, of moisture.

Explosion Hazards in Presence of Various Substances:
Risks of explosion of the product in presence of mechanical impact: Not available. Risks of explosion of the product in presence of static discharge: Not available.

Fire Fighting Media and Instructions:
SMALL FIRE: Use DRY chemical powder. LARGE FIRE: Use water spray, fog or foam. Do not use water jet.

Special Remarks on Fire Hazards:
Dangerous on contact with acids, acid fumes, water or stream. It will produce toxic and flammable vapors of CN-H and sodium oxide. Contact with acids and acid salts causes immediate formation of toxic and flammable hydrogen cyanide gas. When heated to decomposition it emits toxic fumes hydgrogen cyanide and oxides of nitrogen

Special Remarks on Explosion Hazards: Fusion mixtures of metal cyanides with metal chlorates, perchlorated or nitrates causes a violent explosion

Appendix C: Assessment of Ethics in Research Projects:

EBE Faculty: Assessment of Ethics in Research Projects

Any person planning to undertake research in the Faculty of Engineering and the Built Environment at the University of Cape Town is required to complete this form before collecting or analysing data. When completed it should be submitted to the supervisor (where applicable) and from there to the Head of Department. If any of the questions below have been answered YES, and the applicant is NOT a fourth year student, the Head should forward this form for approval by the Faculty EIR committee: submit to Ms Zakiya Chikte (Zakiya.chikte@uct.ac.za): New ERE Building, Ph 021 650 5739). Students must include a copy of the completed form with the dissertation/thesis when it is submitted for examination.

Name of Principal Researcher/Student: Kathija Shaik **Department: Chemical Engineering**

If a Student: **Degree: MSc(Eng)** **Supervisor: Prof Jochen Petersen**

If a Research Contract indicate source of funding/sponsorship:

Research Project Title: The formation of thiocyanate in bioleaching residues and its effect in PGM recovery

Overview of ethics issues in your research project:

Question 1: Is there a possibility that your research could cause harm to a third party (i.e. a person not involved in your project)?	YES	NO ✓
Question 2: Is your research making use of human subjects as sources of data? If your answer is YES, please complete Addendum 2.	YES	NO ✓
Question 3: Does your research involve the participation of or provision of services to communities? If your answer is YES, please complete Addendum 3.	YES	NO ✓
Question 4: If your research is sponsored, is there any potential for conflicts of interest? If your answer is YES, please complete Addendum 4.	YES	NO ✓

If you have answered YES to any of the above questions, please append a copy of your research proposal, as well as any interview schedules or questionnaires (Addendum 1) and please complete further addenda as appropriate.

I hereby undertake to carry out my research in such a way that

- there is no apparent legal objection to the nature or the method of research; and
- the research will not compromise staff or students or the other responsibilities of the University;
- the stated objective will be achieved, and the findings will have a high degree of validity;
- limitations and alternative interpretations will be considered;
- the findings could be subject to peer review and publicly available; and
- I will comply with the conventions of copyright and avoid any practice that would constitute plagiarism.

Signed by:

	Full name and signature	Date
Principal Researcher/Student: Kathija Shaik		12/02/2016

This application is approved by:

Supervisor (if applicable):		12/02/2016
HOD (or delegated nominee): Final authority for all assessments with NO to all questions and for all undergraduate research.		12/02/2016
Chair: Faculty EIR Committee For applicants other than undergraduate students who have answered YES to any of the above questions.		

ADDENDUM 1:
Please append a copy of the research proposal here, as well as any interview schedules or questionnaires:

ADDENDUM 2: To be completed if you answered YES to Question 2:

It is assumed that you have read the UCT Code for Research involving Human Subjects (available at http://web.uct.ac.za/depts/educate/download/uctcodeforresearchinvolvinghumansubjects.pdf) in order to be able to answer the questions in this addendum.

2.1 Does the research discriminate against participation by individuals, or differentiate between participants, on the grounds of gender, race or ethnic group, age range, religion, income, handicap, illness or any similar classification?	YES	NO ✓
2.2 Does the research require the participation of socially or physically vulnerable people (children, aged, disabled, etc) or legally restricted groups?	YES	NO ✓
2.3 Will you not be able to secure the informed consent of all participants in the research? (In the case of children, will you not be able to obtain the consent of their guardians or parents?)	YES	NO ✓
2.4 Will any confidential data be collected or will identifiable records of individuals be kept?	YES	NO ✓
2.5 In reporting on this research is there any possibility that you will not be able to keep the identities of the individuals involved anonymous?	YES	NO ✓
2.6 Are there any foreseeable risks of physical, psychological or social harm to participants that might occur in the course of the research?	YES	NO ✓
2.7 Does the research include making payments or giving gifts to any participants?	YES	NO ✓

If you have answered YES to any of these questions, please describe how you plan to address these issues (append to form):

ADDENDUM 3: To be completed if you answered YES to Question 3:

3.1 Is the community expected to make decisions for, during or based on the research?	YES	NO ✓
3.2 At the end of the research will any economic or social process be terminated or left unsupported, or equipment or facilities used in the research be recovered from the participants or community?	YES	NO ✓
3.3 Will any service be provided at a level below the generally accepted standards?	YES	NO ✓

If you have answered YES to any of these questions, please describe how you plan to address these issues (append to form)

ADDENDUM 4: To be completed if you answered YES to Question 4

4.1 Is there any existing or potential conflict of interest between a research sponsor, academic supervisor, other researchers or participants?	YES	NO ✓
4.2 Will information that reveals the identity of participants be supplied to a research sponsor, other than with the permission of the individuals?	YES	NO ✓
4.3 Does the proposed research potentially conflict with the research of any other individual or group within the University?	YES	NO ✓

If you have answered YES to any of these questions, please describe how you plan to address these issues(append to form)